Critical dynamics near the λ transition in ^{3}He-^{4}He mixtures

V. Dohm

Institut für Festkörperforschung, Kernforschungsanlage Jülich, D-5170 Jülich, Germany

R. Folk[*]

*Institut für Theoretische Physik, Universität Linz, A-4045 Linz, Austria[†]
and Institut für Festkörperforschung, Kernforschungsanlage Jülich, D-5170 Jülich, Germany*

(Received 26 January 1983; revised manuscript received 12 July 1983)

The critical dynamics of the λ transition in ^{3}He-^{4}He mixtures are studied by means of renormalized field theory applied to the model of Siggia and Nelson. A diagonal representation for the equations of motion is introduced, which greatly simplifies the computations in two-loop order. A universal connection is found with the asymptotic critical dynamics of pure ^{4}He in all orders of perturbation theory. The observable critical dynamics of helium mixtures are dominated by nonuniversal crossover effects which can be properly described only within a nonlinear renormalization-group approach. The theory is applied to explain the observable critical and precritical temperature dependence of the mass diffusion D, of the thermal conductivity κ, of the thermal diffusion ratio k_T, and of the dynamic structure factor for $T \geq T_\lambda(X)$. Recent experimental data for the transport coefficients at the molar ^{3}He concentration $X=0.05$ by Gestrich and Meyer are used to identify the nonuniversal parameters of the theory in the range $X \ll 1$. Consistency with the dynamics of pure ^{4}He $(X=0)$ is verified. Predictions without adjustable parameters are made for the dynamic structure factor and the transport coefficients in very dilute mixtures. The Siggia-Kawasaki problem concerning the leading X dependence of $\kappa(T_\lambda)$ in the $X \rightarrow 0$ limit is resolved. It is demonstrated that Siggia's prediction $\kappa(T_\lambda) \sim X^{-1}$ is correct but not observable. Theoretical extrapolations to $X > 0.05$ without adjustable parameters are presented and compared with measured transport coefficients at $X=0.11$ and 0.15. The overall agreement is satisfactory. Deviations of order 15% exist with the thermal conductivity κ at $X=0.15$. This may be attributed to dynamic effects arising from the singular specific heat and mass susceptibility, which are not included in the present analysis.

I. INTRODUCTION

Favorable experimental conditions such as the absence of strains and impurities as well as a rich variety of observable properties have stimulated a large number of dynamic experiments near the λ line $T_\lambda(c)$ of ^{3}He-^{4}He mixtures.[1-26] While the *static* critical behavior near the superfluid transition in pure ^{4}He and in a ^{3}He-^{4}He mixture belong to the same universality class,[27] the critical *dynamics* at finite concentration c of ^{3}He atoms are expected to be quite different from and more complicated than those of pure ^{4}He. This is so because the ^{3}He concentration constitutes a separate hydrodynamic variable[28] which is coupled dynamically to the superfluid order parameter ψ. The most spectacular difference has been found for the measured thermal conductivity κ, which remains finite[2,29] at T_λ for finite ^{3}He concentration whereas κ diverges[30-34] at T_λ in pure ^{4}He. A unique feature of ^{3}He-^{4}He mixtures is the existence of a tricritical point which is well accessible to dynamic experiments[6,11,12,20,21] in contrast to multicritical points in solids. Furthermore, as in pure ^{4}He, the pressure can be varied in order to test predictions concerning critical[34,35] and tricritical[36] universality. Alternatively, universal and nonuniversal dynamic effects can also be identified by performing a series of measurements at various ^{3}He concentrations.[5,7,8,11-17,20-23] Particularly interesting are the crossover phenomena in the dilute and in the tricritical regime. Thus the helium mixtures constitute perhaps the best physical system where the richness of dynamic critical behavior can be fully explored with sufficient accuracy and can be

compared in a conclusive way with the theoretical predictions.

In spite of these experimental advantages the theory of critical dynamics in ³He-⁴He mixtures[28,29,37−45] has remained in a rather incomplete and unsatisfactory status, with a few specific predictions based on scaling arguments and on calculations at the one-loop level.[2,13,29,39,43−45] Although two-loop contributions are generally known to be crucial in the area of critical and multicritical dynamics[46−49] no attempt has been made so far to study the corresponding effects near the λ line of helium mixtures. This lack of information is not only due to the considerable complexity of the underlying stochastic equations of motion[28,43] but also to the serious problems[46] which existed already with the simpler dynamics of pure ⁴He. Therefore, it seemed necessary to await the solution to these problems.

Recent advances[47,50−56] in the understanding of the ⁴He dynamics indicate that there is now the occasion to proceed to a more advanced theory which may explain and predict the various dynamic critical and tricritical phenomena in ³He-⁴He mixtures as well. It is the purpose of the present work to provide the basis for a major step in this direction. We shall not confine ourselves to the traditional questions as to what the asymptotic power laws and their subleading power-law corrections are, but rather investigate the nonuniversal crossover phenomena in the entire region between the noncritical background far from $T_\lambda(c)$ and the asymptotic criticality at $T_\lambda(c)$. This is quite different in spirit from the work of Siggia and Nelson[43] or of Siggia,[44] who studied the crossover from the λ line to tricritical or to pure ⁴He-like behavior in the asymptotic vicinity of $T_\lambda(c)$.

Our approach consists of a nonlinear dynamic renormalization-group analysis[51−56] on the basis of renormalized-field theory[57−59,47] applied to the model of Siggia and Nelson.[43] A diagonal representation for the equations of motion is introduced which greatly simplifies our explicit calculations in two-loop order and which reveals a universal connection between the asymptotic critical dynamics of ⁴He and of ³He-⁴He mixtures in all orders of perturbation theory. In particular, there exist universal amplitudes of the transport coefficients along $T_\lambda(c)$, one of which coincides with the previous universal amplitude R_λ (Refs. 47, 49, and 60) for pure ⁴He. The observable critical behavior is found to be dominated by nonuniversal crossover effects of genuine dynamic origin which cannot be described in terms of power laws.

Specifically, we study the mass diffusion coefficient D, the thermal diffusion ratio k_T, and the thermal conductivity κ (in the absence of mass flow),

for which detailed experimental information is available at a number of different concentrations, in particular due to recent measurements by Ruppeiner, Ryschkewitsch, and Meyer,[20] by Behringer and Meyer,[21,22] and by Gestrich and Meyer.[23] Recent data[23] at the molar ³He concentration $X=0.05$ are used to determine approximately the nonuniversal parameters of our theory in the low-concentration range. Extrapolation to $X=0.11$ and 0.15 without adjustable parameters yields reasonable agreement with available data,[2,13,14,23] except for deviations of order 15% for κ (Refs. 2 and 23) at $X=0.15$. Predictions are made for very dilute mixtures ($X \ll 0.1$) for which new thermal-conductivity measurements by Meyer and co-workers[61] are planned for future publication. In particular, we reexamine the problem of the divergence of $\kappa(T_\lambda)$ in the dilute limit $c \rightarrow 0$ for which there exist contradictory predictions $\kappa(T_\lambda) \sim c^{-1}$ and $\kappa(T_\lambda) \sim c^{-1/3}$ due to Siggia[44] and to Kawasaki and co-workers,[13] respectively, neither of which has been convincingly confirmed by experiment.[13,20,23,62] We resolve this problem by demonstrating that Siggia's result is correct at least up to two-loop order but is not experimentally observable. Furthermore, there are effects of the weak-scaling fixed point[47] which we find to induce a small dynamic transient exponent $\omega_w \ll 1$ not only for ⁴He (Refs. 47 and 49−51) but also for ³He-⁴He mixtures.

Finally, we determine the dynamic structure factor $S(k,\omega)$ for $T \geq T_\lambda(c)$ and discuss its shape and temperature dependence in the hydrodynamic region. This can be compared with future light scattering experiments.

Throughout this paper we neglect, for simplicity, dynamic contributions arising from static couplings of the model-F type.[60] We believe that within this approximation the main features of the observable dynamics for $X \ll 1$ are described with reasonable accuracy comparable to the quality of the previous model-E analysis for pure ⁴He.[51−54] A fully quantitative description does of course require the inclusion of the static couplings as indicated by the model-F analysis for ⁴He.[55,56] The corresponding corrections are expected to be of the order of 15−20% (Refs. 52, 55, and 56) and may eliminate the deviations of the present analysis with the data for κ at $X=0.15$. Also an accurate analysis in the entire range of X up to the tricritical point should be possible. So far, however, the complete renormalization-group flow equations including the static couplings are unknown in two-loop order and are expected to be much more complicated than those for model F.[63]

The outline of this paper is as follows. In Sec. II the parameters and the structure of the model of

Siggia and Nelson[43] are discussed and part of the general procedure of the paper is outlined. Section III presents the definitions and properties related to the field-theoretic renormalization of the model. The temperature dependence of the transport coefficients is calculated in Sec. IV. Exact results concerning the dynamic fixed point, the transient exponents, and the amplitudes of the transport coefficients are given in Sec. V. The results of renormalized perturbation calculations in two-loop order as well as the connection with model E (Ref. 60) are discussed in Sec. VI after the equations of motions have been transformed in a convenient way. Section VII contains the nonlinear renormalization-group analysis of the transport coefficients; this includes a determination of the nonuniversal parameters of the theory, a comparison with existing experimental data, and the prediction of the temperature and concentration dependence in dilute mixtures. In Sec. VIII the theory is applied to the dynamic structure factor.

II. MODEL

A. Model parameters

In studying the critical dynamics of ^{3}He-^{4}He mixtures we shall use the model of Siggia and Nelson.[43] As we wish to carry out a quantitative comparison with experiments it is necessary to specify the precise meaning of the model parameters. In this section we present the various definitions and review the previous identification of the static and dynamic parameters by Siggia and Nelson.

The equilibrium values of the thermodynamic quantities of ^{3}He-^{4}He mixtures can be defined via the Gibbs free energy $G(T,P,N_3,N_4)$, where T, P, and N_i denote the temperature, the pressure, and the number of ^{3}He or ^{4}He atoms. We consider the Gibbs free energy per unit mass $\tilde{g}=G/M$ $=\tilde{g}(T,P,c)$ as a function of T,P, and of the mass concentration of the ^{3}He atoms $c=m_3N_3/M$, with $M=m_3N_3+m_4N_4$ being the total mass and m_i being the mass of a ^{3}He or ^{4}He atom.

The entropy per unit mass σ and the chemical potential Δ conjugate to c are obtained from $\tilde{g}$ according to $\sigma=-(\partial\tilde{g}/\partial T)_{P,c}$ and

$$\Delta=(\partial\tilde{g}/\partial c)_{T,P}=\tilde{\mu}_3/m_3-\tilde{\mu}_4/m_4 ,$$

where $\tilde{\mu}_i$ denotes a chemical potential per particle, $\tilde{\mu}_3=(\partial G/\partial N_3)_{T,P,N_4}$, and $\tilde{\mu}_4=(\partial G/\partial N_4)_{T,P,N_3}$. The slow variables of interest are the long-wavelength fluctuations $\delta\sigma(x)$, $\delta c(x)$, and $\psi_0(x)$ of the entropy per unit mass, of the mass concentration, and of the complex order parameter, respective-

ly.[28] As we shall not study first sound we neglect the fluctuations of the pressure.

We consider an equilibrium state at given T,P,Δ, and a distribution $\sim\exp(-H)$ for the probability of small fluctuations $\psi_0(x)$, $\delta\sigma(x)$, and $\delta c(x)$. We assume

$$H=H_\psi[\psi_0]+H_{\sigma c}[\delta\sigma,\delta c] , \tag{2.1}$$

$$H_\psi=\int d^dx(\tfrac{1}{2}\tau_0|\psi_0|^2+\tfrac{1}{2}|\nabla\psi_0|^2+u_0|\psi_0|^4) , \tag{2.2}$$

where τ_0 is proportional to $T-T_\lambda^{MF}(P,\Delta)$, with T_λ^{MF} being a mean-field (MF) transition temperature. We shall keep only Gaussian fluctuations $\delta\sigma$ and δc. The corresponding functional $H_{\sigma c}$ is bilinear in $\delta\sigma$ and δc with coefficients which can be determined via the requirements[64]

$$\int d^dx \langle \delta\sigma(x)\delta\sigma(0)\rangle$$
$$=\frac{k_BT}{\rho}\left[\frac{\partial\sigma}{\partial T}\right]_{P,\Delta}=\rho^{-1}k_BC_{P,\Delta} , \tag{2.3}$$

$$\int d^dx \langle \delta c(x)\delta\sigma(0)\rangle=\frac{k_BT}{\rho}\left[\frac{\partial c}{\partial T}\right]_{P,\Delta} , \tag{2.4}$$

$$\int d^dx \langle \delta c(x)\delta c(0)\rangle=\frac{k_BT}{\rho}\left[\frac{\partial c}{\partial\Delta}\right]_{P,T}\equiv\chi_c . \tag{2.5}$$

Here $\rho=M/V$ is the mass density and $C_{P,\Delta}$ is the specific heat per unit mass at constant P and Δ. We neglect possible couplings $\sim|\psi_0|^2\delta\sigma$ and $\sim|\psi_0|^2\delta c$ in H. This approximation is analogous to that using model E rather than model F (Ref. 60) for the dynamics of pure ^{4}He, as will be further discussed below.

Following previous authors[43,65-67] we shall eliminate the variable $\delta\sigma(x)$ in favor of a variable $q(x)$ proportional to the fluctuations $\delta T(x)$ of the temperature. This is convenient because $\delta T(x)$ and $\delta c(x)$ are independent fluctuations.[64] Using the relation

$$\delta\sigma(x)=\left[\frac{\partial\sigma}{\partial T}\right]_{P,c}\delta T(x)+\left[\frac{\partial\sigma}{\partial c}\right]_{P,T}\delta c(x) , \tag{2.6}$$

and defining

$$q(x)=k_B^{-1}\rho\left[\frac{\partial\sigma}{\partial T}\right]_{P,c}\delta T(x) , \tag{2.7}$$

we obtain from Eqs. (2.3)–(2.5)

$$\int d^d x \langle q(x)q(0)\rangle$$

$$= k_B^{-1}\rho T \left[\frac{\partial\sigma}{\partial T}\right]_{P,c} = k_B^{-1}\rho C_{P,c} \equiv \chi_q \quad (2.8)$$

and

$$\int d^d x \langle q(x)\delta c(0)\rangle = 0 . \quad (2.9)$$

Here $C_{P,c}$ is the specific heat per unit mass at constant P and c. Thus we have

$$H = H_\psi + \tfrac{1}{2}\int d^d x[\chi_q^{-1}q^2 + \chi_c^{-1}(\delta c)^2] . \quad (2.10)$$

The variable $q(x)$ and the susceptibility χ_q have been defined such that in the limit of zero ^{3}He concentration they can be identified with the entropy variable $m(x)$ and the susceptibility χ of model E for pure ^{4}He (where χ represents the constant pressure specific heat per unit volume divided by k_B).[60]

The appropriate equations of motion for $\psi_0(x,t)$, $q(x,t)$, and $\delta c(x,t)$ must be consistent with the equilibrium distribution determined by Eq. (2.10), with the diffusion equations for binary mixtures,[65] and with the hydrodynamics of superfluid ^{3}He-^{4}He mixtures.[28] In particular, the limit $c \to 0$ should lead to model E for pure ^{4}He. These requirements are met by the Langevin equations of Siggia and Nelson.[43] With the simplified notation $c(x,t)\equiv\delta c(x,t)$ these equations read

$$\frac{\partial}{\partial t}\psi_0 = -2\Gamma_0\frac{\delta H}{\delta\psi_0^*} + i\frac{g_1}{\chi_q}\psi_0 q + i\frac{g_2}{\chi_c}\psi_0 c + \theta_\psi ,$$
$$(2.11)$$

$$\frac{\partial}{\partial t}q = \frac{K_0}{\chi_q}\nabla^2 q + \frac{L_0}{\chi_c}\nabla^2 c$$
$$-2g_1\mathrm{Im}\left[\psi_0^*\frac{\delta H}{\delta\psi_0^*}\right] + \theta_q , \quad (2.12)$$

$$\frac{\partial}{\partial t}c = \frac{\lambda_0}{\chi_c}\nabla^2 c + \frac{L_0}{\chi_q}\nabla^2 q$$
$$-2g_2\mathrm{Im}\left[\psi_0^*\frac{\delta H}{\delta\psi_0^*}\right] + \theta_c , \quad (2.13)$$

where the Gaussian-Langevin forces have the nonvanishing correlations

$$\langle\theta_\psi(x,t)\theta_\psi^*(x',t')\rangle = 4\Gamma_0\delta(x-x')\delta(t-t') ,$$
$$(2.14a)$$

$$\langle\theta_q(x,t)\theta_q(x',t')\rangle = -2K_0\nabla^2\delta(x-x')\delta(t-t') ,$$
$$(2.14b)$$

$$\langle\theta_c(x,t)\theta_c(x',t')\rangle = -2\lambda_0\nabla^2\delta(x-x')\delta(t-t') ,$$
$$(2.14c)$$

$$\langle\theta_q(x,t)\theta_c(x',t')\rangle = -2L_0\nabla^2\delta(x-x')\delta(t-t') .$$
$$(2.14d)$$

The coupling constants g_1 and g_2 of the reversible terms can be identified by comparison with the hydrodynamic equations for the entropy and concentration as given in Eqs. (24.65) of Khalatnikov.[28] With the use of Eqs. (2.6) and (2.7), and expressing the superfluid velocity as $\vec{v}_s = (\hbar/m_4)\vec\nabla\varphi$ these equations become

$$\frac{\partial q}{\partial t} = \frac{\hbar\rho_s}{k_B m_4}\left[\sigma - c\left[\frac{\partial\sigma}{\partial c}\right]_{P,T}\right]\nabla^2\varphi , \quad (2.15)$$

$$\frac{\partial c}{\partial t} = \frac{\hbar\rho_s c}{m_4\rho}\nabla^2\varphi , \quad (2.16)$$

where ρ_s is the superfluid density and $\varphi(x,t)$ is the phase of the complex order parameter below T_λ. The quantities σ, c, and ρ on the right-hand side (rhs) of Eqs. (2.15) and (2.16) represent the equilibrium values defined above. The terms in Eqs. (2.12) and (2.13) which correspond to Eqs. (2.15) and (2.16) are obtained by substituting

$$\psi_0 = |\psi_0|\exp[i\varphi(x,t)]$$

into

$$\mathrm{Im}\left[\psi_0^*\frac{\delta H}{\delta\psi_0^*}\right] = -\frac{1}{2}|\psi_0|^2\nabla^2\varphi = -\frac{\hbar^2\rho_s}{2m_4^2 k_B T}\nabla^2\varphi .$$
$$(2.17)$$

Here we have used the known relation[60] between $|\psi_0|$ and ρ_s. Comparing Eqs. (2.12), (2.13), and (2.17) with Eqs. (2.15) and (2.16), we find

$$g_1 = \frac{Tm_4}{\hbar}\left[\sigma - c\left[\frac{\partial\sigma}{\partial c}\right]_{P,T}\right] , \quad (2.18)$$

$$g_2 = \frac{k_B Tcm_4}{\hbar\rho} . \quad (2.19)$$

As $c \to 0$, g_1 becomes identical with the coupling constant $g_0 = Tm_4\sigma/\hbar$ of model E for pure ^{4}He.[60] Equations (2.17)–(2.19) correct the corresponding equations of Siggia and Nelson[43] and of Siggia.[44] With the use of the identifications (2.18) and (2.19), and eliminating δc in favor of $\delta\Delta$ via

$$\delta\Delta = \left[\frac{\partial\Delta}{\partial c}\right]_{P,T}\delta c - \left[\frac{\partial\sigma}{\partial c}\right]_{P,T}\delta T , \quad (2.20)$$

one can verify that also the reversible parts of Eq.

(2.11) agree with the corresponding hydrodynamic equation[28]

$$\frac{\partial}{\partial t}\vec{v}_s = c\,\vec{\nabla}\Delta + \sigma\vec{\nabla}T \;, \tag{2.21}$$

where, in Khalatnikov's notation, $\Delta \equiv Z/\rho$. We note that the reversible part of Eq. (2.11) is already determined by those of Eqs. (2.12) and (2.13) due to the requirement of consistency with the equilibrium distribution $\exp(-H)$.

In order to identify K_0, λ_0, and L_0 we follow Siggia and Nelson[43] by rewriting the hydrodynamic equations for binary mixtures[65] in terms of $q(x,t)$, $c(x,t)$, $\mathcal{X}_q$, and $\mathcal{X}_c$:

$$\frac{\partial q}{\partial t} = \frac{\kappa}{k_B \mathcal{X}_q}\nabla^2 q + \frac{k_T D}{\mathcal{X}_c}\left[\nabla^2 c + \frac{k_T}{\mathcal{X}_q}\nabla^2 q\right]\;, \tag{2.22}$$

$$\frac{\partial c}{\partial t} = D\left[\nabla^2 c + \frac{k_T}{\mathcal{X}_q}\nabla^2 q\right]\;. \tag{2.23}$$

Here D is the ^{3}He mass diffusion coefficient and k_T is the thermal diffusion ratio. κ represents the thermal conductivity in the absence of ^{3}He mass flow in which case Eq. (2.22) reduces to

$$\frac{\partial q}{\partial t} = \frac{\kappa}{\rho C_{P,c}}\nabla^2 q\;. \tag{2.24}$$

Comparison with Eqs. (2.12) and (2.13), and neglecting the reversible terms, yields the identification

$$D = \lambda_0/\mathcal{X}_c = \rho\lambda_0\left[\frac{\partial\Delta}{\partial c}\right]_{P,T}\!\!\Big/k_B T\;, \tag{2.25}$$

$$k_T = L_0/D\;, \tag{2.26}$$

$$\kappa/k_B = K_0 - L_0^2/\lambda_0\;, \tag{2.27}$$

in agreement with Siggia and Nelson (apart from factors k_B and $k_B T$). In summary, the model has four dynamic nonuniversal parameters Γ_0, λ_0, L_0, and K_0 to be determined by comparison with dynamic experiments, whereas τ_0, u_0, $\mathcal{X}_q$, $\mathcal{X}_c$, g_1, and g_2 are determined by static quantities.

B. Orthogonal transformation

In order to discuss the structure of the equations of motion it is convenient to introduce two-component vectors

$$\vec{Q}(x,t) = \begin{bmatrix} q(x,t)\,\mathcal{X}_q^{-1/2} \\ c(x,t)\,\mathcal{X}_c^{-1/2} \end{bmatrix}\;, \tag{2.28}$$

$$\vec{G} = \begin{bmatrix} g_1\,\mathcal{X}_q^{-1/2} \\ g_2\,\mathcal{X}_c^{-1/2} \end{bmatrix}\;, \tag{2.29}$$

$$\vec{\theta} = \begin{bmatrix} \theta_q\,\mathcal{X}_q^{-1/2} \\ \theta_c\,\mathcal{X}_c^{-1/2} \end{bmatrix}\;, \tag{2.30}$$

and the matrix

$$\underline{\Lambda}_0 = \begin{bmatrix} K_0\mathcal{X}_q^{-1} & L_0(\mathcal{X}_q\mathcal{X}_c)^{-1/2} \\ L_0(\mathcal{X}_q\mathcal{X}_c)^{-1/2} & \lambda_0\mathcal{X}_c^{-1} \end{bmatrix}\;. \tag{2.31}$$

Then, Eqs. (2.11)–(2.13) can be rewritten in the more compact form

$$\frac{\partial}{\partial t}\psi_0 = -2\Gamma_0\frac{\delta H}{\delta\psi_0^*} + i\psi_0\vec{G}\cdot\vec{Q} + \theta_\psi\;, \tag{2.32}$$

$$\frac{\partial}{\partial t}\vec{Q} = \underline{\Lambda}_0\nabla^2\vec{Q} - 2\vec{G}\,\mathrm{Im}\left[\psi_0^*\frac{\delta H}{\delta\psi_0^*}\right] + \vec{\theta}\;. \tag{2.33}$$

Now the following invariance property is easily verified. Consider an orthogonal 2×2 matrix $\underline{R}_0$ with $(\underline{R}_0)^{-1} = (\underline{R}_0)^T$, for example,

$$\underline{R}_0 = \begin{bmatrix} \cos\varphi_0 & \sin\varphi_0 \\ -\sin\varphi_0 & \cos\varphi_0 \end{bmatrix} \tag{2.34}$$

with arbitrary φ_0, and introduce the transformed quantities

$$\vec{Q}' = \underline{R}_0\vec{Q},\,\vec{G}' = \underline{R}_0\vec{G},\,\vec{\theta}' = \underline{R}_0\,\vec{\theta},\,\underline{\Lambda}_0' = \underline{R}_0\underline{\Lambda}_0\underline{R}_0^T\;. \tag{2.35}$$

Rewriting Eqs. (2.32) and (2.33) in terms of the transformed quantities simply amounts to replacing $\vec{Q},\vec{G},\vec{\theta},\underline{\Lambda}_0$ by $\vec{Q}',\vec{G}',\vec{\theta}',\underline{\Lambda}_0'$ without changing the structure of the equations of motion, because the scalar product $\vec{G}\cdot\vec{Q}$ in Eq. (2.32) is invariant under the transformation $\underline{R}_0$, $\vec{G}\cdot\vec{Q} = \vec{G}'\cdot\vec{Q}'$. This invariance property will be exploited in deriving exact relations between Z factors in the renormalized theory in Sec. VI A.

We note that the invariance of the scalar products $\vec{Q}\cdot\vec{Q}$, $\vec{G}\cdot\vec{G}$, and $\vec{G}\cdot\vec{Q}$ implies the invariance of the following static quantities under the transformation $\underline{R}_0$: namely, the Hamiltonian H, Eq. (2.10),

$$H = H_\Psi + \tfrac{1}{2}\int d^dx\,\vec{Q}^2 = H_\Psi + \tfrac{1}{2}\int d^dx\,\vec{Q}'^2\;, \tag{2.36}$$

the second-sound velocity c_2 below T_λ,

$$c_2^2 = |\Psi_0|^2\vec{G}^2 = |\Psi_0|^2\vec{G}'^2 \tag{2.37}$$

[compare Eq. (24.74) of Ref. 28], and the rhs of the hydrodynamic equation (2.21),

$$\frac{\partial}{\partial t}\vec{v}_s = c\,\vec{\nabla}\Delta + \sigma\vec{\nabla}T = \frac{\hbar}{m_4}\vec{\nabla}(\vec{G}\cdot\vec{Q}) = \frac{\hbar}{m_4}\vec{\nabla}(\vec{G}'\cdot\vec{Q}')$$

$$= \vec{\nabla}\tilde{\mu}_4/m_4\;, \tag{2.38}$$

where $\tilde{\mu}_4$ is the chemical potential defined in Sec. II A above. The last part of Eq. (2.38) follows from Khalatnikov's[28] Eq. (24.30). The variables $\vec{Q}$ or $\vec{Q}'$ are seen to be most convenient as opposed to the vector $(\delta\sigma, \delta c)$, for example. In terms of the latter variables Eqs. (2.32) and (2.36)—(2.38) would involve an off-diagonal matrix of susceptibilities, which in the present formulation has been reduced to a unity matrix.

Among the class of variables $\vec{Q}'$ generated by the orthogonal transformation $\underline{R}_0$ there is one particular $\vec{Q}'$ corresponding to a diagonal matrix of kinetic coefficients,

$$\underline{\Lambda}'_0 = \underline{R}_0 \underline{\Lambda}_0 \underline{R}_0^T = \begin{bmatrix} K'_0 & 0 \\ 0 & \lambda'_0 \end{bmatrix} . \qquad (2.39)$$

The corresponding transformation is a rotation $\underline{R}_0$, Eq. (2.34), with matrix elements

$$\cos\varphi_0 = \left[\frac{1}{2\Omega_0}(K_0\chi_q^{-1} - \lambda_0\chi_c^{-1} + \Omega_0) \right]^{1/2} , \qquad (2.40a)$$

$$\sin\varphi_0 = \left[\frac{1}{2\Omega_0}(\lambda_0\chi_c^{-1} - K_0\chi_q^{-1} + \Omega_0) \right]^{1/2} , \qquad (2.40b)$$

where

$$\Omega_0 = [(K_0\chi_q^{-1} - \lambda_0\chi_c^{-1})^2 + 4L_0^2\chi_q^{-1}\chi_c^{-1}]^{1/2} . \qquad (2.41)$$

The transformed kinetic coefficients are given by

$$K'_0 = \tfrac{1}{2}(K_0\chi_q^{-1} + \lambda_0\chi_c^{-1} + \Omega_0) , \qquad (2.42a)$$

$$\lambda'_0 = \tfrac{1}{2}(K_0\chi_q^{-1} + \lambda_0\chi_c^{-1} - \Omega_0) . \qquad (2.42b)$$

Since $\underline{\Lambda}'_0$ is diagonal, the components Q'_1 and Q'_2 of

$$\vec{Q}' = \begin{bmatrix} Q'_1 \\ Q'_2 \end{bmatrix} \qquad (2.43)$$

are coupled to one another only through the reversible couplings

$$\vec{G}' = \begin{bmatrix} G'_1 \\ G'_2 \end{bmatrix} . \qquad (2.44)$$

We shall be interested in the situation where the dynamics of ψ_0 and Q'_1 are decoupled from Q'_2. This situation arises when the model parameters are such that the coupling

$$G'_2 = -g_1\chi_q^{-1/2}\sin\varphi_0 + g_2\chi_c^{-1/2}\cos\varphi_0 \qquad (2.45)$$

vanishes. This is trivially the case in the absence of ³He where $g_2 = 0$ and $L_0 = 0$, which implies $\sin\varphi_0 = 0$. A nontrivial case, however, is

$$\frac{g_1}{K_0^{1/2}} = \frac{g_2}{\lambda_0^{1/2}} , \qquad (2.46)$$

$$\frac{L_0^2}{K_0\lambda_0} = 1 . \qquad (2.47)$$

Equation (2.47) implies

$$\lambda'_0 = 0 , \qquad (2.48)$$

$$K'_0 = K_0\chi_q^{-1} + \lambda_0\chi_c^{-1} , \qquad (2.49)$$

and Eq. (2.46) yields

$$G'_2 = 0 , \qquad (2.50)$$

$$G'_1 = \left[\frac{K'_0}{K_0} \right]^{1/2} g_1 = \left[\frac{K'_0}{\lambda_0} \right]^{1/2} g_2 . \qquad (2.51)$$

Then ψ_0 and

$$Q'_1 = \left[\frac{K_0}{K'_0} \right]^{1/2} \frac{q}{\chi_q} + \left[\frac{\lambda_0}{K'_0} \right]^{1/2} \frac{c}{\chi_c} \qquad (2.52)$$

satisfy the simplified equations of motion

$$\frac{\partial}{\partial t}\psi_0 = -2\Gamma_0\frac{\delta H}{\delta\psi_0^*} + i\psi_0 G'_1 Q'_1 + \theta_\psi , \qquad (2.53)$$

$$\frac{\partial}{\partial t}Q'_1 = K'_0\nabla^2 Q'_1 - 2G'_1\,\mathrm{Im}\left[\psi_0\frac{\delta H}{\delta\psi_0^*} \right] + \theta'_1 . \qquad (2.54)$$

They are identical in structure with the equations of motion of model E for pure ⁴He,[60] with a ratio of relaxation rates

$$w'_0 \equiv \frac{\Gamma_0}{K'_0} = \left[\frac{K_0}{\Gamma_0\chi_q} + \frac{\lambda_0}{\Gamma_0\chi_c} \right]^{-1} \qquad (2.55)$$

and with a dimensionless coupling

$$f'_0 = \frac{G'^2_1 K_d\mu^{-\epsilon}}{\Gamma_0 K'_0} = \frac{g_1^2 K_d\mu^{-\epsilon}}{\Gamma_0 K_0} = \frac{g_2^2 K_d\mu^{-\epsilon}}{\Gamma_0\lambda_0} , \qquad (2.56)$$

where μ denotes a reference wave number, and

$$K_d^{-1} = 2^{d-1}\pi^{d/2}\Gamma(d/2) .$$

The parameters w'_0, f'_0 correspond to the usual model-E parameters w_0, f_0. We shall see in Sec. V that the renormalized parameters are driven to fixed-point values which satisfy conditions equivalent to Eqs. (2.46)—(2.51). This will imply a

universal connection between the asymptotic critical dynamics of pure ^{4}He and of ^{3}He-^{4}He mixtures.

C. General procedure

We shall be interested mainly in the critical temperature dependence of the transport coefficients D, k_T, and κ given in Eqs. (2.25)–(2.27). Our procedure will be to calculate a correlation function that contains these transport coefficients, for example

$$C_{qq}(k,\omega) = \int d^dx \int dt \langle q(x,t)q(0,0)\rangle$$
$$\times \exp[-i(kx - \omega t)] .$$

$$(2.57)$$

A convenient way is to express C_{qq} in terms of vertex functions and to compute the critical behavior of the latter by means of the field-theoretic renormalization-group approach.[47,59] In order to obtain conclusive results a calculation of the renormalization-group flow equations beyond one-loop order is necessary.

Instead of the Langevin equations (2.11)–(2.13) we shall use the corresponding dynamic functional[68,69] $J(q,\tilde{q},c,\tilde{c},\psi_0,\tilde{\psi}_0,\psi_0^*,\tilde{\psi}_0^*)$, where $\tilde{q}(x,t)$, $\tilde{c}(x,t)$, $\tilde{\psi}_0(x,t)$, and $\tilde{\psi}_0^*(x,t)$ denote response fields[68-70] conjugate to q, c, ψ_0, and ψ_0^*, respectively. In terms of the notation employed in Eqs. (2.28)–(2.33) this functional reads

$$J = \int dt \int d^dx(J_\psi + J_Q + J^{(1)}) ,$$

$$(2.58)$$

$$J_\psi = \frac{1}{2}\Gamma_0\tilde{\psi}_0\tilde{\psi}_0^* - \frac{1}{2}\tilde{\psi}_0[\partial_t + \Gamma_0(\tau_0 - \nabla^2)]\psi_0^*$$
$$- 2\Gamma_0 u_0 \tilde{\psi}_0^*\psi_0^2\psi_0^* + \text{c.c.} ,$$

$$(2.59)$$

$$J_Q = -\vec{\tilde{Q}}\cdot\underline{\Lambda}_0\nabla^2\vec{\tilde{Q}} - \vec{\tilde{Q}}\cdot(\partial t - \underline{\Lambda}_0\nabla^2)\vec{Q} ,$$

$$(2.60)$$

$$J^{(1)} = \frac{i}{2}\vec{G}\cdot\vec{\tilde{Q}}(\tilde{\psi}_0\psi_0^* + \tilde{\psi}_0^*\psi_0)$$
$$+ \frac{i}{2}\vec{G}\cdot\vec{\tilde{Q}}(\psi_0^*\nabla^2\psi_0 - \psi_0\nabla^2\psi_0^*) .$$

$$(2.61)$$

Here we have used the vector of response fields

$$\vec{\tilde{Q}} = \begin{vmatrix} \tilde{q}\chi_q^{1/2} \\ \tilde{c}\chi_c^{1/2} \end{vmatrix}$$

$$(2.62)$$

conjugate to $\vec{Q}$. One-particle irreducible vertex functions can now be defined in the usual way via the appropriate generating functional constructed from J and can be computed from the corresponding one-particle irreducible diagrams.

The correlation function C_{qq} can be expressed in terms of two-point vertex functions $\Gamma_{\alpha\beta}(k,\omega)$; the

indices α and β denote one of the fields $q,c,\tilde{q},\tilde{c}$ and indicate the type of (truncated) external legs of the diagrams which contribute to the respective vertex function. The connection between C_{qq} and $\Gamma_{\alpha\beta}$ follows from the general relation

$$C_{\alpha\beta} = (\underline{\Gamma}^{-1})_{\alpha\beta}$$

$$(2.63)$$

between the matrices $\underline{C}$ and $\underline{\Gamma}$ of two-point correlation (or response) functions and of two-point vertex functions. Inverting $\underline{\Gamma}$, we thus obtain

$$C_{qq}(k,\omega) = -\frac{N_{qq}(k,\omega)}{|M(k,\omega)|^2} ,$$

$$(2.64)$$

with

$$N_{qq} = \Gamma_{\tilde{q}\tilde{q}}|\Gamma_{c\tilde{c}}|^2 + \Gamma_{\tilde{c}\tilde{c}}|\Gamma_{c\tilde{q}}|^2 - 2\,\text{Re}(\Gamma_{\tilde{c}\tilde{q}}\Gamma_{c\tilde{c}}\Gamma_{\tilde{q}c})$$

$$(2.65)$$

and

$$M = \Gamma_{q\tilde{q}}\Gamma_{c\tilde{c}} - \Gamma_{q\tilde{c}}\Gamma_{c\tilde{q}} ,$$

$$(2.66)$$

which is analogous to Eqs. (1)–(3) of Ref. 71. In Sec. VIII we shall also need the correlation functions $C_{qc}(k,\omega)$ and $C_{cc}(k,\omega)$ which enter the light scattering spectrum. From Eq. (2.63) we find

$$C_{qc}(k,\omega) = -\frac{N_{qc}(k,\omega)}{|M(k,\omega)|^2} ,$$

$$(2.67)$$

$$C_{cc}(k,\omega) = -\frac{N_{cc}(k,\omega)}{|M(k,\omega)|^2} ,$$

$$(2.68)$$

with

$$N_{qc} = \Gamma_{q\tilde{q}}(\Gamma_{\tilde{q}c}\Gamma_{\tilde{c}c} - \Gamma_{\tilde{q}c}\Gamma_{\tilde{c}c})$$
$$+ \Gamma_{q\tilde{c}}(\Gamma_{\tilde{q}c}\Gamma_{\tilde{c}q} - \Gamma_{\tilde{q}\tilde{q}}\Gamma_{\tilde{c}c})$$

$$(2.69)$$

and

$$N_{cc} = \Gamma_{\tilde{c}\tilde{c}}|\Gamma_{q\tilde{q}}|^2 + \Gamma_{\tilde{q}\tilde{q}}|\Gamma_{q\tilde{c}}|^2$$
$$- 2\,\text{Re}(\Gamma_{\tilde{q}\tilde{c}}\Gamma_{q\tilde{q}}\Gamma_{\tilde{c}q}) .$$

$$(2.70)$$

The correlation function $C_{cq}(k,\omega)$ is obtained from Eqs. (2.67) and (2.69) by exchanging q and c.

III. RENORMALIZATION

We shall study the critical behavior of the model by means of the field-theoretic renormalization-group approach using the dimensional regularization and minimal subtraction procedure.[47,58,72] The necessary renormalizations are

$$\psi = Z_\psi^{-1/2}\psi_0, \quad \psi^* = Z_\psi^{-1/2}\psi_0^* ,$$

$$(3.1)$$

$$\tilde{\psi} = \tilde{Z}_\psi^{-1/2}\tilde{\psi}_0, \quad \tilde{\psi}^* = \tilde{Z}_\psi^{-1/2}\tilde{\psi}_0^* ,$$

$$(3.2)$$

$$\tau = Z_\tau^{-1}\tau_0 , \tag{3.3}$$

$$u = \mu^{-\epsilon}Z_u^{-1}Z_\psi^2 K_d u_0 , \tag{3.4}$$

$$\Gamma = Z_\Gamma^{-1}\Gamma_0 , \tag{3.5}$$

$$K = Z_K^{-1}K_0\chi_q^{-1} , \tag{3.6}$$

$$\lambda = Z_\lambda^{-1}\lambda_0\chi_c^{-1} , \tag{3.7}$$

$$L = Z_L^{-1}L_0\chi_q^{-1/2}\chi_c^{-1/2} . \tag{3.8}$$

The fields q and c need not be renormalized since their static fluctuations are Gaussian. Also the response fields $\widetilde{q}$ and $\widetilde{c}$ remain unrenormalized as follows from the conservation properties of the fields q and c. Furthermore, a Ward identity[45,47,59(b),60] implies that the mode coupling constants g_1 and g_2 are not renormalized. The nonuniversal reference wave number μ will be specified in Sec. VII.

Substituting Eqs. (3.1)—(3.8) into Eqs. (2.58)—(2.61) yields the dynamic functional in renormalized form:

$$J = \int dt \int d^dx (J_\psi + J_Q + J^{(1)}) , \tag{3.9}$$

$$J_\psi = \tfrac{1}{2}Z_\Gamma \widetilde{Z}_\psi \Gamma \widetilde{\psi}\widetilde{\psi}^*$$

$$-\tfrac{1}{2}(Z_\psi\widetilde{Z}_\psi)^{1/2}\widetilde{\psi}[\partial_t + Z_\Gamma\Gamma(Z_\tau\tau - \nabla^2)]\psi^*$$

$$-2Z_\Gamma Z_u(\widetilde{Z}_\psi/Z_\psi)^{1/2}\Gamma u\mu^{-\epsilon}K_d^{-1}\widetilde{\psi}^*\psi^2\psi^* + \text{c.c.} , \tag{3.10}$$

$$J_Q = -\widetilde{\vec{Q}}\cdot\underline{\Lambda}\nabla^2\widetilde{\vec{Q}} - \widetilde{\vec{Q}}\cdot(\partial_t - \underline{\Lambda}\nabla^2)\vec{Q} , \tag{3.11}$$

$$J^{(1)} = \frac{i}{2}(Z_\psi\widetilde{Z}_\psi)^{1/2}\vec{G}\cdot\vec{Q}(\widetilde{\psi}\psi^* + \widetilde{\psi}^*\psi)$$

$$+\frac{i}{2}Z_\psi\vec{G}\cdot\widetilde{\vec{Q}}(\psi^*\nabla^2\psi - \psi\nabla^2\psi^*) , \tag{3.12}$$

with

$$\underline{\Lambda} = \begin{bmatrix} Z_K K & Z_L L \\ Z_L L & Z_\lambda \lambda \end{bmatrix} . \tag{3.13}$$

We shall employ the dimensionless couplings

$$F_1 = g_1 \left[\frac{K_d}{\mu^\epsilon K\Gamma\chi_q}\right]^{1/2} , \quad F_2 = g_2 \left[\frac{K_d}{\mu^\epsilon \Gamma\lambda\chi_c}\right]^{1/2} , \tag{3.14}$$

and the dimensionless ratios

$$w_1 = \frac{\Gamma}{K}, \quad w_2 = \frac{\Gamma}{\lambda}, \quad w_3 = \frac{L}{(K\lambda)^{1/2}} . \tag{3.15}$$

The renormalized two-point vertex functions $\Gamma_{\alpha\beta}$ satisfy the renormalization-group equation

$$\left[\mu\partial_\mu + \zeta_\lambda\lambda\partial_\lambda + \zeta_\tau\tau\partial_\tau + \sum_i \beta_i\partial_i + \tfrac{1}{2}\zeta_\alpha + \tfrac{1}{2}\zeta_\beta\right]\Gamma_{\alpha\beta}$$

$$= 0 , \tag{3.16}$$

where $i = w_1, w_2, w_3, F_1, F_2$, and u and $\alpha,\beta = q,\widetilde{q},c,\widetilde{c},\psi,\widetilde{\psi},\psi^*,\widetilde{\psi}^*$. The β functions are defined as

$$\beta_i = (\mu\partial_\mu i)_0 , \tag{3.17}$$

with $i = w_1, w_2, w_3, F_1, F_2$, and u, where the derivative is to be taken at fixed bare parameters. The dynamic β functions have the structure

$$\beta_{w_1} = w_1(\zeta_\Gamma - \zeta_K) , \tag{3.18}$$

$$\beta_{w_2} = w_2(\zeta_\Gamma - \zeta_\lambda) , \tag{3.19}$$

$$\beta_{w_3} = w_3(\zeta_L - \tfrac{1}{2}\zeta_K - \tfrac{1}{2}\zeta_\lambda) , \tag{3.20}$$

$$\beta_{F_1} = -\frac{F_1}{2}(\epsilon + \zeta_\Gamma + \zeta_K) , \tag{3.21}$$

$$\beta_{F_2} = -\frac{F_2}{2}(\epsilon + \zeta_\Gamma + \zeta_\lambda) . \tag{3.22}$$

The ζ functions in Eqs. (3.16) and (3.18)—(3.22) are independent of the dimension $d = 4 - \epsilon$ and are defined as

$$\zeta_j = (\mu\partial_\mu \ln Z_j^{-1})_0 , \tag{3.23}$$

with $j = \Gamma, K, \lambda, L, \tau, \psi, \psi^*, \widetilde{\psi}$, and $\widetilde{\psi}^*$. Since the fields $q,c,\widetilde{q},\widetilde{c}$ are not renormalized $(Z_q = Z_c = \widetilde{Z}_q = \widetilde{Z}_c = 1)$ we have $\zeta_q = \zeta_c = \zeta_{\widetilde{q}} = \zeta_{\widetilde{c}} = 0$ for the corresponding ζ functions. From previous work[47,58,73] we know

$$\beta_u = u(-\epsilon + 40u - 960u^2) + O(u^4) , \tag{3.24}$$

$$\zeta_\tau = -16u + 160u^2 + O(u^3) , \tag{3.25}$$

$$Z_\psi = 1 - \frac{16u^2}{\epsilon} + O(u^3) , \tag{3.26}$$

$$(Z_\psi\widetilde{Z}_\psi)^{1/2} = 1 - \frac{96u^2}{\epsilon}\ln\frac{4}{3} + O(u^3) . \tag{3.27}$$

We shall calculate the remaining functions ζ_Γ, ζ_K, ζ_λ, and ζ_L up to two-loop order in Sec. VI.

Integrating the renormalization-group equation (3.16) yields for the Fourier transforms of the renormalized vertex functions

$$\Gamma_{\alpha\beta}(k,\omega;w_1,w_2,w_3,F_1,F_2,u;\tau,\lambda;\mu)$$

$$= \exp\left[\int_1^l \tfrac{1}{2}(\zeta_\alpha + \zeta_\beta)\frac{dl'}{l'}\right]$$

$$\times \Gamma_{\alpha\beta}(k,\omega;\overline{w}_1,\overline{w}_2,\overline{w}_3,\overline{F}_1,\overline{F}_2,\overline{u};\overline{\tau},\overline{\lambda};\mu l) , \tag{3.28}$$

with

$$\bar{\tau} \equiv \tau(l) = \tau \exp\left[\int_1^l \zeta_\tau \frac{dl'}{l'}\right] , \tag{3.29}$$

$$\bar{\lambda} \equiv \lambda(l) = \lambda \exp\left[\int_1^l \zeta_\lambda \frac{dl'}{l'}\right] . \tag{3.30}$$

The effective parameters $\bar{u} \equiv u(l)$, $\bar{w}_i \equiv w_i(l)$, $i = 1,2,3$, and $\bar{F}_j \equiv F_j(l)$, $j = 1,2$ are determined by the renormalization-group flow equations

$$l\frac{du(l)}{dl} = \beta_u(\bar{u}) , \tag{3.31}$$

$$l\frac{dw_i(l)}{dl} = \beta_{w_i}(\bar{w}_1, \bar{w}_2, \bar{w}_3, \bar{F}_1, \bar{F}_2, \bar{u}) , \tag{3.32}$$

$$l\frac{dF_j(l)}{dl} = \beta_{F_j}(\bar{w}_1, \bar{w}_2, \bar{w}_3, \bar{F}_1, \bar{F}_2, \bar{u}) . \tag{3.33}$$

The initial values at $l = 1$ coincide with the renormalized parameters,

$$u(1) \equiv u, \quad w_i(1) \equiv w_i, \quad F_j(1) \equiv F_j , $$
$$\tau(1) \equiv \tau, \quad \lambda(1) \equiv \lambda . \tag{3.34}$$

They are nonuniversal quantities to be determined by comparison with experiment. As $l \to 0$, the effective parameters attain their (stable) fixed-point values

$$u(0) \equiv u^*, \quad w_i(0) \equiv w_i^*, \quad F_j(0) \equiv F_j^* . \tag{3.35}$$

From Eq. (3.24) we have

$$u^* = \epsilon(1 + 3\epsilon/5)/40 + O(\epsilon^3) . \tag{3.36}$$

The dynamic fixed-point values w_i^* and F_j^* are determined by the zeros of β_{w_i} and β_{F_j}. The stability of the fixed point is governed by the transient exponents which are the eigenvalues of the 5×5 matrix

$$\left[\frac{\partial \beta_m}{\partial n}\right] , \tag{3.37}$$

with $m, n = w_1, w_2, w_3, F_1, F_2$ taken at the fixed point. We shall see that there exist only three different dynamic transient exponents at the stable fixed point.

The usual static critical exponents are obtained as

$$\nu = (2 - \zeta_\tau^*)^{-1} , \quad \eta = -\zeta_\psi^* , \tag{3.38}$$

with $\zeta_\tau^* \equiv \zeta_\tau(u^*)$ and $\zeta_\psi^* = \zeta_\psi(u^*)$. There are four

dynamic critical exponents

$$z_\psi = 2 + \zeta_\Gamma^* , \quad z_q = 2 + \zeta_K^* , $$
$$z_c = 2 + \zeta_\lambda^*, \quad z_L = 2 + \zeta_L^* , \tag{3.39}$$

where ζ_i^* denote the fixed-point values of the ζ functions.

IV. TRANSPORT COEFFICIENTS ABOVE T_λ

The main application of our nonlinear renormalization-group treatment will be a quantitative prediction of the observable critical temperature dependence of the mass diffusion coefficient D, of the thermal diffusion ratio k_T, and the thermal conductivity κ. Another transport coefficient (of primarily theoretical interest) is

$$\kappa_s = \kappa + k_T^2 D k_B / X_c , \tag{4.1}$$

which, according to Eq. (2.22), represents the thermal conductivity in the absence of a concentration gradient. In the following, we calculate these transport coefficients in terms of the effective dynamic parameters $w_i(l)$ and $F_i(l)$.

We consider the vertex functions

$$\Gamma_{q\bar{q}}(k,\omega) = -i\omega + K_0 X_q^{-1} k^2 + X_q^{-1} \Sigma_{q\bar{q}}(k,\omega) , \tag{4.2}$$

$$\Gamma_{c\bar{c}}(k,\omega) = -i\omega + \lambda_0 X_c^{-1} k^2 + X_c^{-1} \Sigma_{c\bar{c}}(k,\omega) , \tag{4.3}$$

$$\Gamma_{q\bar{c}}(k,\omega) = X_c X_q^{-1} \Gamma_{c\bar{q}}(k,\omega)$$
$$= L_0 X_q^{-1} k^2 + X_q^{-1} \Sigma_{q\bar{c}}(k,\omega) , \tag{4.4}$$

which enter the denominator of the correlation function C_{qq}, Eq. (2.64). By inspection of the corresponding diagrams we see that the perturbation parts $\Sigma_{\alpha\bar{\beta}}$ differ only by their two external vertices, according to the different external (truncated) legs, but their internal structure is identical in all orders of perturbation theory. Therefore, the different vertex functions have the diagrammatic contributions

$$\Sigma_{q\bar{q}}(k,\omega) = g_1^2 I(k,\omega) , \tag{4.5}$$

$$\Sigma_{c\bar{c}}(k,\omega) = g_2^2 I(k,\omega) , \tag{4.6}$$

$$\Sigma_{q\bar{c}}(k,\omega) = g_1 g_2 I(k,\omega) , \tag{4.7}$$

which are determined by a single function $I(k,\omega)$. In one-loop order it reads

$$I^{(1)}(k,\omega) = \int \frac{d^d p}{(2\pi)^d} \frac{4(\vec{p} \cdot \vec{k})^2}{[(\vec{p} - \frac{1}{2}\vec{k})^2 + \tau_0][(\vec{p} + \frac{1}{2}\vec{k})^2 + \tau_0][2\Gamma_0(p^2 + \frac{1}{4}k^2 + \tau_0) - i\omega]} , \tag{4.8}$$

which is the analytic expression for the standard diagram shown in Fig. 2 of Ref. 49. The one-loop expressions for the vertex functions entering the numerator $N(k,\omega)$, Eq. (2.65), of C_{qq} are obtained from Eqs. (4.2)–(4.8) as

$$\Gamma_{\tilde{q}\tilde{q}}(k,\omega) = -2\mathcal{X}_q \, \mathrm{Re}[\Gamma_{q\tilde{q}}(k,\omega)] , \qquad (4.9)$$

$$\Gamma_{\tilde{c}\tilde{c}}(k,\omega) = -2\mathcal{X}_c \, \mathrm{Re}[\Gamma_{c\tilde{c}}(k,\omega)] , \qquad (4.10)$$

$$\Gamma_{\tilde{q}\tilde{c}}(k,\omega) = -2\mathcal{X}_q \, \mathrm{Re}[\Gamma_{q\tilde{c}}(k,\omega)]$$
$$= -2\mathcal{X}_c \, \mathrm{Re}[\Gamma_{c\tilde{q}}(k,\omega)] . \qquad (4.11)$$

In the hydrodynamic region we need to consider only

$$I^{(1)}(k,0) = \frac{2}{\Gamma_0} \int \frac{d^d p}{(2\pi)^d} \frac{(\vec{p}\cdot\vec{k})^2}{(p^2+\tau_0)^3} + O(k^4) \qquad (4.12)$$

$$= \frac{K_d}{2\Gamma_0 \epsilon} k^2 \left[1 - \frac{\epsilon}{2} - \frac{\epsilon}{2}\ln\tau_0 + O(\epsilon^2) \right]$$
$$+ O(k^4) . \qquad (4.13)$$

Expressing the bare parameters in terms of the renormalized ones according to Eqs. (3.3)–(3.8), (3.14), and (3.15), and requiring the Z factors to cancel the pole terms $\sim\epsilon^{-1}$ yields

$$Z_K = 1 - F_1^2/2\epsilon , \qquad (4.14)$$

$$Z_\lambda = 1 - F_2^2/2\epsilon , \qquad (4.15)$$

$$Z_L = 1 - F_1 F_2/2w_3\epsilon . \qquad (4.16)$$

The remaining finite parts of the vertex functions are

$$\Gamma_{q\tilde{q}} = -i\omega + Kk^2 \left[1 - \tfrac{1}{4}F_1^2 \left[1 + \ln\frac{\tau}{\mu^2} \right] \right] , \qquad (4.17)$$

$$\Gamma_{c\tilde{c}} = -i\omega + \lambda k^2 \left[1 - \tfrac{1}{4}F_2^2 \left[1 + \ln\frac{\tau}{\mu^2} \right] \right] , \qquad (4.18)$$

$$\Gamma_{q\tilde{c}} = \left[\frac{\mathcal{X}_c}{\mathcal{X}_q} \right]^{1/2}$$
$$\times Lk^2 \left[1 - \tfrac{1}{4}F_1 F_2 w_3^{-1} \left[1 + \ln\frac{\tau}{\mu^2} \right] \right] . \qquad (4.19)$$

Now we employ Eq. (3.28) in order to express the

vertex functions in terms of the effective parameters $F_i(l)$, $w_i(l)$, and $\tau(l)$. As usual, we choose the flow parameter l such that the logarithmic terms in the perturbation parts drop out,[57,74]

$$\frac{\tau(l)}{\mu^2 l^2} = 1 . \qquad (4.20)$$

This choice connects l with the relative temperature

$$t_\Delta = \frac{T - T_\lambda(P,\Delta)}{T_\lambda(P,\Delta)} \qquad (4.21)$$

according to[53]

$$l\mu = \xi_0^{-1}t_\Delta^\nu = \xi_\Delta^{-1} , \qquad (4.22)$$

with ξ_0 being the amplitude of the correlation length ξ_Δ above T_λ. In Eq. (4.22) we have neglected static corrections to scaling. The resulting vertex functions can be written as

$$\Gamma_{q\tilde{q}}(k,\omega) = -i\omega + K(l)k^2[1 - \tfrac{1}{4}F_1(l)^2] , \qquad (4.23)$$

$$\Gamma_{c\tilde{c}}(k,\omega) = -i\omega + \lambda(l)k^2[1 - \tfrac{1}{4}F_2(l)^2] , \qquad (4.24)$$

$$\Gamma_{q\tilde{c}}(k,\omega) = (\mathcal{X}_c/\mathcal{X}_q)^{1/2}L(l)$$
$$\times k^2[1 - \tfrac{1}{4}F_1(l)F_2(l)w_3(l)^{-1}] , \qquad (4.25)$$

where

$$K(l) = K \exp\int_1^l \zeta_K \frac{dl'}{l'}$$
$$= g_1\xi_\Delta^{\epsilon/2}K_d^{1/2}[w_1(l)F_1(l)^2\mathcal{X}_q]^{-1/2} , \qquad (4.26)$$

$$\lambda(l) = \lambda \exp\int_1^l \zeta_\lambda \frac{dl'}{l'}$$
$$= g_2\xi_\Delta^{\epsilon/2}K_d^{1/2}[w_2(l)F_2(l)^2\mathcal{X}_c]^{-1/2} , \qquad (4.27)$$

$$L(l) = w_3(l)K(l)^{1/2}\lambda(l)^{1/2} . \qquad (4.28)$$

The rhs of Eqs. (4.26) and (4.27) follow from the exact relations

$$\zeta_K = -\tfrac{1}{2}(\epsilon + 2\beta_{F_1}/F_1 + \beta_{w_1}/w_1) , \qquad (4.29)$$

$$\zeta_\lambda = -\tfrac{1}{2}(\epsilon + 2\beta_{F_2}/F_2 + \beta_{w_2}/w_2) . \qquad (4.30)$$

The hydrodynamic form of the vertex functions, Eqs. (4.23)–(4.25), and the identification of the bare model parameters according to Eqs. (2.25)–(2.27), suggest the following identification of the temperature-dependent transport coefficients D, k_T, and κ_s:

$$D = \frac{\partial}{\partial k^2}\Gamma_{c\tilde{c}}(k,0)\bigg|_{k=0} = \lambda(l)[1 - \tfrac{1}{4}F_2(l)^2] , \qquad (4.31)$$

$$k_T D = X_q \frac{\partial}{\partial k^2} \Gamma_{q\bar{c}}(k,0) \bigg|_{k=0}$$

$$= (X_q X_c)^{1/2} L(l)[1 - \tfrac{1}{4} F_1(l) F_2(l) w_3(l)^{-1}] , \tag{4.32}$$

$$\kappa_s = k_B X_q \frac{\partial}{\partial k^2} \Gamma_{q\bar{q}}(k,0) \bigg|_{k=0}$$

$$= k_B X_q K(l)[1 - \tfrac{1}{4} F_1(l)^2] . \tag{4.33}$$

In order to verify consistency with general hydrodynamics[37] we substitute Eqs. (4.9)—(4.11) and (4.23)—(4.25) into the expression for $C_{qq}(k,\omega)$ given in Eqs. (2.63)—(2.65). Using Eqs. (4.31)—(4.33) we obtain

$$C_{qq}(k,\omega) = 2k^2 X_q$$

$$\times \frac{D_s \omega^2 + D_T D^2 k^4}{|-\omega^2 - (D+D_s)i\omega k^2 + DD_T k^4|^2} , \tag{4.34}$$

with the thermal diffusivities

$$D_T = \frac{\kappa}{k_B X_q} , \quad D_s = \frac{\kappa_s}{k_B X_q} . \tag{4.35}$$

This can be rewritten in the hydrodynamic form

$$C_{qq}(k,\omega) = 2k^2 X_q \frac{D_s \omega^2 + \Gamma_0 \Gamma_2 D}{(\omega^2 + \Gamma_0^2)(\omega^2 + \Gamma_2^2)} , \tag{4.36}$$

with the linewidths

$$\Gamma_{0,2} = \frac{k^2}{2} \{D + D_s \pm [(D+D_s)^2 - 4DD_T]^{1/2}\} . \tag{4.37}$$

Equation (4.37) agrees with Eq. (15) of Griffin.[37]

From Eqs. (4.5)—(4.7), we see that there are identical higher-order corrections to the one-loop expressions given in Eqs. (4.31)—(4.33). Thus we have the general structure

$$D = \lambda(l)\{1 - \tfrac{1}{4} F_2(l)^2[1 + P(l)]\} , \tag{4.38}$$

$$k_T D = (X_q X_c)^{1/2} L(l)$$

$$\times \{1 - \tfrac{1}{4} F_1(l) F_2(l) w_3(l)^{-1}[1 + P(l)]\} , \tag{4.39}$$

$$\kappa_s = k_B X_q K(l)\{1 - \tfrac{1}{4} F_1(l)^2[1 + P(l)]\} , \tag{4.40}$$

where

$$P(l) = P[w_1(l), w_2(l), w_3(l), F_1(l), F_2(l)] \tag{4.41}$$

is determined by contributions of order two loops and higher. Equations (4.38)—(4.40) together with Eqs. (4.1) and (4.26)—(4.28) provide the connection of our theory with the observable transport coefficients.

So far, within the present model, the parameters X_q, X_c, g_1, and g_2 represent temperature-independent background values. On the other hand, if the static couplings $\sim q |\psi_0|^2$ and $\sim c |\psi_0|^2$ are included in the Hamiltonian, the susceptibilities X_q and X_c develop a dependence on the flow parameter l corresponding to a critical temperature dependence of the specific heat and of the mass susceptibility. This holds true also for the susceptibility $(\partial\sigma/\partial c)_{P,T}$, which causes a nontrivial temperature dependence of g_1, Eq. (2.18), as emphasized by Ahlers.[75] We shall account for these nonnegligible static effects by considering X_q, X_c, and g_1 in our final expressions as experimentally determined, temperature-dependent quantities. This is in the same spirit as for the susceptibility X in the previous model-E analysis of the superfluid transition in pure ${}^4\mathrm{He}$.[51–54,60]

V. EXACT RESULTS

Since g_1 and g_2 are not renormalized there are only four dynamic ζ functions determining the five β functions, Eqs. (3.18)—(3.22). Consequently, there exists a general relation between the β functions. The relation reads

$$\frac{2}{F_1}\beta_{F_1} - \frac{2}{F_2}\beta_{F_2} = \frac{1}{w_1}\beta_{w_1} - \frac{1}{w_2}\beta_{w_2} . \tag{5.1}$$

With the use of the flow equations (3.32) and (3.33) one obtains

$$l\frac{d}{dl}\ln\frac{F_1(l)^2 w_2(l)}{F_2(l)^2 w_1(l)} = 0 . \tag{5.2}$$

Hence the ratio

$$\frac{F_1(l)^2 w_2(l)}{F_2(l)^2 w_1(l)} = \frac{F_1(1)^2 w_2(1)}{F_2(1)^2 w_1(1)} = \frac{g_1^2 X_c}{g_2^2 X_q} \tag{5.3}$$

is independent of l within the present model. This exact relation holds, in particular, in the limit $l \to 0$:

$$\frac{F_1^{*2} w_2^*}{F_2^{*2} w_1^*} = \frac{g_1^2 X_c}{g_2^2 X_q} . \tag{5.4}$$

Another exact property follows from the general form, Eqs. (4.2)—(4.7), of the vertex functions $\Gamma_{q\bar{q}}$,

$\Gamma_{c\tilde{c}}$, $\Gamma_{c\tilde{q}}$, and $\Gamma_{q\tilde{c}}$. Since they have higher-order contributions which are identical up to prefactors, their pole terms and the corresponding Z factors Z_K, Z_λ, and Z_L will exhibit this property as well.[76] This implies a common structure of the higher-order terms of the ensuing ζ functions ζ_K, ζ_λ, and ζ_L. From Eqs. (4.14)–(4.16) we have in one-loop order

$$\zeta_K^{(1)} = -\frac{F_1^2}{2} \, , \quad \zeta_\lambda^{(1)} = -\frac{F_2^2}{2} \, , \quad \zeta_L^{(1)} = -\frac{F_1 F_2}{2w_3} \, .$$

$$(5.5)$$

Thus we are led to the general form

$$\zeta_K = -\frac{F_1^2}{2}(1+Q) \, , \tag{5.6}$$

$$\zeta_\lambda = -\frac{F_2^2}{2}(1+Q) \, , \tag{5.7}$$

$$\zeta_L = -\frac{F_1 F_2}{2w_3}(1+Q) \, , \tag{5.8}$$

where Q is determined by the pole terms of n-loop diagrams with $n \geq 2$. The explicit form of Q in two-loop order will be given in Sec. VI.

In order to exploit this result it is useful to consider the β functions associated with w_3 and F_2/F_1. From Eqs. (3.20)–(3.22) and (5.6)–(5.8) one obtains

$$\beta_{w_3} = \tfrac{1}{4}(1+Q)(w_3 F_1^2 + w_3 F_2^2 - 2F_1 F_2) \, , \tag{5.9}$$

$$\beta_{F_2/F_1} = \frac{F_2}{4F_1}(1+Q)(F_1+F_2)(F_2-F_1) \, . \tag{5.10}$$

This implies as a general result to all orders (provided that F_i^* and $1+Q^*$ are finite)

$$F_1^* = F_2^* \, , \tag{5.11}$$

$$w_3^* = 1 \, , \tag{5.12}$$

in agreement with the one-loop result of Siggia and Nelson.[43] Substituting Eq. (5.11) into Eq. (5.4) yields the exact relation

$$\frac{w_2^*}{w_1^*} = \frac{g_1^2 \chi_c}{g_2^2 \chi_q} \, . \tag{5.13}$$

It is important to observe that Eqs. (5.11) and (5.12) represent the fixed-point version of the conditions given in Eqs. (2.46) and (2.47). Consequently, there is a close connection between the fixed-point values of the present model and of model E. Specifically, on the basis of the analogy between Eqs. (2.53) and (2.54) and the model-E equations, we conclude from Eq. (2.55)

$$\frac{1}{w^*} = \frac{1}{w_1^*} + \frac{1}{w_2^*} \, , \tag{5.14}$$

and from Eq. (2.56)

$$f^* = F_1^{*2} = F_2^{*2} \, . \tag{5.15}$$

Here w^* and f^* represent the usual fixed-point values of model E.[47,49,60] Equations (5.11)–(5.15) completely determine the dynamic fixed point of the present model.

An interesting consequence of the relation (5.13) is that the fixed-point values w_1^* and w_2^* depend on nonuniversal static quantities, in contrast to w^*. From Eqs. (5.13) and (5.14) we obtain

$$w_1^* = (1+B^{-1})w^* \, , \tag{5.16}$$

$$w_2^* = (1+B)w^* \, , \tag{5.17}$$

with the purely static parameter[77]

$$B = \frac{g_1^2 \chi_c}{g_2^2 \chi_q} = \frac{T[\sigma - c(\partial \sigma / \partial c)_{P,T}]^2}{c^2 C_{P,c}} \left[\frac{\partial c}{\partial \Delta} \right]_{P,T} \, . \tag{5.18}$$

It is determined by the finite specific heat and mass susceptibility at T_λ and depends on the pressure P and the mass concentration c. This implies finite nonuniversal fixed-point values $w_1^*(P,c)$ and $w_2^*(P,c)$ along the λ line (provided that w^* is finite). The disagreement with the concentration-independent values $w_1^* = \tfrac{3}{7}$ and $w_2^* = \infty$ found by Siggia and Nelson [Eqs. (4.6) and (4.14) of Ref. 43] is due to their incomplete static treatment which takes into account the coupling $\sim c \, |\psi_0|^2$ but not $\sim q \, |\psi_0|^2$. In $O(\epsilon)$ this implies a divergent χ_c with χ_q remaining noncritical and finite, hence B and w_2^* become infinite in this treatment. We shall use finite values for B (see Sec. VII) and a two-loop value $w^* \ll 1$, which yields both $w_1^* \ll 1$ and $w_2^* \ll 1$ along the λ line, except for $c \to 0$ and $c \to c_{\text{tricrit}}$ where B diverges.

We proceed to a discussion of the transport coefficients. From Eqs. (4.38)–(4.40) and (5.3) we obtain

$$k_T = \frac{g_1 \chi_c F_2(l)}{g_2 F_1(l)} \frac{w_3(l) - \tfrac{1}{4}F_1(l)F_2(l)[1+P(l)]}{1 - \tfrac{1}{4}F_2(l)^2[1+P(l)]}$$

$$(5.19)$$

and

$$\frac{D_s}{D} = \frac{g_1^2 \chi_c F_2(l)^2}{g_2^2 \chi_q F_1(l)^2} \frac{1 - \tfrac{1}{4}F_1(l)^2[1+P(l)]}{1 - \tfrac{1}{4}F_2(l)^2[1+P(l)]} \, .$$

$$(5.20)$$

Using the above fixed-point values we arrive at the exact results

$$\lim_{T\to T_\lambda} k_T = \frac{g_1 \chi_c}{g_2}$$

$$= T_\lambda c^{-1} \left[\frac{\partial c}{\partial \Delta} \right]_{P,T} \left[\sigma - c \left(\frac{\partial \sigma}{\partial c} \right)_{P,T} \right] \quad (5.21)$$

and

$$\lim_{T\to T_\lambda} \frac{D_s}{D} = B , \quad (5.22)$$

with B given by Eq. (5.18). The asymptotic value of k_T at T_λ given in Eq. (5.21) agrees with the conjectures by Papoular[41] and by Lucas and Tyler[10] based on the hydrodynamics below T_λ and on continuity arguments at T_λ. Here we have presented a general proof. We conclude that there exist two dimensionless ratios

$$R_{k_T} = \frac{g_2 k_T}{g_1 \chi_c}$$

$$= \frac{F_2(l)}{F_1(l)} \frac{w_3(l) - \frac{1}{4} F_1(l) F_2(l)[1 + P(l)]}{1 - \frac{1}{4} F_2(l)^2 [1 + P(l)]} \quad (5.23)$$

and

$$R_B = \frac{D_s}{DB} = \frac{F_2(l)^2}{F_1(l)^2} \frac{1 - \frac{1}{4} F_1(l)^2 [1 + P(l)]}{1 - \frac{1}{4} F_2(l)^2 [1 + P(l)]}$$

$$(5.24)$$

which attain the concentration-independent universal values

$$R_{k_T}^* = R_B^* = 1 \quad (5.25)$$

in the limit $T \to T_\lambda$.

Another dimensionless ratio of interest is introduced by

$$R_{He} = \xi_\Delta^{-\epsilon/2} \left[\frac{D_s \chi_q^{1/2}}{g_1 (1 + B^{-1})^{1/2}} + \frac{D \chi_c^{1/2}}{g_2 (1 + B)^{1/2}} \right] .$$

$$(5.26)$$

From Eqs. (4.38) and (4.40), with (4.26) and (4.27), we find

$$R_{He} = \left[\frac{K_d}{w_1(l) F_1(l)^2 (1 + B^{-1})} \right]^{1/2} \{ 1 - \frac{1}{4} F_1(l)^2 [1 + P(l)] \} + \left[\frac{K_d}{w_2(l) F_2(l)^2 (1 + B)} \right]^{1/2} \{ 1 - \frac{1}{4} F_2(l)^2 [1 + P(l)] \} ,$$

$$(5.27)$$

which in the limit $l \to 0$ tends to the value

$$R_{He}^* = \left[\frac{K_d}{w^* f^*} \right]^{1/2} \{ 1 - \frac{1}{4} f^* [1 + P(0)] \} . \quad (5.28)$$

Here w^* and f^* denote the (concentration-independent) fixed-point values of model E. R_{He}^* is identical with the universal ratio[47,49,60]

$$R_\lambda = (K_d / w^* f^*)^{1/2} [1 - \frac{1}{4} f^* + O(f^{*2})]$$

entering the asymptotic scaling form of the thermal conductivity of pure ^{4}He.

In summary, there are three *universal*, i.e., concentration- and pressure-independent ratios along the λ line of ^{3}He-^{4}He mixtures which involve only D, k_T, κ_s (or κ), and static quantities. In particular, there exists an analog of R_λ of pure ^{4}He. The opposite statements of Siggia and Nelson[43] are incorrect.

From Eqs. (5.18), (5.22), and (5.26)—(5.28) we obtain in three dimensions the asymptotic power law

$$D = g_2 \chi_c^{-1/2} (1 + B)^{-1/2} R_{He}^* \xi_\Delta^{1/2} \quad (5.29)$$

for $T \to T_\lambda$. The exponent $-\nu/2$ agrees with earlier predictions based on dynamic scaling,[2,78] on mode coupling,[29,39] and on renormalization-group[43] calculations provided that R_{He}^* is finite ($w^* > 0$). The corresponding power law for D_s reads

$$D_s = g_1 \chi_q^{-1/2} (1 + B^{-1})^{-1/2} R_{He}^* \xi_\Delta^{1/2} , \quad (5.30)$$

whose exponent also agrees with earlier predictions.[29,43] Here we have presented the complete expressions for the asymptotic *amplitudes*. Our theory will predict that these exponents and amplitudes are not experimentally observable.

Next we consider the dynamic transient exponents. Because of the relation (5.3) we can eliminate w_2 in terms of w_1 and F_2/F_1. Hence we need to consider only the transient exponents associated with the parameters w_1, F_1 and $w_3, F_2/F_1$. Owing to the simple structure of Eqs. (5.9) and (5.10) we can determine the transient exponents ω_{w_3} and ω_{F_2/F_1} independently of those associated with w_1 and F_1. Using Eqs. (5.12) and (5.15) we obtain from Eqs. (5.9) and (5.10) the general result

$$\omega_{w_3} = \omega_{F_2/F_1} = \frac{f^*}{2}(1+Q^*) . \tag{5.31}$$

At present it is not established whether $w^* > 0$ or $w^* = 0$ is the stable fixed point for ⁴He in three dimensions.[47,49,79,80] Assuming that $w^* > 0$, as suggested by the two-loop results,[47,49,79,81] we have $0 < w_1^* < \infty$, $0 < w_2^* < \infty$. Then we obtain from Eqs. (3.18), (3.19), (3.22), (5.6), and (5.7)

$$\zeta_\Gamma^* = \zeta_K^* = \zeta_\lambda^* = \zeta_L^* = -\frac{f^*}{2}(1+Q^*) = -\frac{\epsilon}{2} . \tag{5.32}$$

The last equality follows from Eqs. (3.21) and (3.22). Thus we have the exact transient exponents

$$\omega_{w_3} = \omega_{F_2/F_1} = \frac{\epsilon}{2} , \tag{5.33}$$

and from Eq. (3.39) the scaling exponents[30,60,78]

$$z_\psi = z_q = z_c = z_L = \frac{d}{2} . \tag{5.34}$$

Equation (5.33) implies a fast approach of the effective parameters $w_3(l)$ and $F_2(l)/F_1(l)$ to their fixed-point value 1 with a transient exponent $\frac{1}{2}$ in three dimensions. As $l \to 0$ we obtain from Eqs.

(5.9) and (5.10) the representations

$$w_3(l) = 1 - A_3(l)(\mu l)^{\epsilon/2} , \tag{5.35}$$

$$F_2(l)/F_1(l) = 1 + A_F(l)(\mu l)^{\epsilon/2} , \tag{5.36}$$

with finite subleading amplitudes $A_3(0) > 0$ and $A_F(0)$. As soon as w_3 and F_2/F_1 have come close to 1, the remaining flow of the parameters as $l \to 0$ will be governed by model-E (or model-F) flow equations, as follows from the structure of Eqs. (2.53) and (2.54). Hence we conclude, without explicit calculation, that the remaining two transient exponents are identical with ω_w and ω_f of model E. Because of the smallness of $\omega_w \ll 1$ there will be a slow approach of $w_1(l)$, $w_2(l)$, $F_1(l)$, and $F_2(l)$ to their fixed-point values. Thus we predict significant departures from the asymptotic behavior in the experimentally accessible regime for the same reason as for pure ⁴He.[50,51]

Finally, we consider the thermal conductivity κ. Substituting our results for κ_s, k_T, and D into Eq. (4.1) yields

$$\kappa = k_B \chi_q^{1/2} g_1 [K_d/w_1(l)F_1(l)^2]^{1/2} A_\kappa(l) , \tag{5.37}$$

with

$$A_\kappa(l) = (\mu l)^{-\epsilon/2}\left[1 - \frac{1}{4}F_1(l)^2[1+P(l)] - \frac{\{w_3(l) - \frac{1}{4}F_1(l)F_2(l)[1+P(l)]\}^2}{1-\frac{1}{4}F_2(l)^2[1+P(l)]}\right] . \tag{5.38}$$

With the use of the representations (5.35) and (5.36), one obtains

$$A_\kappa(l) = 2A_3(l) + B_\kappa(l)(\mu l)^{\epsilon/2} , \tag{5.39}$$

with a finite amplitude $B_\kappa(0)$. This implies

$$\lim_{T \to T_\lambda} \kappa = k_B \chi_q^{1/2} g_1 (K_d/w_1^* f^*)^{1/2} 2A_3(0) . \tag{5.40}$$

By continuity κ must approach the ⁴He behavior at finite distance from T_λ for sufficiently small c. In this regime the nonasymptotic temperature dependence of κ is affected by $\omega_w \ll 1$, which enters mainly through the slow approach of $w_1(l)$ to $w_1^* \ll 1$. For larger c, however, this effect is compensated by a similar slow approach of $A_3(l)$ to $A_3(0)$. Instead of κ we shall work with the ratio

$$R_\kappa = \frac{\kappa\mu^{1/2}}{k_B\chi_q^{1/2}g_1} \tag{5.41}$$

which tends to the asymptotic (nonuniversal) value

$$R_\kappa^* = 2A_3(0)(2\pi^2 w_1^* f^*)^{-1/2}\mu^{1/2} . \tag{5.42}$$

If the weak-scaling fixed point[47] $w^* = 0$ of pure

⁴He turns out to be stable in three dimensions, then both $w_1^* = 0$ and $w_2^* = 0$, with w_2^*/w_1^* remaining finite for $c > 0$ according to Eq. (5.13). In this case Eqs. (5.33) and (5.34) have to be replaced by

$$\omega_{w_3} = \omega_{F_2/F_1} = \frac{1}{2}(\epsilon + \omega_w) \tag{5.43}$$

and

$$z_\psi = \frac{1}{2}(d + \omega_w), \quad z_q = z_c = z_L = \frac{1}{2}(d - \omega_w) . \tag{5.44}$$

Correspondingly, Eqs. (5.29) and (5.30) yield $D, D_s \sim \xi_\Delta^{(1+\omega_w)/2}$ but κ remains finite because $A^3(l) \sim l^{\omega_w/2} \sim w_1(l)^{1/2}$. At finite distance from criticality the weak-scaling case is almost indistinguishable from the scaling case $0 < w^* \ll 1$ with $\omega_w \ll 1$. In the present paper we consider only the scaling case in accord with the two-loop results.[47,49]

Finally, we note that the static terms $\sim q |\psi_0|^2$ and $\sim c |\psi_0|^2$ modify the relation (5.1) and lead to smoothly l-dependent corrections both to our formulas for the transport coefficients and to the flow equations to be derived in Sec. VI. These corrections vanish in the critical limit $l \to 0$ except at the

tricritical point where the term $\sim c \mid \psi_0 \mid^2$ becomes quite important. This will be investigated in a separate paper.

VI. RENORMALIZED PERTURBATION THEORY

A. Diagonal representation

A major inconvenience for perturbation calculations beyond one-loop order is the dynamic coupling of the fields $q, \tilde{q}$ to $c, \tilde{c}$ through the kinetic coefficient L even in the absence of the reversible couplings g_1 and g_2. We shall circumvent this complication by performing an orthogonal transformation

$$\begin{bmatrix} q' \\ c' \end{bmatrix} = \underline{R} \begin{bmatrix} q\chi_q^{-1/2} \\ c\chi_c^{-1/2} \end{bmatrix}, \quad \begin{bmatrix} \tilde{q}' \\ \tilde{c}' \end{bmatrix} = \underline{R} \begin{bmatrix} \tilde{q}\chi_q^{1/2} \\ \tilde{c}\chi_c^{1/2} \end{bmatrix}, \quad (6.1)$$

$$\underline{R} = \begin{bmatrix} \cos\varphi & \sin\varphi \\ -\sin\varphi & \cos\varphi \end{bmatrix}, \quad (6.2)$$

such that the fields q' and $\tilde{q}'$ are decoupled from c' and $\tilde{c}'$ in lowest order in g_1 and g_2. This is achieved by transforming the matrix of kinetic coefficients, Eq. (3.13),

$$\underline{R} \begin{bmatrix} Z_K K & Z_L L \\ Z_L L & Z_\lambda \lambda \end{bmatrix} \underline{R}^{-1} = \begin{bmatrix} Z_K' K' & A'L' \\ A'L' & Z_\lambda' \lambda' \end{bmatrix} \equiv \underline{\Delta}', \quad (6.3)$$

such that $\underline{\Delta}'$ becomes diagonal in the absence of g_1 and g_2. Thus we require in lowest order in g_1 and g_2

$$Z_K'^{(0)} = 1, \quad Z_\lambda'^{(0)} = 1, \quad A'^{(0)} = 0. \quad (6.4)$$

The transformation is completed by introducing new couplings

$$\begin{bmatrix} g_1' \\ g_2' \end{bmatrix} = \underline{R} \begin{bmatrix} g_1\chi_q^{-1/2} \\ g_2\chi_c^{-1/2} \end{bmatrix} \quad (6.5)$$

[compare Eqs. (2.29) and (2.35) above]. This permits us to rewrite the dynamic functional J in terms of primed quantities without any change in structure, as pointed out in Sec. II.

The latter invariance property implies that the transformed couplings g_1' and g_2' are not renormalized for the same reason as for the original couplings g_1 and g_2. As an important consequence, the matrix elements of $\underline{R}$ in Eq. (6.5) must have no pole terms $\sim \epsilon^{-n}$. Therefore, we can determine R from Eq. (6.3) by dropping all pole terms arising from Λ and Λ'. This yields

$$\underline{R} \begin{bmatrix} K & L \\ L & \lambda \end{bmatrix} \underline{R}^{-1} = \begin{bmatrix} K' & 0 \\ 0 & \lambda' \end{bmatrix}, \quad (6.6)$$

which identifies the matrix elements of $\underline{R}$ as

$$\cos\varphi = \left[\frac{1}{2\Omega}(K - \lambda + \Omega) \right]^{1/2}, \quad (6.7)$$

$$\sin\varphi = \left[\frac{1}{2\Omega}(\lambda - K + \Omega) \right]^{1/2}, \quad (6.8)$$

with

$$\Omega = [(K - \lambda)^2 + 4L^2]^{1/2}. \quad (6.9)$$

Furthermore,

$$K' = \tfrac{1}{2}(K + \lambda + \Omega), \quad (6.10)$$

$$\lambda' = \tfrac{1}{2}(K + \lambda - \Omega). \quad (6.11)$$

From

$$\underline{\Lambda} = \underline{R}^{-1}\underline{\Lambda}'\underline{R} \quad (6.12)$$

we now obtain exact expressions for Z_K, Z_λ, and Z_L in terms of Z_K', Z_λ', and A' by substituting Eqs. (6.7) and (6.8) into $\underline{R}$ and $\underline{R}^{-1}$. This leads to

$$Z_K = \frac{1}{2K\Omega}[(K - \lambda + \Omega)Z_K'K' + (\lambda - K + \Omega)Z_\lambda'\lambda' - 4LA'L'], \quad (6.13)$$

$$Z_\lambda = \frac{1}{2\lambda\Omega}[(\lambda - K + \Omega)Z_K'K' + (K - \lambda + \Omega)Z_\lambda'\lambda' + 4LA'L'], \quad (6.14)$$

$$Z_L = \frac{1}{2L\Omega}[2(K - \lambda)A'L' + 2L(Z_K'K' - Z_\lambda'\lambda')]. \quad (6.15)$$

The remaining task is to compute the pole terms of Z_K', Z_λ', $A'L'$, and Z_Γ as functions of

$$F_1' = g_1' \left[\frac{\mu^{-\epsilon}K_d}{\Gamma K'} \right]^{1/2}, \quad F_2' = g_2' \left[\frac{\mu^{-\epsilon}K_d}{\Gamma \lambda'} \right]^{1/2}, \quad (6.16)$$

and of

$$w_1' = \frac{\Gamma}{K'}, \quad w_2' = \frac{\Gamma}{\lambda'}, \quad w_3' = \frac{L'}{(K'\lambda')^{1/2}} \quad (6.17)$$

within the transformed theory. Rewriting the dynamic functional, Eqs. (3.9)–(3.12), in terms of renormalized primed quantities yields

$$J = \int dt \int d^d x \, (J_\psi + J_q' + J_c' + J'^{(1)}), \quad (6.18)$$

where J_ψ is given by Eq. (3.10), and

$$J'_q = -Z'_K K' \widetilde{q}\,' \nabla^2 \widetilde{q}\,' - \widetilde{q}\,'(\partial_t - Z'_K K' \nabla^2)q' \ ,$$

$$(6.19)$$

$$J'_c = -Z'_\lambda \lambda' \widetilde{c}\,' \nabla^2 \widetilde{c}\,' - \widetilde{c}\,'(\partial_t - Z'_\lambda \lambda' \nabla^2)c' \ , \quad (6.20)$$

$$J'^{(1)} = -A'L'[\widetilde{q}\,' \nabla^2(\widetilde{c}\,' - c') + \widetilde{c}\,' \nabla^2(\widetilde{q}\,' - q')]$$
$$+ \frac{i}{2}(\widetilde{Z}_\psi Z_\psi)^{1/2}(\widetilde{\psi}\psi^* + \psi\widetilde{\psi}^*)(g'_1 q' + g'_2 c')$$
$$+ \frac{i}{2}Z_\psi(g'_1 \widetilde{q}\,' + g'_2 \widetilde{c}\,')(\psi^* \nabla^2 \psi - \psi \nabla^2 \psi^*) \ .$$

$$(6.21)$$

The perturbation calculation is now substantially simplified owing to the absence of off-diagonal couplings in zeroth order. Instead, the terms $\sim A'L'$ in $J'^{(1)}$ can be treated conveniently as two-point interactions. They will play the role of counter terms which absorb pole terms $\sim g'_1 g'_2 / \epsilon$.

The Z factors Z_K, Z_λ, Z_L, and Z_Γ are finally obtained as functions of the unprimed parameters w_i and F_i by means of Eqs. (6.13)–(6.15) and by expressing w'_i and F'_i in terms of w_i and F_i. The latter expressions follow from Eqs. (6.16) and (6.17) after substituting Eqs. (6.5), (6.10), and (6.11). The result is

$$w'_1 = 2w_1 w_2 (w_1 + w_2 + \theta)^{-1} \ , \quad (6.22)$$

$$w'_2 = 2w_1 w_2 (w_1 + w_2 - \theta)^{-1} \ , \quad (6.23)$$

$$\theta = [(w_1 + w_2)^2 + 4w_1 w_2(w_3^2 - 1)]^{1/2} \ , \quad (6.24)$$

$$F'_1 = (w'_1)^{1/2}(w_1^{-1/2} F_1 \cos\varphi + w_2^{-1/2} F_2 \sin\varphi) \ ,$$

$$(6.25)$$

$$F'_2 = (w'_2)^{1/2}(w_2^{-1/2} F_2 \cos\varphi - w_1^{-1/2} F_1 \sin\varphi) \ ,$$

$$(6.26)$$

$$\cos\varphi = (2\theta)^{-1/2}(w_2 - w_1 + \theta)^{1/2} \ , \quad (6.27)$$

$$\sin\varphi = (2\theta)^{-1/2}(w_1 - w_2 + \theta)^{1/2} \ . \quad (6.28)$$

At the fixed point determined by Eqs. (5.12), (5.14), and (5.15) these expressions become

$$w'_1{}^* = w_1^* w_2^* (w_1^* + w_2^*)^{-1} = w^* \ , \quad (6.29)$$

$$w'_2{}^* = \infty \ , \quad (6.30)$$

$$\theta^* = w_1^* + w_2^* \ , \quad (6.31)$$

$$F'_1{}^* = F_1^* = (f^*)^{1/2} \ , \quad (6.32)$$

$$F'_2{}^* = 0 \ , \quad (6.33)$$

$$\cos\varphi^* = (w^*/w_1^*)^{1/2} \ , \quad (6.34)$$

$$\sin\varphi^* = (w^*/w_2^*)^{1/2} \ . \quad (6.35)$$

The crucial consequence of Eq. (6.33) is this: At the fixed point the fluctuations described by the variables c' and $\widetilde{c}\,'$ are decoupled from q', $\widetilde{q}\,'$ and $\psi, \widetilde{\psi}$ in all orders of perturbation theory. Therefore, at the fixed point, all correlation and response functions involving $q', \widetilde{q}\,'$ and $\psi, \widetilde{\psi}$ are identical with those of model E,[47,49,60] which involve the variables $m, \widetilde{m}$ and $\psi, \widetilde{\psi}$. This is in agreement with the fixed-point values $w'_1{}^* = w^*$ and $(F'_1{}^*)^2 = f^*$, Eqs. (6.29) and (6.32), which are those of model E. As a particular consequence, the *asymptotic universal* part of the dynamic order-parameter correlation function $C_{\psi\psi}(k,\omega)$ for ³He-⁴He mixtures is identical with that for pure ⁴He in all orders of perturbation theory.

Similar statements can be made about the correlation function $C_{q'q'}(k,\omega)$ in relation to $C_{mm}(k,\omega)$ of model E, and in particular about the asymptotic critical behavior of the effective kinetic coefficient which plays the role analogous to the thermal conductivity in model E. Here this is K', Eq. (6.10). Consequently, there exists a universal ratio which is analogous to R_λ of ⁴He,[47,49,60] namely

$$R_{K'} = \frac{1}{2} \lim_{l \to 0} \frac{K(l) + \lambda(l) + \Omega(l)}{(\mu l)^{-1/2} g'_1} \left[1 - \frac{f^*}{4}(1 + P^*) \right]$$

$$(6.36)$$

$$= \lim_{l \to 0} \frac{K(l) + \lambda(l)}{(\mu l)^{-1/2} g'_1} \left[1 - \frac{f^*}{4}(1 + P^*) \right] \ .$$

$$(6.37)$$

Here P^* describes the higher-order contributions which are identical with those appearing in R_λ of model E. Using in Eq. (6.37)

$$g'_1 = \left[\frac{w^*}{w_1^* \chi_q} \right]^{1/2} g_1 + \left[\frac{w^*}{w_2^* \chi_c} \right]^{1/2} g_2 \ , \quad (6.38)$$

and comparing Eq. (6.37) with Eqs. (4.38), (4.40), and (5.26)–(5.28), one can show that $R_{K'}$ also coincides with R_{He}^*, at least in two-loop order.

B. Dynamic Z factors in two-loop order

The Z factors Z'_K and Z'_λ appearing in the dynamic functional, Eq. (6.18), are determined by the requirement that the derivatives of the renormalized vertex functions

$$\left. \frac{\partial}{\partial k^2} \Gamma_{q'\widetilde{q}\,'}(k,0) \right|_{k=0} \quad (6.39)$$

and

$$\left. \frac{\partial}{\partial k^2} \Gamma_{c'\widetilde{c}\,'}(k,0) \right|_{k=0} \quad (6.40)$$

have no poles $\sim \epsilon^{-n}$ at $d = 4$. Inspection of the diagrams in the diagonal representation shows that the two-point interaction $\sim A'$ in $J'^{(1)}$, Eq. (6.21), does not contribute to $\Gamma_{q'\bar{q}'}$ and $\Gamma_{c'\bar{c}'}$ up to two-loop order. Consequently, the perturbation calculation is analogous to that for $\Gamma_{m\bar{m}}$ of model E. Thus the diagonal representation enables us to infer from model E, without any additional calculation,

$$Z_K' = 1 - \frac{(F_1')^2}{2\epsilon}(1 + \tfrac{1}{2}Q) , \tag{6.41}$$

$$Z_\lambda' = 1 - \frac{(F_2')^2}{2\epsilon}(1 + \tfrac{1}{2}Q) , \tag{6.42}$$

where, in two-loop order,

$$Q = (F_1')^2 N(w_1') + (F_2')^2 N(w_2') \tag{6.43}$$

with the model-E function[47,49]

$$N(w) = \frac{1}{2(1+w)}\left[\tfrac{1}{2} + w - w^2(2+w)\ln\frac{(1+w)^2}{(2+w)w}\right] . \tag{6.44}$$

In Eqs. (6.41) and (6.42) we have dropped pole terms $\sim \epsilon^{-n}$ with $n > 1$ since they do not contribute to the ζ functions within the minimal renormalization procedure.

Next we consider the renormalization factor A', which is determined by the pole terms of

$$\frac{\partial}{\partial k^2}\Gamma_{q'\bar{c}'}(k,0)\bigg|_{k=0} . \tag{6.45}$$

Again, inspection of the diagrams shows that no additional calculation is necessary, only the couplings entering the external vertices have to be modified. This yields in two-loop order

$$A' = -\frac{F_1'F_2'}{2w_3'\epsilon}(1 + \tfrac{1}{2}Q) . \tag{6.46}$$

Substituting these results into the relations (6.13)–(6.15) yields

$$Z_K = 1 - \frac{F_1^2}{2\epsilon}(1 + \tfrac{1}{2}Q) , \tag{6.47}$$

$$Z_\lambda = 1 - \frac{F_2^2}{2\epsilon}(1 + \tfrac{1}{2}Q) , \tag{6.48}$$

$$Z_L = 1 - \frac{F_1F_2}{2w_3\epsilon}(1 + \tfrac{1}{2}Q) . \tag{6.49}$$

Here Q is regarded as a function of the unprimed parameters which is obtained from Eq. (6.43) by substituting Eqs. (6.22)–(6.28).

The remaining Z factor Z_Γ is determined by the poles of

$$\frac{\partial}{\partial\tau}\Gamma_{\psi^*\tilde{\psi}}(k,\omega)\bigg|_{k=0,\omega=0} . \tag{6.50}$$

Within the diagonal representation it is obvious that the contributions proportional to $(F_1')^{2n}$ and $(F_2')^{2n}$ can be taken immediately from the terms proportional to f^n in model E. Thus Z_Γ must read in two-loop order

$$\begin{aligned}
Z_\Gamma = {} & 1 - \frac{(F_1')^2}{(1+w_1')\epsilon}[1 - \tfrac{1}{2}(F_1')^2 M(w_1')] \\
& - \frac{(F_2')^2}{(1+w_2')\epsilon}[1 - \tfrac{1}{2}(F_2')^2 M(w_2')] \\
& + \frac{(F_1')^2(F_2')^2}{2\epsilon(1+w_1')(1+w_2')}H(w_1',w_2') \\
& - \frac{u^2}{36\epsilon}(6\ln\tfrac{4}{3} - 1) + O(\epsilon^{-2}) ,
\end{aligned} \tag{6.51}$$

with the model-E function[47,49]

$$M(w) = \frac{1}{2(1+w)^2}\left[\tfrac{1}{2}(1+w)(27\ln\tfrac{4}{3} - 6) + w + (1+2w)\ln\frac{(1+w)^2}{1+2w}\right] . \tag{6.52}$$

The mixed term proportional to $(F_1')^2(F_2')^2$, however, must be computed explicitly from new two-loop diagrams which have both an internal q and c line. Furthermore, one must verify that there are no contributions proportional to $F_1'(F_2')^3$ and $(F_1')^3 F_2'$. The function $H(x,y)$ determining the mixed term in Eq. (6.51) is calculated as

$$\begin{aligned}
H(x,y) = {} & \tfrac{27}{2}\ln\tfrac{4}{3} - 3 + \frac{y}{2(1+y)}\left[1 + \ln\frac{y(1+x)}{x+y} + \frac{x}{y}(1+x+y)\ln\frac{x+xy+x^2}{(1+x)(x+y)}\right] \\
& + \frac{x}{2(1+x)}\left[1 + \ln\frac{x(1+y)}{x+y} + \frac{y}{x}(1+x+y)\ln\frac{y+xy+y^2}{(1+y)(x+y)}\right] \\
& - x\ln\frac{x+xy+x^2}{(1+x)(x+y)} - y\ln\frac{y+xy+y^2}{(1+y)(x+y)} - \ln\frac{1+x+y}{(1+x)(1+y)} . \tag{6.53}
\end{aligned}$$

Again all primed parameters in Eq. (6.51) have to be considered as functions of the unprimed parameters according to Eqs. (6.22)–(6.28). The complexity of the resulting expressions demonstrates the great advantage of having avoided a direct off-diagonal perturbation calculation in two-loop order.

The ζ functions are finally obtained from the Z factors Z_K, Z_λ, and Z_L in the form anticipated in Eqs. (5.6)–(5.8), with Q given by Eqs. (6.43), (6.44), and (6.22)–(6.28). The remaining ζ function ζ_Γ reads

$$\zeta_\Gamma = -\frac{(F_1')^2}{1+w_1'}[1-(F_1')^2 M(w_1')] - \frac{(F_2')^2}{1+w_2'}[1-(F_2')^2 M(w_2')] + \frac{(F_1')^2(F_2')^2}{(1+w_1')(1+w_2')}H(w_1',w_2')$$

$$-\frac{u^2}{18\epsilon}(6\ln\tfrac{4}{3}-1) \tag{6.54}$$

with the primed parameters expressed in terms of unprimed parameters according to Eqs. (6.22)–(6.28). This completes the determination of the β functions, Eqs. (3.18)–(3.22), and of the renormalization-group flow equations (3.32) and (3.33) in two-loop order.

VII. NONLINEAR RENORMALIZATION-GROUP ANALYSIS

There are several reasons for carrying out a nonlinear renormalization-group analysis of the critical dynamics in ^{3}He-^{4}He mixtures: (i) the smallness of the dynamic transient exponent $\omega_w \ll 1$ which makes the asymptotic critical region experimentally inaccessible and which invalidates the conventional power-law description in the accessible region even very close to criticality ($10^{-6} \lesssim t \lesssim 10^{-4}$); (ii) our interest in explaining the crossover behavior in the range $10^{-4} \lesssim t \lesssim 10^{-1}$ and in providing a semiquantitative connection with the noncritical background properties; (iii) the possibility of predicting the concentration dependence of various physical quantities for arbitrary $c \ll 1$ without adjustable parameters once the initial values $w_i(l_0)$ and $F_i(l_0)$ have been identified in the background region $l_0 \gtrsim O(10^{-1})$ at a particular concentration $c_0 \ll 1$. These points require a global integration of the nonlinear renormalization-group flow equations rather than the usual linearization in the vicinity of the fixed point.

A. Effective dynamic parameters

In the following we shall illustrate some features of the effective dynamic parameters by numerical integration of the two-loop flow equations. For simplicity we shall neglect the effect of static corrections to scaling and therefore set $u(l)=u^*=\epsilon/40$ in Eq. (6.54). In the remaining five-dimensional space the dynamic parameters vary in the range

$$0 \leq F_i \leq \infty, \quad i=1,2 \tag{7.1}$$

$$0 \leq w_i \leq \infty, \quad i=1,2 \tag{7.2}$$

and

$$-1 \leq w_3 \leq 1 . \tag{7.3}$$

The range $|w_3| > 1$ is excluded as it corresponds to an unphysical, negative eigenvalue λ', Eq. (6.11), of the matrix of kinetic coefficients. Also the large F_i domain, $F_i > O(1)$, will not be discussed since our perturbation results are not conclusive in this domain. By contrast, the dependence of the β functions on w_i, $i=1,2,3$, is exact within the loop expansion and fully nonlinear. This permits us to include the entire range (7.2) and (7.3) in our analysis, with the restriction $F_i \lesssim O(1)$. Fortunately, as for pure ^{4}He,[53] it is indeed the small F_i region which turns out to be relevant for the dynamics of ^{3}He-^{4}He mixtures in three dimensions. The large F_i domain may become relevant near two dimensions.[53,80–82]

As shown in Sec. V, the parameters $w_3(l)$ and $F_2(l)/F_1(l)$ have a fast approach to their fixed-point values $w_3^* = F_2^*/F_1^* = 1$ in three dimensions. Therefore, for a preliminary study, it is of some interest to illustrate the flow of the remaining parameters in the simpler subspace

$$w_3(l)=1 , \tag{7.4}$$

$$F_1(l)=F_2(l) , \tag{7.5}$$

which was also considered by Siggia and Nelson.[43] As we shall see below, the most serious restriction is that of Eq. (7.4), which excludes the crossover behavior in the precritical region $t > 10^{-4}$. Substituting Eq. (7.5) into the exact relation (5.3) determines the ratio of $w_1(l)$ and $w_2(l)$ as $w_2(l)/w_1(l)=B$, with B given by Eq. (5.18). Thus within the subspace defined by Eqs. (7.4) and (7.5) it suffices to study the flow of the parameters

$$f(l)=F_1(l)^2=F_2(l)^2 \tag{7.6}$$

and

$$w(l)=[w_1(l)^{-1}+w_2(l)^{-1}]^{-1} . \tag{7.7}$$

The resulting flow diagram for f and w is identical with that for model E, for reasons given in Secs. II and V, and is shown in Fig. 1(b) of Ref. 53 for $d = d^* \approx 3$. Here d^* denotes the borderline dimension below which the weak-scaling fixed point $w^* = 0$ becomes stable. We note that the previous one-loop theory[43] with $w^* = 1 + O(\epsilon)$ implies a flow diagram of the type shown in Fig. 1(a) of Ref. 53 and is therefore misleading. For a detailed discussion of the two-loop flow diagram we refer to Refs. 51 and 53.

Outside the subspace defined by Eqs. (7.4) and (7.5) the global topology of the flow diagram may become quite complicated. We have not systematically investigated the entire five-dimensional parameter space but only the region that is expected to be relevant for ^{3}He-^{4}He mixtures in three dimensions. By continuity it is clear *a priori* that for low concentrations the projections of the ^{3}He-^{4}He trajectory onto the f_1-w_1 plane must yield a trajectory similar to that for pure ^{4}He. The latter was first identified by Dohm and Folk as shown in Fig. 7 of Ref. 53.

Using our two-loop result for the renormalization-group flow equations and comparing with the recent measurements of Gestrich and Meyer[23] at $c \approx 0.04$ we have approximately determined a trajectory typical for ^{3}He-^{4}He mixtures at low concentration. The corresponding effective dynamic parameters $w_i(l)$ and $f_i(l) = F_i(l)^2$ are shown in Figs. 1(a)–1(e). We see that both $f_1(l)$ and $w_1(l)$ are consistent with $f(l)$ and $w(l)$ of pure ^{4}He.[53] The new information is contained in our approximate determination of the l dependence of $f_2(l)$, $w_2(l)$, and $w_3(l)$. In the following we discuss the procedure that leads to this identification.

B. Theoretical amplitudes

In order to clearly separate the genuine dynamic properties from purely static effects it is appropriate to rewrite the transport coefficients in terms of static prefactors multiplied by dimensionless dynamic amplitudes R_D, R_{k_T}, and R_κ. From the expression derived in Secs. IV and V we obtain in three dimensions

$$D = g_2 \xi_\Delta^{1/2} \chi_c^{-1/2} R_D , \tag{7.8}$$

$$k_T = g_1 g_2^{-1} \chi_c R_{k_T} , \tag{7.9}$$

$$\kappa = g_1 \chi_q^{1/2} k_B \mu^{-1/2} R_\kappa , \tag{7.10}$$

where

$$R_D = [2\pi^2 w_2(l) f_2(l)]^{-1/2} [1 - \tfrac{1}{4} f_2(l)] , \tag{7.11}$$

$$R_{k_T} = \frac{F_2(l)}{F_1(l)} \frac{w_3(l) - \tfrac{1}{4} F_1(l) F_2(l)}{1 - \tfrac{1}{4} f_2(l)} , \tag{7.12}$$

$$R_\kappa = \left[\frac{l^{-1}}{2\pi^2 w_1(l) f_1(l)} \right]^{1/2}$$

$$\times \left[1 - \tfrac{1}{4} f_1(l) - \frac{[w_3(l) - \tfrac{1}{4} F_1(l) F_2(l)]^2}{1 - \tfrac{1}{4} f_2(l)} \right] . \tag{7.13}$$

These amplitudes contain the relevant information about the critical dynamics since they depend only on the dynamic parameters $w_i(l)$ and $F_i(l)$. In the limit $l \to 0$, they attain finite values $R_{k_T}^*$, R_κ^* [see Eqs. (5.25) and (5.40)], and

$$R_D^* = (2\pi^2 w_2^* f^*)^{-1/2} (1 - \tfrac{1}{4} f^*) . \tag{7.14}$$

Note that R_κ^* and R_D^* are nonuniversal dynamic quantities. They cannot be expressed in terms of purely static quantities, contrary to what is implied in Ref. 41 concerning R_D^*.[83]

Alternatively, one can work with the set of amplitudes R_{k_T}, R_{He}, and R_B defined in Sec. V, which become universal quantities for $l \to 0$. They are appropriate for demonstrating the nonuniversal departures from the asymptotic values in the experimentally accessible regime. On the other hand, the experimental values corresponding to R_{He} and R_B are not directly measurable in a single experiment but must be extracted simultaneously from three separate measurements (D, k_T, and κ) at the same concentration. Therefore, it seems preferable to employ the amplitudes given in Eqs. (7.11)–(7.13).

In order to compare with experiments one must specify the absolute temperature scale in the connection between l and t_Δ, Eq. (4.22). For reasons given previously[53] we choose

$$l = t_\Delta^\nu . \tag{7.15}$$

This corresponds to the identification

$$\mu = \xi_0^{-1} . \tag{7.16}$$

For simplicity we shall approximate $\xi_0(P, \Delta)$ by the ^{4}He value[84]

$$\xi_0 = 1.41 \times 10^{-8} , \tag{7.17}$$

in units of cm. The remaining task consists of determining the nonuniversal initial values $w_i(l_0)$ and $F_i(l_0)$ by means of comparison with experiment.
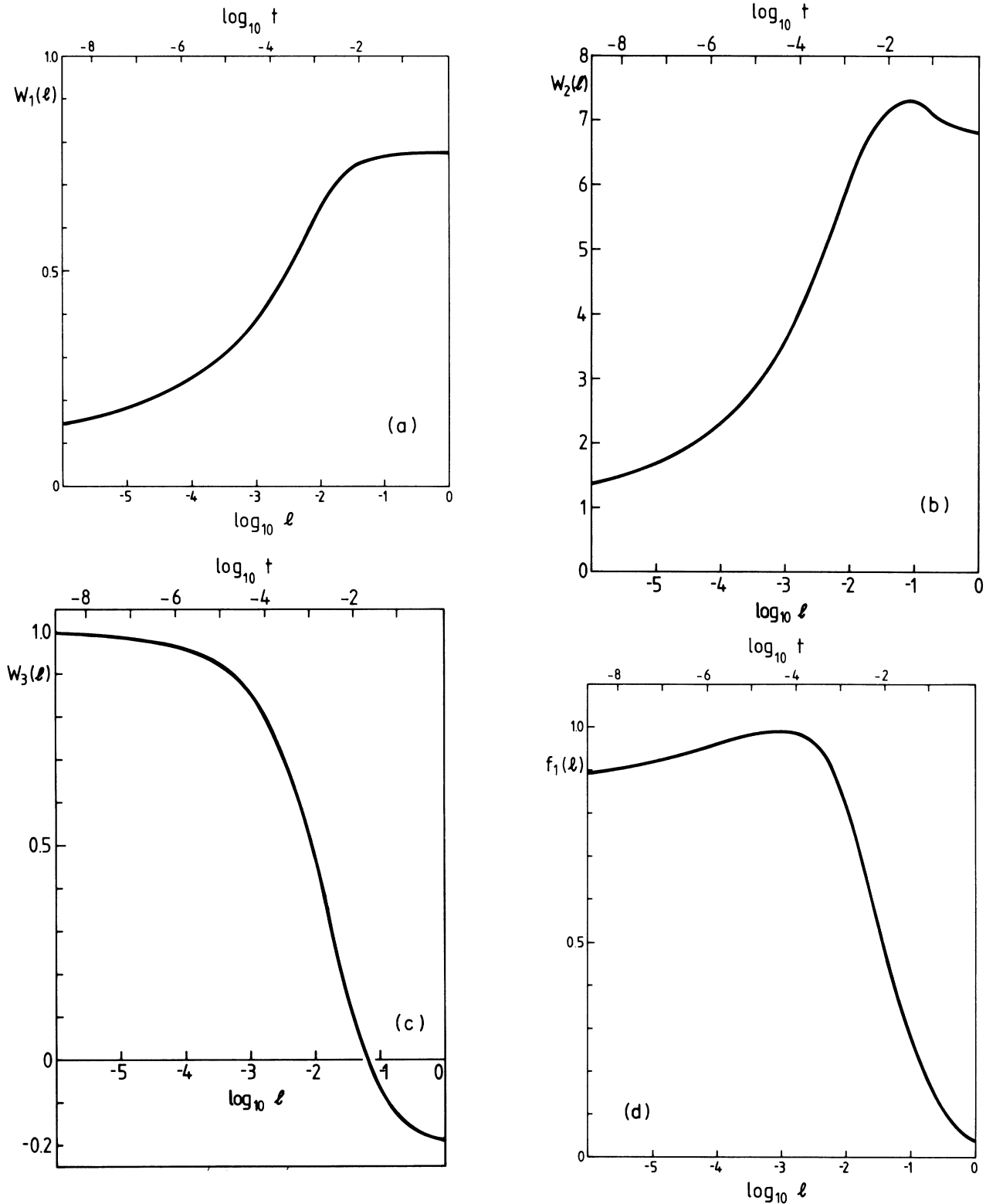
FIG. 1. Effective dynamic parameters vs flow parameter l as calculated by numerical integration of the flow equations (3.18)—(3.22), (5.6)—(5.8), (6.43), and (6.54) with the initial conditions given by Eqs. (7.24)—(7.28) at $l_0=0.0884$. The initial conditions have been determined by a four-parameter fit of the amplitudes Eqs. (7.11)—(7.13) to the data for the amplitudes Eqs. (7.18)—(7.20) at $X=0.05$ shown in Fig. 2. The flow parameter l is related to t (see top scale) according to Eq. (A12). The fixed-point values are $w_1^*=0.02$, $w_2^*=0.19$, $w_3^*=1$, $f_1^*=f_2^*=f^*=0.83$.
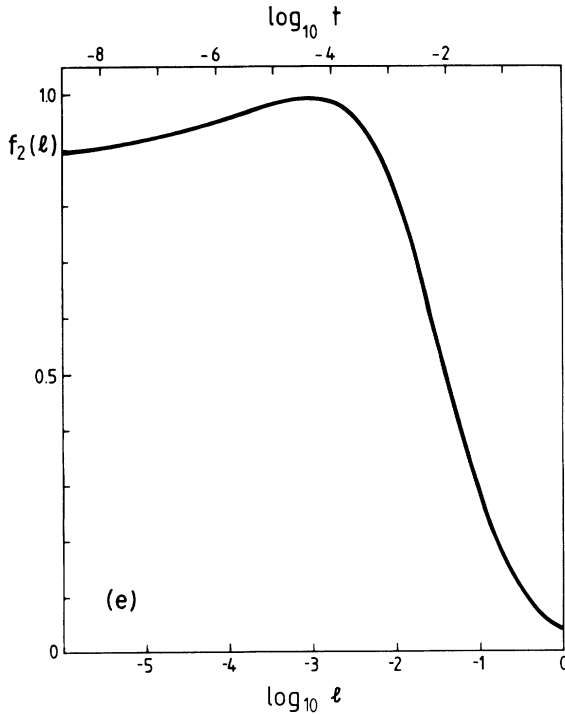
FIG. 1. (Continued.)

C. Experimental quantities

The experimental values corresponding to the theoretical amplitudes, Eqs. (7.11)—(7.13), are obtained as

$$R_D^{\text{expt}} = \frac{D\hbar}{\text{cm}_4} \left[\frac{\rho}{k_B T \xi_\Delta} \left| \frac{\partial c}{\partial \Delta} \right|_{P,T} \right]^{1/2}, \qquad (7.18)$$

$$R_{k_T}^{\text{expt}} = \frac{k_T c}{T\bar{\sigma}} \left| \frac{\partial \Delta}{\partial c} \right|_{P,T}, \qquad (7.19)$$

$$R_\kappa^{\text{expt}} = \frac{\kappa \hbar}{\bar{\sigma} T m_4} \left[\frac{\xi_0^{-1}}{\rho k_B C_{P,c}} \right]^{1/2}, \qquad (7.20)$$

with

$$\bar{\sigma} = \sigma - c \left| \frac{\partial \sigma}{\partial c} \right|_{P,T}. \qquad (7.21)$$

Since the experiments are performed at constant c rather than at constant Δ one must take into account the well-known effects of the Fisher renormalization.[85] Furthermore, the various static quantities have to be rewritten in terms of the molar concentration X and the molar chemical potential ϕ used in the experimental literature.[24-26] These points are summarized in the Appendix.

The dynamic quantities D, k_T, and κ have been measured at several concentrations above T_λ.[2,4-6,9,10,12-14,16,18-23] At the present stage of

our analysis we are primarily interested in a complete set of data for D, k_T, and κ at one particular concentration. This permits a simultaneous identification of all five initial conditions $w_i(l_0)$ and $F_i(l_0)$ at this concentration. Furthermore, it seems advisable to start with an analysis of measurements at low concentration $X \ll 1$ in order to be able to make contact with our previous analysis of pure ^{4}He ($X = 0$) and to verify continuity in X. Fortunately such measurements have been performed very recently at $X = 0.053$ by Gestrich and Meyer.[23] The corresponding data for the amplitudes R_D^{expt}, $R_{k_T}^{\text{expt}}$, and R_κ^{expt} are readily obtained from Eqs. (7.18)—(7.20) by using the known experimental results for the various static quantities, as described in the Appendix. The data are shown in Figs. 2(a)—2(c) as a function of the relative temperature

$$t = \frac{T - T_\lambda(c)}{T_\lambda(c)} = \frac{T - T_\lambda[X]}{T_\lambda[X]}, \qquad (7.22)$$

where $T_\lambda[X] = T_\lambda(c(X)) = 2.10$ K at $X = 0.053$ or $c = 0.04$ according to

$$c(X) = \frac{m_3 X}{m_3 X + m_4(1 - X)}. \qquad (7.23)$$

All data exhibit a more or less systematic temperature dependence even close to T_λ which is consistent with our prediction of the importance of dynamic transients in the accessible region. Owing to the fast transient $\omega_{w_3} = \omega_{F_2/F_1} = \frac{1}{2}$, $R_{k_T}^{\text{expt}}$ is not far from its asymptotic value $R_{k_T}^* = 1$ in the experimentally accessible region $t \lesssim 10^{-4}$, as predicted in Sec. V. According to Fig. 2 we expect $R_{k_T}^{\text{expt}} \approx R_{k_T}^*$ and $R_\kappa^{\text{expt}} \approx R_\kappa^*$ near $t = 10^{-6}$ whereas R_D^{expt} should increase further even for $t < 10^{-6}$. We note that the scatter of the data for R_D may partly be due to the logarithmic representation of the original data for D which introduces some uncertainty on our nonlogarithmic scale. There might also be systematic errors introduced from static quantities such as $\bar{\sigma}$, $\partial c/\partial \Delta$, etc.

D. Determination of the initial conditions

Our procedure of identifying the ^{3}He-^{4}He trajectory is an extension of that introduced previously[52,53] for ^{4}He. Here we have to determine five initial values $w_i(l_0), F_i(l_0)$. We have found that this is possible only if all of the three theoretical amplitudes, Eqs. (7.11)—(7.13), are fitted simultaneously to their experimental counterparts, Eqs. (7.18)—(7.20). The data for only one or two of these amplitudes do not provide sufficient information for this purpose. This is plausible according to the dependence on w_i and F_i in Eqs. (7.11)—(7.13). For
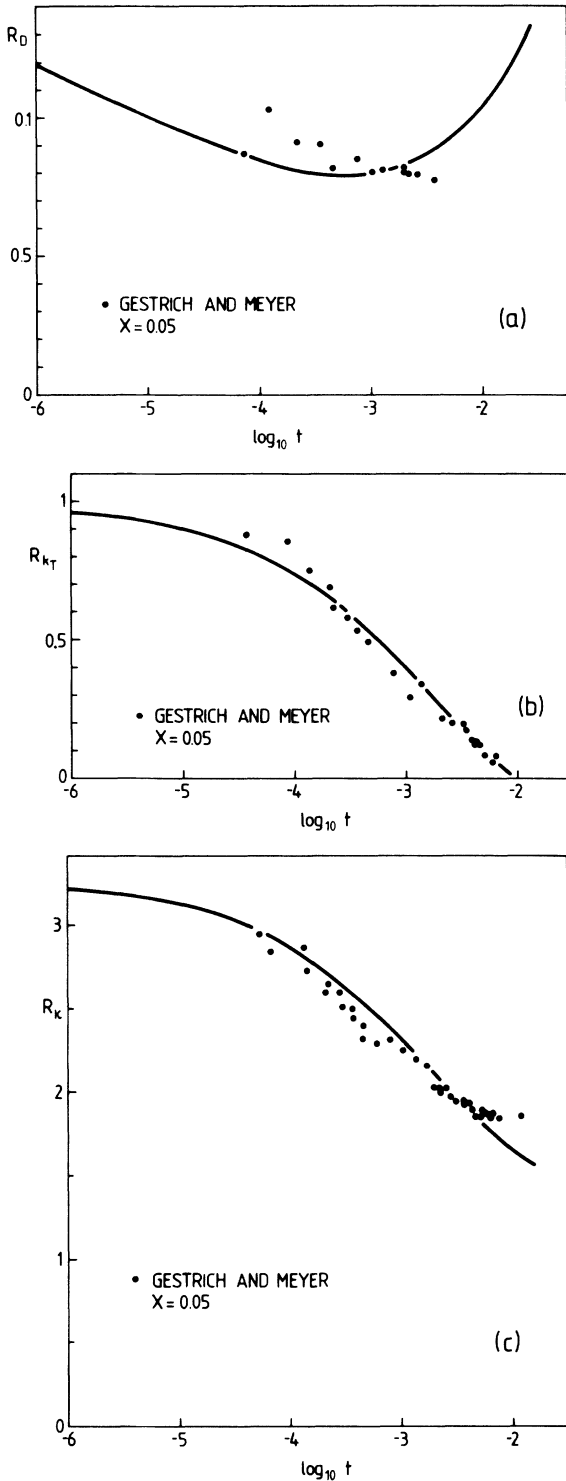
FIG. 2. Amplitudes according to Eqs. (7.11)—(7.13) and (7.18)—(7.20) for the transport coefficients D, k_T, and κ vs t, Eq. (7.22) at $X=0.05$. The data are taken from the dynamic measurements of Ref. 23 using the values for static quantities given in the Appendix. The curves are four-parameter fits of Eqs. (7.11)—(7.13) to the data, with adjustable $w_1(l_0)$, $w_3(l_0)$, $f_1(l_0)$, and $f_2(l_0)$, and with $w_2(l_0)$ determined by Eq. (7.24). The corresponding effective parameters are shown in Fig. 1.

example, R_D and R_{k_T} are quite sensitive to the parameters $w_2(l_0)$ and $w_3(l_0)$, but not to $w_1(l_0)$. There exists only an indirect coupling of R_D and R_{k_T} to $w_1(l)$ through the flow equations. Thus the data of R_κ^{expt} are needed as well in order to identify $w_1(l_0)$ unambiguously via Eq. (7.13).

Besides $w_3(l_0)$ there are only three of the four parameters $w_i(l_0)$,$F_i(l_0)$, $i=1,2$, that can be considered as freely adjustable. The remaining parameter, for example $w_2(l_0)$, is determined by the exact relation (5.3). It contains the nonuniversal quantity B, Eq. (5.18), which within the present model plays the role of a temperature-independent background parameter. We use an experimental value for B which is taken from static quantities at $t_0=10^{-1.5}$. For $X=0.05$ we find $B^{\mathrm{expt}}(t_0)=9.26$ (see Appendix).

We have carried out a four-parameter least-squares fit of R_α to R_α^{expt} ($\alpha=D,k_T,\kappa$) by numerical integration of the flow equations for $w_1(l)$, $w_2(l)$, $w_3(l)$, $F_1(l)$, and $F_2(l)$ with adjustable initial conditions $w_1(l_0)$, $w_3(l_0)$, $F_1(l_0)$, and $F_2(l_0)$ at $t_0=10^{-3/2}$ and with $w_2(l_0)$ determined by

$$w_2(l_0)=9.26w_1(l_0)f_2(l_0)/f_1(l_0) . \tag{7.24}$$

We used equal weights for the data points of $R_{k_T}^{\mathrm{expt}}$ and R_κ^{expt} shown in Fig. 2. Since there are only a few data points for R_D^{expt} we attached weights to these points which are twice as large as the weights for $R_{k_T}^{\mathrm{expt}}$ and R_κ^{expt} in order to have comparable overall weights for the different amplitudes (the results are rather insensitive to these details).[86] The fit leads to the following initial conditions (at $t_0=10^{-3/2}$, $l_0=0.088$)

$$w_1(l_0)=0.764 , \tag{7.25}$$

$$w_3(l_0)=-0.050 , \tag{7.26}$$

$$f_1(l_0)=F_1(l_0)^2=0.298 , \tag{7.27}$$

$$f_2(l_0)=F_2(l_0)^2=0.308 . \tag{7.28}$$

The corresponding value for $w_2(l_0)$ is 7.31.

The ensuing l dependence of the flow parameters is shown in Figs. 1(a)—1(e) and the corresponding theoretical amplitudes are shown in Figs. 2(a)—2(c) (solid curves). The good quantitative agreement with the three different experimental amplitudes over two decades of relative temperature is nontrivial since in our four-parameter fit there are only two entirely new parameters, namely $f_2(l_0)$ and $w_3(l_0)$, whereas $f_1(l_0)$ and $w_1(l_0)$ are expected a priori to be comparable to our previous ^{4}He values $f(l_0)=0.253$, $w(l_0)=0.572$ (model-E, cell-D data), or $f(l_0)=0.186$, $w(l_0)=0.759$ (model-E, cell-A

data). The latter difference between the two sets of values for $f(l_0)$ and $w(l_0)$ arises from the as yet unexplained dependence of the ^{4}He thermal conductivity on the cell size.[32,55] The same kind of uncertainty may be expected for the ^{3}He-^{4}He thermal-conductivity data and for the ensuing values of the fit parameters given in Eqs. (7.25)–(7.28).

Another source of uncertainty in determining $w_i(l_0)$ and $f_i(l_0)$ is the neglect of the static couplings $\sim q \, |\psi_0|^2$ and $\sim c \, |\psi_0|^2$ in the present model. Including these couplings would lead to additional terms in the flow equations and to an l dependence of the quantity B in Eq. (5.3). Using experimental values for B yields the nonnegligible temperature dependence shown in Fig. 3. The decrease of $B^{\text{expt}}(t)$ toward a small value $B^{\text{expt}}(0) \ll 1$ at T_λ is due to the increase of $C_{P,c}$ for $t \to 0$. In order to test the sensitivity of the present results to this variation of B we have repeated the fit with a smaller value of B. We have found that the fit quality is not very sensitive to a change of B within the range $1 \lesssim B \lesssim 10$, but the initial values $w_i(l_0), f_i(l_0)$ do change. For example, for $B = 3.0$ (corresponding to B^{expt} at $t = 10^{-3}$, $X = 0.05$) we find $w_1(l_0) = 1.24$, $w_2(l_0) = 7.63$, $w_3(l_0) = -0.019$, $f_1(l_0) = 0.137$, and $f_2(l_0) = 0.281$, instead of Eqs. (7.24)–(7.28).[87] These differences yield a reasonable estimate for the uncertainty of the present determination of the background values. Nevertheless, we believe that our present analysis is sufficiently conclusive to explain the main features in the range $X \lesssim O(0.1)$. A fully quantitative treatment of all nonuniversal details is not the purpose of this paper and would require extensive additional computations such as those for model F in the ^{4}He case,[63] as noted in the Introduction.

In Figs. 2(a)–2(c) we have extended toward T_λ

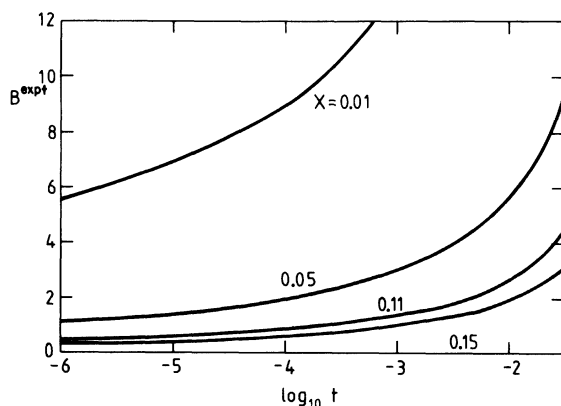FIG. 3. Experimental values for $B^{\text{expt}} = g_1^2 X_c / g_2^2 X_q$ vs t for various X. The curves are obtained from Eqs. (A2), (A4), (A7), and (A8) and from the curves in Fig. 14 in the Appendix.

the theoretical amplitudes (solid curves) outside the range of the experimental data employed for the fit. Thus our theory predicts a measurable increase of R_κ^{expt}, R_D^{expt}, and $R_{k_T}^{\text{expt}}$ in the range $10^{-6} \lesssim t \lesssim 10^{-4}$. It would be interesting to test this prediction. At present it is not possible to determine reliably the true asymptotic value R_D^* since it is quite sensitive to w^* and to the asymptotic value of B^{expt} at T_λ which is not accurately known. Nevertheless, because of $w_2^* \ll 1$, we predict R_D^* to be considerably larger than the observable amplitude $R_D \sim 0.1$. By contrast, R_{k_T} should remain close to $R_{k_T}^*$ for $t < 10^{-4}$ because of the fast transient $\omega_{w_3} = \omega_{F_1}/F_2 = \frac{1}{2}$.

Farther from T_λ our theory predicts an increasing R_D with increasing t for $t > 10^{-3}$ [Fig. 2(a)], due to the strong decrease of $f_2(l)$ as $l \to 1$ according to Fig. 1(e). Furthermore, since $w_3(l)$ changes sign in the background region [Fig. 1(c)] our theoretical R_{k_T} becomes negative for $t \gtrsim 10^{-2}$. These points require further theoretical investigation since the present model is not expected to be fully quantitative in the background region. Additional measurements in the range $t > 10^{-2}$ would be quite interesting.

Finally, in Figs. 4(a)–4(c) we show the comparison between our fits (solid curves) and the data of Gestrich and Meyer[23] for the complete transport coefficients. The solid curves are obtained from Eqs. (7.8)–(7.13), where the static prefactors are taken from experiments (see Appendix). The theoretical and the experimental temperature dependence of R_D in Fig. 2(a) implies an effective critical exponent for D in Fig. 4(a) which deviates slightly from the dynamic-scaling exponent[30,78]-$\nu/2$ in the accessible region (in addition there is an almost negligible effect from the Fisher renormalization[85]). For $t < 10^{-3}$ this deviation is mainly due to the l dependence of $w_2(l)$ shown in Fig. 1(b). A corresponding statement applies to the dashed and dot-dashed curves in Fig. 4(a), which will be explained below.

E. Concentration dependence

It has been demonstrated experimentally[5,13,14,20–23] that the critical behavior of D, k_T, and κ depends on the equilibrium concentration c or X in a nontrivial way. So far this has been studied theoretically[13,44] only for the special case of κ at $T_\lambda(c)$ in the dilute limit $c \to 0$, with conflicting asymptotic results $\kappa(T_\lambda) \sim c^{-1}$ and $\kappa(T_\lambda) \sim c^{-\nu/2}$ due to Siggia[44] and to Kawasaki,[13] respectively. Neither of these results was convincingly confirmed by experiment.[13,20,23,62] Our theory permits us to resolve this problem by predicting the *observable* c
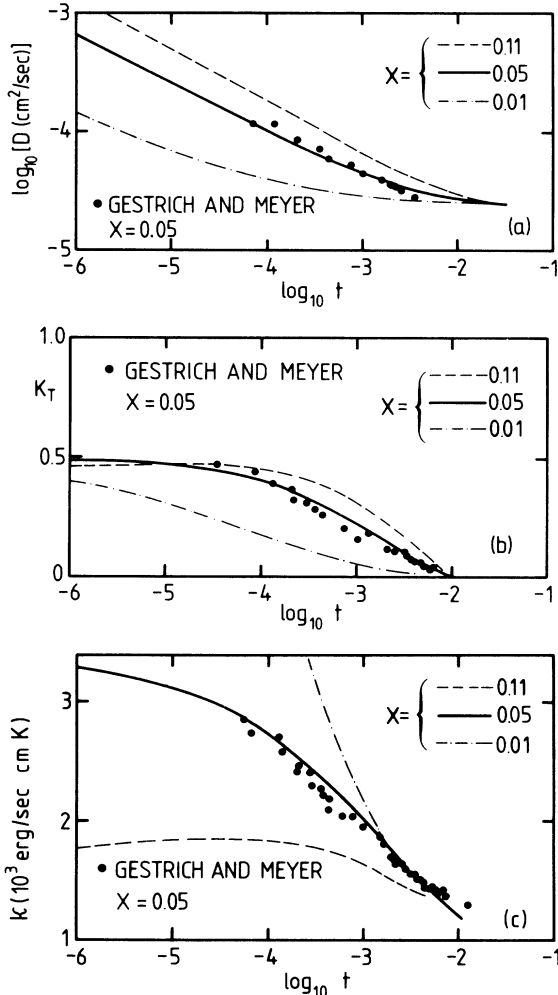
FIG. 4. Transport coefficients D, k_T, and κ vs t. The fit (solid curves) and the data correspond to $X=0.05$ and are obtained from those in Fig. 2 according to Eqs. (7.8)—(7.13) and (7.18)—(7.20), respectively. The dashed and dot-dashed curves are theoretical predictions without adjustable parameters based on extrapolations from $X=0.05$ to $X=0.11$ and 0.01 as described in the text. The corresponding initial conditions are given in Eqs. (7.39) and (7.40) and in Table II.

dependence of κ in the accessible temperature range near T_λ. Furthermore, we present predictions of the present model for the c dependence of D and k_T.

Following Siggia[44] we incorporate the dependence on c via the bare model parameters which represent noncritical background values. The c dependence of the parameters X_c, X_q, g_1, and g_2 is already determined by Eqs. (2.5), (2.8), (2.18), and (2.19) in terms of static quantities which can be taken from experiment. Therefore, we only need to specify the c or X dependence of the bare dynamic parameters Γ_0, K_0, λ_0, and L_0.

We expect that $\Gamma_0(X)$ and $K_0(X)$ are smooth func-

tions of X with finite limiting values for $X \to 0$. The parameters $\Gamma_0(0)$ and $K_0(0)$ are clearly finite since they represent the kinetic coefficients for pure ^{4}He. Furthermore, we expect that in the background the mass diffusivity $D(X)$ and the thermal diffusion factor

$$\alpha_T(X) = \frac{k_T(X)}{X(1-X)} \tag{7.29}$$

depend on X only smoothly. From kinetic theory it is known[88] that $D(X)$ and $\alpha_T(X)$ have finite limiting value as $X \to 0$. According to Eqs. (2.25) and (2.26) we therefore expect that $\lambda_0(X)X_c^{-1}$ and $L_0(X)X^{-1}(1-X)^{-1}$ are the appropriate quantities to be considered as smooth functions of X. In terms of the bare model parameters

$$f_{10} = \frac{g_1^2 \xi_0}{2\pi^2 \Gamma_0 K_0}, \quad f_{20} = \frac{g_2^2 \xi_0}{2\pi^2 \lambda_0 \Gamma_0} \tag{7.30}$$

and

$$w_{10} = \frac{\Gamma_0 X_q}{K_0}, \quad w_{20} = \frac{\Gamma_0 X_c}{\lambda_0},$$

$$w_{30} = \frac{L_0}{(K_0 \lambda_0)^{1/2}}, \tag{7.31}$$

this means that $w_{10}(X)$, $w_{20}(X)$, and $f_{10}(X)$, as well as

$$\frac{w_{30}(X)X_c^{1/2}}{X(1-X)} \equiv \tilde{w}_3 \tag{7.32}$$

and

$$\frac{f_{20}(X)X_c}{g_2^2} \equiv \tilde{f}_2, \tag{7.33}$$

should be smoothly X dependent. Therefore, it suffices to determine w_{10}, w_{20}, f_{10}, $\tilde{w}_3$, and $\tilde{f}_2$ at a few different concentrations and to interpolate smoothly between $X=0$ and $X_t=0.675$. Employing the resulting background values as noncritical initial conditions for our renormalization-group flow equations should then permit a complete treatment of the critical dynamics along the λ line above and below T_λ. Here we have assumed that at some $l_0 \gtrsim O(10^{-1})$ in the background region the renormalized parameters $w_i(l_0)$ and $f_i(l_0)$ have approximately the same concentration dependence as the bare parameters w_{i0} and f_{i0}.

In the following we shall consider only the low-concentration range $X \ll 1$, where Γ_0, K_0, λ_0/X_c, $\tilde{w}_3$, and $\tilde{f}_2$ can be taken to be roughly independent of X. Identifying the initial values given in Eqs. (7.24)—(7.28) with the bare parameters defined in Eqs. (7.30) and (7.31), and using experimental values

for χ_q, χ_c, g_1, and g_2 (at $X = 0.05$, $t_0 = 10^{-3/2}$, see Appendix), we obtain

$$\Gamma_0 = 0.568 \times 10^{-4} \ \mathrm{cm^2/sec} \ , \tag{7.34}$$

$$K_0 = 2.02 \times 10^{18} \ \mathrm{cm^{-1} sec^{-1}} \ , \tag{7.35}$$

$$\lambda_0/\chi_c \equiv D_0 = 7.77 \times 10^{-6} \ \mathrm{cm^2/sec} \ , \tag{7.36}$$

$$\widetilde{w}_3 = -1.18 \times 10^{-12} \ \mathrm{cm^{3/2}} \ , \tag{7.37}$$

$$\widetilde{f}_2 = 1.62 \ \mathrm{sec^2/cm^3} \ . \tag{7.38}$$

These numbers should be considered only as order-of-magnitude estimates for the background values of the transport coefficients.[89–93]

Keeping the parameters (7.34)–(7.38) fixed we can use Eqs. (7.30)–(7.33) to calculate $w_{i0}(X)$ and $f_{i0}(X)$ for arbitrary X within the range $X \ll 1$. This enables us to determine the X dependence of the effective parameters $w_i(l), f_i(l)$ by integrating the flow equations with the initial conditions $w_i(l_0) = w_{i0}(X)$, $f_i(l_0) = f_{i0}(X)$. Consequently, we can predict the critical behavior of the transport coefficients for arbitrary $X \ll 1$ without adjustable parameters. The reliability of this procedure does of course depend on the accuracy of the present model and on the experimental data at $X = 0.05$ which were crucial for identifying the background values given by Eqs. (7.24)–(7.28) or Eqs. (7.34)–(7.38). Note that some uncertainty enters also through the ambiguity for an appropriate value of t_0 or l_0.

We shall apply our concept to the following points: (i) predicting the critical behavior at $X = 0.11$ and 0.15, and comparison with existing data,[2,5,13,14,23] (ii) predicting the results of measurements in very dilute mixtures,[61] and testing consistency with the thermal conductivity[34,94] in pure ^{4}He by extrapolating to $X = 0$, and (iii) resolving the Siggia-Kawasaki problem[44,13] concerning the X dependence of $\kappa(T_\lambda)$.

1. Extrapolation to $X = 0.11$ and 0.15

Our results for $X = 0.11$ are shown by the dashed curves in Figs. 4(a)–4(c). They have been calculated from Eqs. (7.8)–(7.13) with experimental values for the static prefactors. The initial conditions $w_i(l_0)$ and $f_i(l_0)$ have been determined without adjustable parameters by substituting the values given in Eqs. (7.34)–(7.38) into Eqs. (7.30)–(7.33). The result is

$$w_1(l_0) = 0.784, \quad w_2(l_0) = 7.31 \ ,$$
$$w_3(l_0) = -0.0648 \tag{7.39}$$

and

$$f_1(l_0) = 0.281, \quad f_2(l_0) = 0.592 \tag{7.40}$$

at $l_0 = 0.082$ corresponding to $t_0 = 10^{-3/2}$ for $X = 0.11$ (see also Appendix).

We see that the difference with the $X = 0.05$ case is most pronounced for κ [Fig. 4(c)]. The dashed curve shows a weakly nonmonotonous behavior very close to T_λ which results from the temperature dependence[75] of g_1. This feature becomes more pronounced at larger X as indicated by preliminary extrapolations. Whether this should be an observable effect can be answered conclusively only by means of a more complete theory including the static couplings $\sim q |\psi|^2$ and $\sim c |\psi|^2$.

The direct comparison of our theory with the data of Tanaka and Ikushima[14] for κ and k_T is shown in Figs. 5(a) and 5(b). The agreement with the κ data is excellent, which is perhaps partly fortuitous. Also for the k_T data the agreement is well within the expected accuracy of the present model (and of the data). It should be noted that the k_T data of Tanaka and Ikushima are higher than suggested by interpolating between the $X = 0.15$ and 0.05 data of Gestrich and Meyer.[23] Furthermore, the k_T data of Tanaka and Ikushima[14] (for $X = 0.23$ and 0.33) do not show the expected X dependence $(k_T \sim X)$ in the background region.

A conclusive comparison between our dashed curves in Fig. 4(a) and the measurements by Ahlers and Pobell[5] at $X = 0.10$ is not possible since the relation which converts their measured relaxation time τ into the desired values for D is not accurately known. With simplifying assumptions about the geometry of the cell and about the boundary conditions one would expect the relation[95] $D = (L/\pi)^2 \tau^{-1}$ corresponding to Eq. (19) of Behringer and Meyer[21] for $n = 1$, where L is a characteristic length of the cell. Use of this relation and identification of L with the height[5] $H = 0.6$ cm yields experimental values for D which agree with our dashed curve in Fig. 4(a) within 15%.

In this context we comment on the indirect estimate of the damping coefficient D_2 for second sound presented by Tanaka and Ikushima.[14] These authors employed values for D which were calculated from the data[5] for τ via the Ahlers-Pobell formula[5] $D = L^2/\tau$ with $L \sim 0.7$ cm, and obtained values for D_2 which disagreed with those of Ahlers[96] and of Crooks and Robinson[97] by a factor of 5 (see also Ikushima,[26] Secs. 3.3.5 and 3.3.6). We have found that using the Behringer-Meyer relation $D = (H/\pi)^2 \tau^{-1}$ essentially eliminates the major inconsistencies. Nevertheless, we expect the simple procedure of Tanaka and Ikushima[14] to yield an order-of-magnitude estimate only; in particular, their formula for D_2 does not take into account the non-negligible contribution D_ζ related to the order-parameter damping below T_λ.[98]
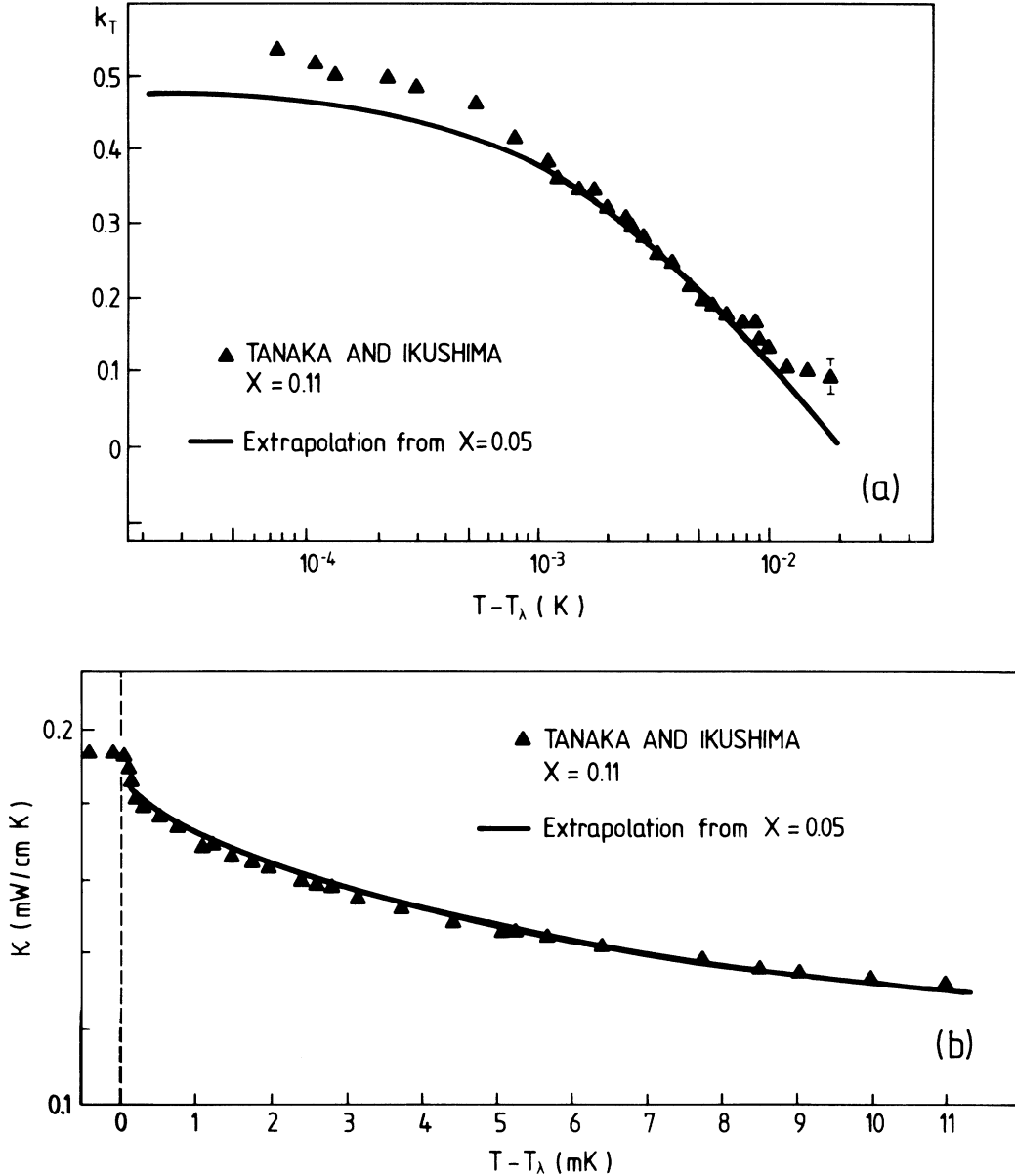
FIG. 5. Comparison between our theoretical extrapolations (solid curves) and experimental data of Ref. 14 for k_T and κ at $X=0.11$. The curves are calculated without adjustable parameters and are identical with the dashed curves in Fig. 4.

Next we present our extrapolation to $X=0.15$. Substituting the parameters of Eqs. (7.34)—(7.38) into Eqs. (7.30)—(7.33) yields the initial conditions

$$w_1(l_0)=0.787, \quad w_2(l_0)=7.31 ,$$
$$w_3(l_0)=-0.072 \tag{7.41}$$

and

$$f_1(l_0)=0.266, \quad f_2(l_0)=0.810 \tag{7.42}$$

at $l_0=0.077$ corresponding to $t_0=10^{-3/2}$ for $X=0.15$ (see also Appendix). The resulting transport coefficients can be calculated from Eqs.

(7.8)—(7.13) without adjustable parameters. They are shown in Figs. 6(a)—6(c) (solid curves) and are compared with the data of Gestrich and Meyer[23] and of Ahlers.[2] The agreement with D and k_T [Figs. 6(a) and 6(b)] is reasonable and well within the expected accuracy of the present theory.[99] The same statement holds for κ for $t > 10^{-3.5}$ [Fig. 6(c)]. The deviations of $O(15\%)$ for $t < 10^{-3.5}$, however, seem to indicate a systematic inaccuracy of the present model. In particular, the decrease of κ for $t < 10^{-4}$, which in the present treatment results from the temperature dependence of g_1,[75] is not supported by the data. We consider the neglect of the static couplings
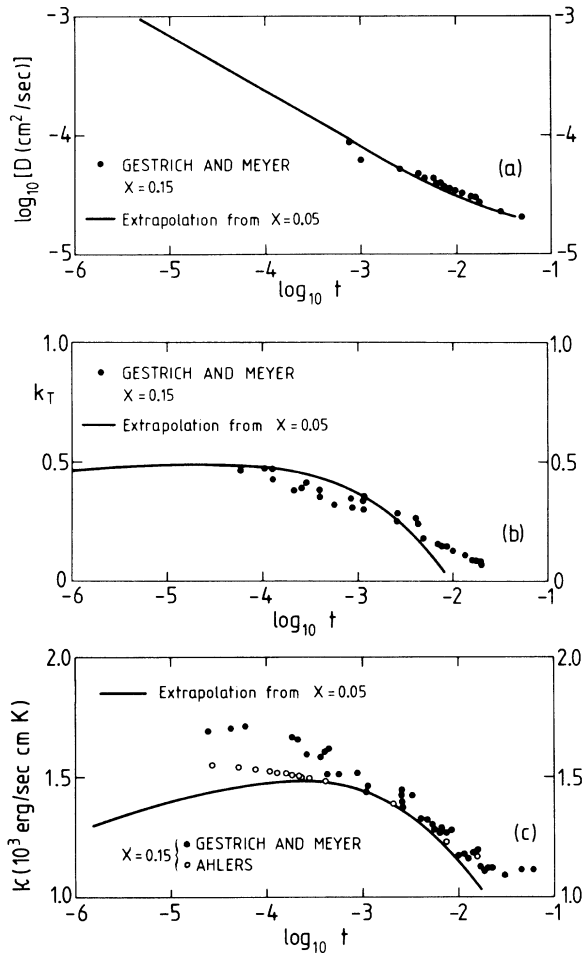
FIG. 6. Comparison between our theoretical extrapolations (solid curves) and experimental data for D, k_T, and κ of Ref. 23 and for κ of Ref. 2 at $X=0.15$. The curves are calculated without adjustable parameters in the same way as the solid curves in Figs. 4 and 5, with initial conditions given in Eqs. (7.41) and (7.42).

$\sim q \, |\Psi|^2$ and $\sim c \, |\Psi|^2$ in the present analysis as the main source of inaccuracies on the theoretical side. Also the extrapolation procedure employing the X-independent parameters of Eqs. (7.34)—(7.38) should be corrected for $X > 0.1$. It remains to be seen whether the systematic deviations from the data in Fig. 6(c) are eliminated in a more complete analysis of the model-F type. It should be noted, on the other hand, that also the data[2,23] themselves are not highly precise, as indicated by the differences in Fig. 6(c), and may be subject to uncertainties due to cell-size effects similar to those in pure ^{4}He,[32,55,94] which are as yet unexplained.

2. Extrapolation to dilute mixtures

The study of very dilute mixtures is of particular interest since at small X the temperature dependence

of κ is expected to exhibit a nontrivial crossover between pure ^{4}He-like behavior farther from T_λ and the ultimate λ-line behavior very close to T_λ. Corresponding measurements are planned by Meyer and co-workers.[61]

Our theoretical results for the transport coefficients at $X=0.01$ are shown by the dot-dashed curves in Figs. 4(a)—4(c). In addition, Fig. 7 shows the predicted temperature dependence of κ for $X=0.01$ and 0.005. [The corresponding initial conditions $w_i(l_0)$ and $f_i(l_0)$ are given in the Appendix.] It is understood that these predictions are not to be considered as highly precise since the present model is not yet complete. Nevertheless, our curves should correctly predict the trend of the observable temperature dependence.

As a test for our procedure we have also performed the $X \to 0$ limit (based on the data[23] at $X=0.053$). The resulting curve for κ can then be compared with existing thermal-conductivity data[94] for pure ^{4}He. This comparison is shown in Fig. 7
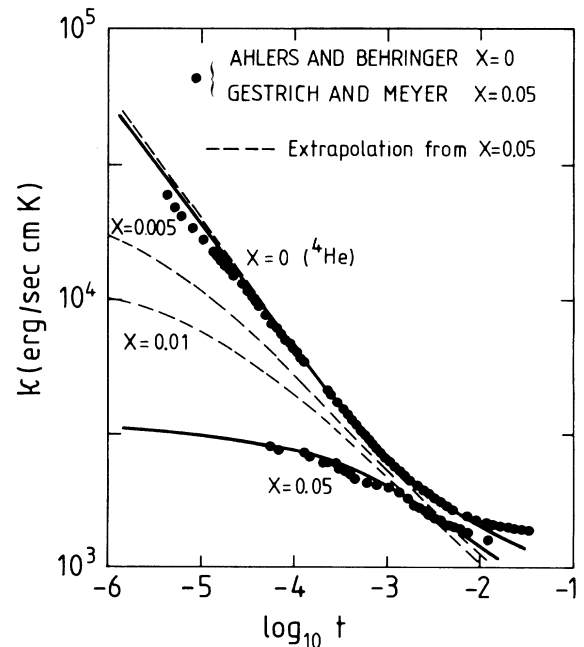

FIG. 7. Thermal conductivity κ vs t on logarithmic scales. The lower data refer to $X=0.05$ and are identical with those shown in Fig. 4(c). The upper set of data are the cell-A data for pure ^{4}He from Ref. 55. The lower solid curve is the four-parameter fit corresponding to the solid curves in Figs. 2(c) and 4(c). The upper solid curve is a (two-parameter) model-E fit using the data for $t < 10^{-2}$ (with the weights suggested in Ref. 55). The dashed curves are theoretical extrapolations from $X=0.05$ to $X=0.01$, 0.005, and 0, respectively, without adjustable parameters. The corresponding initial conditions are given in Table II.

(upper dashed curve and upper set of data). We at-
tribute the systematic deviations from the ^{4}He data
for $t < 10^{-5}$ and $t > 10^{-3}$ mainly to the inaccuracy
of the present model rather than to our extrapola-
tion procedure. For comparison we have also shown
the best fit to the ^{4}He data using model E (upper
solid curve in Fig. 7). The deviations of the data
from the upper solid and dashed curves provide a
realistic estimate for the degree of inaccuracy that
we have to expect at the present stage of the theory
for ^{3}He-^{4}He mixtures.

3. The Siggia-Kawasaki problem

Since $\kappa(T_\lambda)$ is infinite in pure ^{4}He and finite in
^{3}He-^{4}He mixtures it is an interesting theoretical
problem[13,44] to predict the type of divergence of
$\kappa(T_\lambda)$ as a function of the concentration c in the di-
lute limit $c \rightarrow 0$. On the other hand, we have seen in
Fig. 7 that the asymptotic value $\kappa(T_\lambda)$ is not observ-
able for small c. Therefore, the more relevant ques-
tion is to study the concentration dependence of κ at
finite relative temperature $t > 0$. With the extrapola-
tion procedure described above our theory provides a
quantitative answer which is illustrated in Fig. 8.
At the accessible relative temperatures $t = 10^{-3.5}$,
$10^{-4.5}$, and $10^{-5.5}$ the curves predict an increasing κ
with decreasing X which saturates at roughly
$X = 10^{-2.5}$, 10^{-3}, and $10^{-3.5}$, respectively. Thus we
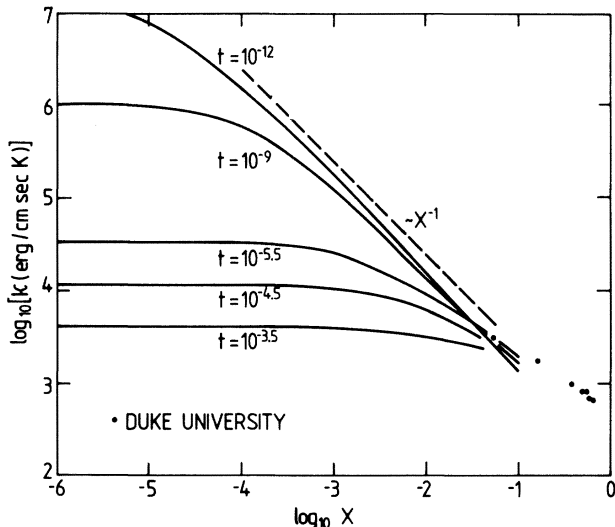

FIG. 8. Thermal conductivity κ vs X on logarithmic
scales at constant t. The dots correspond to the maximal
values of the data of Refs. 20 and 23 very close to T_λ, ac-
cording to Ref. 61. The curves are our theoretical extra-
polations without adjustable parameters, based on the fit
at $X = 0.05$ shown in Figs. 2 and 4, as described in the text
and in the Appendix. The dashed line has the slope -1
corresponding to a power law $\sim X^{-1}$ and is shown for
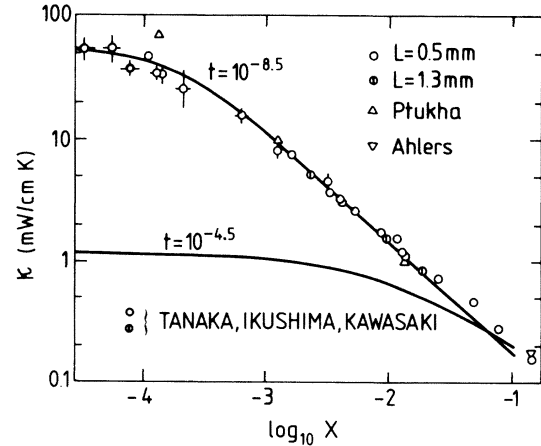comparison with the curve at $t = 10^{-12}$.

FIG. 9. Thermal conductivity κ vs X on logarithmic
scales. The data are identical with those shown in Fig. 2
of Ref. 13 and in Fig. 19 of Ref. 26. The solid curves are
our theoretical extrapolations without adjustable parame-
ters. The lower curve is identical with the curve at
$t = 10^{-4.5}$ shown in Fig. 8; the upper curve is calculated at
$t = 10^{-8.5}$.

do not expect a simple power-law behavior but rath-
er a crossover behavior in the experimentally acces-
sible regime, in contrast to the previous predictions
by Siggia[44] and by Kawasaki.[13]

The reason for the unobservability of a power law
is mainly the shrinking (as $X \rightarrow 0$) of the asymptotic
region where $w_3(l) \approx 1$ [see Fig. 1(c)]. In order to il-
lustrate this point we have extended our analysis to
$t = 10^{-9}$ and 10^{-12}, corresponding to the two upper
curves in Fig. 8. Now we see that κ does indeed ap-
proach a power-law behavior $\sim X^{-1}$ at extremely
small t over two decades in X until, for $X \rightarrow 0$, it
shows the final crossover to a finite ^{4}He value be-
cause t is finite. From these results which are based
on numerical integration of our two-loop flow equa-
tions we infer that at T_λ the thermal conductivity κ
diverges as

$$\kappa(T_\lambda) \sim X^{-1} \sim c^{-1} . \tag{7.43}$$

This agrees with Siggia's prediction[44] based on a
one-loop calculation, but disagrees with the predic-
tion $\kappa(T_\lambda) \sim X^{-\nu/2}$, $\nu/2 \approx \frac{1}{3}$ of Tanaka, Ikushima,
and Kawasaki[13] based on an ad hoc scaling assump-
tion. We note that according to Eq. (5.40) the ana-
lytic proof of Eq. (7.43) would consist of determin-
ing the X dependence of the subleading amplitude
$A_3(0)$ of $w_3(l)$, Eq. (5.35). We conjecture that the
asymptotic power law (7.43) remains valid in all or-
ders of perturbation theory.

Our nonasymptotic theory is consistent with the
data of Meyer and co-workers[20,23] for κ very close to

T_λ (dots in Fig. 8) which do not exhibit the asymptotic X dependence $\sim X^{-1}$ for $X > 0.05$. This is seen to be in agreement with our theoretical prediction at some t between $t = 10^{-4.5}$ and $10^{-5.5}$. (For a comment on new data at $X < 0.05$ see *Note added in Proof.*)

Finally we turn to the work of Tanaka, Ikushima, and Kawasaki.[13] Their data for κ very close to T_λ together with those of Ptukha[1] (extrapolated from below T_λ) and of Ahlers[2] are shown in Fig. 9. Unfortunately, we do not precisely know at what distance t from T_λ these data have been actually measured. A realistic assumption may be $t = 10^{-4.5}$. Our corresponding theoretical curve, which is based on extrapolations from the $X = 0.05$ data without adjustable parameters, is shown as the lower curve in Fig. 9. This is in considerable disagreement with the data for $X < 10^{-2}$. We can reproduce the data only if we extrapolate our theoretical result to the unrealistic value $t \sim 10^{-8.5}$ (upper curve in Fig. 9). We doubt, however, whether for $X < 0.01$ these data can be considered as quantitatively reliable since the data at $X = 0$ shown in Fig. 1 of Ref. 13 and in Fig. 2 of Ref. 26 are much higher than the pure ^{4}He data of Ahlers[34] and of Ahlers and Behringer.[94] New measurements very close to T_λ and at very small X are therefore highly desirable. (See *Note added in proof.*)

VIII. LIGHT SCATTERING SPECTRUM FOR $T \geq T_\lambda(c)$

An important application of our theory is the prediction of the dynamic structure factor $S(k,\omega)$ near $T_\lambda(c)$ without adjustable parameters. This provides the possibility of an independent test of the theory by means of light scattering experiments.

As noted by Rockwell, Benjamin, and Greytak,[40] Brillouin scattering from ^{3}He-^{4}He mixtures is predominantly determined by the local fluctuations $\delta n(\vec{x},t)$ of the number density $n = (N_3 + N_4)/V$ of helium atoms,

$$S(k,\omega) = \text{const} \int d^3x \int dt \langle \delta n(\vec{x},t)\delta n(0,0)\rangle$$

$$\times \exp[-i(\vec{k}\cdot\vec{x} - \omega t)] . \tag{8.1}$$

Neglecting fluctuations of the pressure one can express δn in terms of fluctuations of the mass concentration δc and of the temperature $\delta T \sim q$ according to

$$\delta n(\vec{x},t) = T\chi_q^{-1}\left[\frac{\partial n}{\partial T}\right]_{P,c} q(\vec{x},t)$$

$$+ \left[\frac{\partial n}{\partial c}\right]_{P,T} \delta c(\vec{x},t) , \tag{8.2}$$

with q and χ_q defined in Eqs. (2.7) and (2.8). Thus we obtain

$$S(k,\omega) = \text{const}\{ a_{qq}C_{qq}(k,\omega)$$

$$+ a_{qc}[C_{qc}(k,\omega) + C_{cq}(k,\omega)]$$

$$+ a_{cc}C_{cc}(k,\omega)\} , \tag{8.3}$$

where $C_{\alpha\beta}$ denotes correlation functions analogous to that defined in Eq. (2.57). The static coefficients are

$$a_{qq} = T^2\chi_q^{-2}\left[\left[\frac{\partial n}{\partial T}\right]_{P,c}\right]^2 , \tag{8.4}$$

$$a_{qc} = T\chi_q^{-1}\left[\frac{\partial n}{\partial T}\right]_{P,c}\left[\frac{\partial n}{\partial c}\right]_{P,T} , \tag{8.5}$$

$$a_{cc} = \left[\left[\frac{\partial n}{\partial c}\right]_{P,T}\right]^2 . \tag{8.6}$$

A. Evaluation in one-loop order

We use our expressions for the correlation functions $C_{\alpha\beta}$ given in Eqs. (2.64)–(2.70) as well as our one-loop results for the vertex functions $\Gamma_{\alpha\beta}$ according to Eqs. (4.2)–(4.11). No new computations are necessary since we can employ the previous analytic result for the one-loop integral $I^{(1)}(k,\omega)$, Eq. (4.8), as given in Eqs. (4.7)–(4.10) of Ref. 49 for arbitrary k,ω, and τ_0 in $4 - \epsilon$ dimensions. We only need to substitute the effective parameters $w_i(l)$, $F_i(l)$, and $\tau(l)$, in complete analogy to Eqs. (3.2) and (3.3) of Ref. 53 for the case of pure ^{4}He. This leads to the results

$$\Gamma_{q\bar{q}} = -i\omega + K(l)k^2[1 + f_1(l)\Pi(k,\omega)] , \tag{8.7}$$

$$\Gamma_{c\bar{c}} = -i\omega + \lambda(l)k^2[1 + f_2(l)\Pi(k,\omega)] , \tag{8.8}$$

$$\Gamma_{q\bar{c}} = (\chi_c/\chi_q)^{1/2}L(l)k^2$$

$$\times [1 + F_1(l)F_2(l)w_3(l)^{-1}\Pi(k,\omega)] , \tag{8.9}$$

where

$$\Pi(k,\omega)=F(y,\theta)-\tfrac{1}{4}\ln[(\theta-y)k^2/\mu^2l^2] ,$$

(8.10)

with

$$F(y,\theta)=y+(2y^2-y+\theta-\tfrac{1}{4})\ln\left|\frac{\theta-\tfrac{1}{4}}{\theta-y}\right|$$

$$+2y(y^2-y+\theta)^{1/2}\ln\left|\frac{2y-1+2(y^2-y+\theta)^{1/2}}{2y+1-y\theta^{-1}+2(y^2-y+\theta)^{1/2}}\left(1-\frac{y}{\theta}\right)\right| .$$

(8.12)

The other vertex functions $\Gamma_{\tilde{q}\tilde{q}}$, $\Gamma_{\tilde{c}\tilde{c}}$, $\Gamma_{\tilde{q}\tilde{c}}$, $\Gamma_{\tilde{c}\tilde{q}}$, $\Gamma_{\tilde{q}q}$, and $\Gamma_{\tilde{c}c}$ are determined in one-loop order by Eqs. (4.9)—(4.11) and by the relations

$$\Gamma_{\tilde{c}\tilde{q}}(k,\omega)=\Gamma_{\tilde{q}\tilde{c}}(k,\omega) ,$$

(8.13)

$$\Gamma_{\tilde{q}q}(k,\omega)=\Gamma_{q\tilde{q}}(k,-\omega) ,$$

(8.14)

$$\Gamma_{\tilde{c}c}(k,\omega)=\Gamma_{c\tilde{c}}(k,-\omega) .$$

(8.15)

The effective kinetic coefficient $\Gamma(l)$ in Eq. (8.11) can be rewritten as

$$\Gamma(l)=w_1(l)K(l)=w_2(l)\lambda(l) ,$$

with $K(l)$ and $\lambda(l)$ given by Eqs. (4.26) or (4.27), respectively. Since our results are valid both in the hydrodynamic and in the critical region we relate l to k and ω by generalizing Eq. (4.20) to

$$\left|\frac{\tau(l)}{\mu^2l^2}+\frac{k^2}{4\mu^2l^2}-\frac{i\omega}{2\Gamma(l)\mu^2l^2}\right|=1 ,$$

(8.16)

as suggested by the logarithmic term in Eq. (8.10). This implies

$$\Pi(k,\omega)=F(y,\theta)-\frac{i}{4}\arctan\frac{2\omega}{\Gamma(l)[k^2+4\tau(l)]} .$$

(8.17)

The dynamic structure factor is finally obtained by substituting our results into Eq. (8.3). It predicts the dependence of the light scattering spectrum on k and ω for $T\geq T_\lambda(c)$ without adjustable parameters, provided that the effective parameters $w_i(l)$ and $F_i(l)$ have been identified. In the limit $c\to 0$, $S(k,\omega)$ reduces to the entropy correlation function which was presented by Dohm and Folk [Eqs. (3.2)—(3.7) of Ref. 53] and was subsequently discussed by Hohenberg and Sarkar.[100]

B. Application to the hydrodynamic region

In the following we present explicit results for the hydrodynamic region $k\xi\ll 1$. There Eq. (8.16)

$$y\equiv\frac{i\omega}{2\Gamma(l)k^2} , \quad \theta\equiv\tfrac{1}{4}+\frac{\tau(l)}{k^2} ,$$

(8.11)

and

reduces to Eq. (4.20), and instead of Eq. (8.12) we only need the limiting hydrodynamic value[49]

$$F(0,\infty)=-\tfrac{1}{4} .$$

(8.18)

In this limit Eqs. (8.7)—(8.9) simplify to Eqs. (4.23)—(4.25). This leads to Eq. (4.36) and to

$$C_{qc}(k,\omega)=2k^2k_TD\frac{\omega^2-\Gamma_0\Gamma_2}{(\omega^2+\Gamma_0^2)(\omega^2+\Gamma_2^2)}=C_{cq}(k,\omega)$$

(8.19)

and

$$C_{cc}(k,\omega)=2k^2\chi_c\frac{D\omega^2+D_s\Gamma_0\Gamma_2}{(\omega^2+\Gamma_0^2)(\omega^2+\Gamma_2^2)} ,$$

(8.20)

with the linewidths Γ_0,Γ_2 given by Eq. (4.37). Using Eq. (8.3) we arrive at the following hydrodynamic expression for the dynamic structure factor:

$$S(k,\omega)=\text{const}\times 2k^2\frac{a\omega^2+b\Gamma_0\Gamma_2}{(\omega^2+\Gamma_0^2)(\omega^2+\Gamma_2^2)} ,$$

(8.21)

$$a=a_{qq}\chi_qD_s+2a_{qc}k_TD+a_{cc}\chi_cD ,$$

(8.22)

$$b=a_{qq}\chi_qD-2a_{qc}k_TD+a_{cc}\chi_cD_s .$$

(8.23)

The dependence of D, D_s, k_T, and of $\Gamma_{0,2}$ on temperature and concentration is predicted by our theory while the coefficients $a_{\alpha\beta}$ can be taken from static experiments as described in the Appendix.

Equation (8.21) can be written as the sum of two Lorentzians,

$$S(k,\omega)=\text{const}\times 2\left[A_0\frac{\Gamma_0}{\omega^2+\Gamma_0^2}+A_2\frac{\Gamma_2}{\omega^2+\Gamma_2^2}\right] ,$$

(8.24)

which correspond to the normal modes related to concentration fluctuations and thermal fluctuations analogous to those given in Eqs. (33)—(36) of Ref.

40 below T_λ. From Eqs. (4.36) and (8.19)—(8.21) we can identify the amplitudes as

$$A_0 = \frac{a\Gamma_0 - b\Gamma_2}{\Gamma_0^2 - \Gamma_2^2} k^2 , \qquad (8.25)$$

$$A_2 = \frac{b\Gamma_0 - a\Gamma_2}{\Gamma_0^2 - \Gamma_2^2} k^2 . \qquad (8.26)$$

Integration over ω yields the static structure factor

$$S_0 = \int_{-\infty}^{\infty} \frac{d\omega}{2\pi} S(k,\omega) = \text{const}(A_0 + A_2) , \qquad (8.27)$$

with

$$A_0 + A_2 = a_{qq}\chi_q + a_{cc}\chi_c . \qquad (8.28)$$

Here the contributions $\sim a_{qc}$ are canceled. This is due to the vanishing of the equal-time correlation function

$$\int_{-\infty}^{\infty} d\omega\, C_{qc}(k,\omega) = 0 , \qquad (8.29)$$

since there is no static coupling between q and c within the present model. Including the couplings $\gamma_1 q \, |\psi|^2$ and $\gamma_2 c \, |\psi|^2$ in the Hamiltonian would yield an additional term proportional to $\gamma_1(l)\gamma_2(l)$ on the rhs of Eqs. (8.28) and (8.29). We expect the corresponding corrections to Eqs. (8.25) and (8.26) to be small for $c \ll 1$.

The hydrodynamic structure factor, Eq. (8.24), is completely characterized by the linewidths Γ_0, Γ_2 and the amplitudes A_0, A_2. Their dependence on temperature and concentration in the range $X \leq 0.05$ is shown in Figs. 10 and 11. These predictions follow from using in Eqs. (4.37) and (8.22)—(8.26) the results for the transport coefficients D, k_T, and κ de-
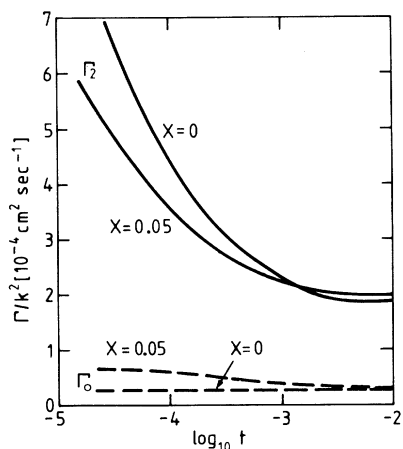

FIG. 10. Hydrodynamic linewidths Γ_0 (dashed curves) and Γ_2 (solid curves) entering the dynamic structure factor $S(k,\omega)$, Eq. (8.24). For $X=0$ (pure ^{4}He) compare Fig. 8 of Ref. 53, Fig. 9 of Ref. 54, Fig. 6 of Ref. 100, and Fig. 7 of Ref. 105. The vertical scale is normalized to k^2.
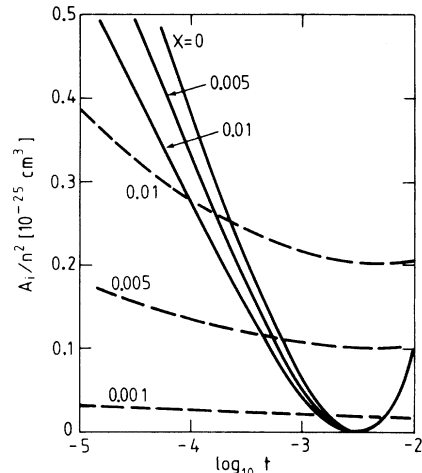

FIG. 11. Hydrodynamic amplitudes A_0 (dashed curves) and A_2 (solid curves) entering the dynamic structure factor $S(k,\omega)$, Eq. (8.24). The intersections between the dashed and solid curves at a particular concentration X determine the crossover temperature $t_c(X)$, where $A_0/A_2 = 1$. The vertical scale is normalized to n^2 with $n = (N_3 + N_4)/V$ being the density of He particles.

rived in Sec. VII. The curves at $X = 0.05$ correspond to the solid curves in Fig. 4. The curves for $X < 0.05$ are extrapolations without adjustable parameters corresponding to the extrapolation procedure of Sec. VII E (see also the Appendix). The applicability of these results is of course limited to the hydrodynamic region. For a finite wave number $k \sim 10^5$ cm^{-1} this means that the curves in Figs. 10 and 11 can be used only for $t > 10^{-4}$ corresponding to $k\xi < 1$.

We briefly discuss the consequences for the shape of the dynamic structure factor. The linewidths Γ_0 and Γ_2 are only weakly X dependent for $X \ll 1$, with finite limiting values $k^2 D$ and $k^2 D_s = k^2 D_T$, respectively, for $X \to 0$, $t > 0$ (see Fig. 10). The shape of the dynamic structure factor is governed by the strong X dependence of the ratio A_0/A_2. In the range $0 \leq X \leq 0.05$ it varies between $A_0/A_2 \gg 1$ at $X = 0.05$ and $A_0/A_2 = 0$ for $X = 0$. In these two cases we have a Lorentzian shape, with a halfwidth at half-height Γ_0 of $\Gamma_0/k^2 \sim 0.5 \times 10^{-4}$ cm^2/sec typical for the λ line, and with a halfwidth Γ_2 of $\Gamma_2/k^2 \sim 2 \times 10^{-4}$ cm^2/sec typical for pure ^{4}He, respectively. More interesting is the crossover between these two types of Lorentzians. According to Fig. 11 our theory provides a prediction where this crossover region with $A_0/A_2 \sim O(1)$ should occur. This depends on t due to the temperature dependence of A_2 (Fig. 11). The strong decay of A_2 toward the minimum near $t = 10^{-2.5}$ is a combined effect of the vanishing of a_{qq} (due to the vanishing of
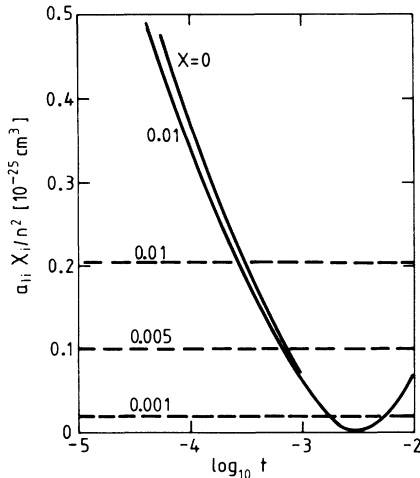
FIG. 12. Contributions $a_{cc}X_c$ (dashed lines) and $a_{qq}X_q$ (solid curves) to the static structure factor S_0, Eqs. (8.27) and (8.28), as obtained from experimental values according to the Appendix. The intersections between the dashed and solid curves determine the static crossover temperature where $a_{cc}X_c/a_{qq}X_q = 1$. The vertical scale is normalized to n^2 (compare Fig. 11).

the thermal expansion coefficient; see the Appendix) and of the smallness of k_T in this regime. We note that the dynamic crossover temperature $t_c(X)$, where $A_0/A_2 \sim O(1)$, is comparable to the static crossover temperature, where $a_{cc}X_c/a_{qq}X_q \sim O(1)$, as illustrated in Fig. 12. Both crossover temperatures would be identical if $k_T = 0$, in which case $A_0/A_2 = a_{cc}X_c/a_{qq}X_q$. In Fig. 13 two shapes typical for the crossover region are presented, with a ratio $A_0/A_2 = 0.35$ in both cases. The non-Lorentzian structure is well pronounced. It would be interesting if these predictions could be tested by light scattering experiments of sufficiently high resolution.

Note added in proof. Very recently new measurements of κ in the range $10^{-3} \lesssim X \lesssim 10^{-2}$ and $10^{-6} \lesssim |t| \lesssim 10^{-1}$ have been made by Gestrich, Dingus, and Meyer (private communication). Their data confirm our prediction presented in Fig. 8 that for $X \ll 0.1$ the asymptotic value $\kappa(T_\lambda)$ is not experimentally observable on the normal side $(T > T_\lambda)$ of the λ line. This can be explained, according to Eqs. (5.37)–(5.41), in terms of the amplitude $A_3(l)$ or of $w_3(l)$, Eq. (5.35). For very small X, w_3 is very small in the background region, therefore it takes many decades of l until $w_3(l)$ reaches its asymptotic region $w_3 \approx 1$, hence R_κ comes close to R_κ^* only extremely close to T_λ if $X \ll 1$. For larger $X \gtrsim 0.1$, R_κ is close to R_κ^* already near $t \sim 10^{-6}$ because in this case $w_3(l) \approx 1$ already for $t \sim 10^{-6}$ [see Fig. 1(c)]. In summary, although the small transient exponent ω_w is the reason for the smallness of the asymptotic region for κ_s and D, this is not the case for k_T and κ.
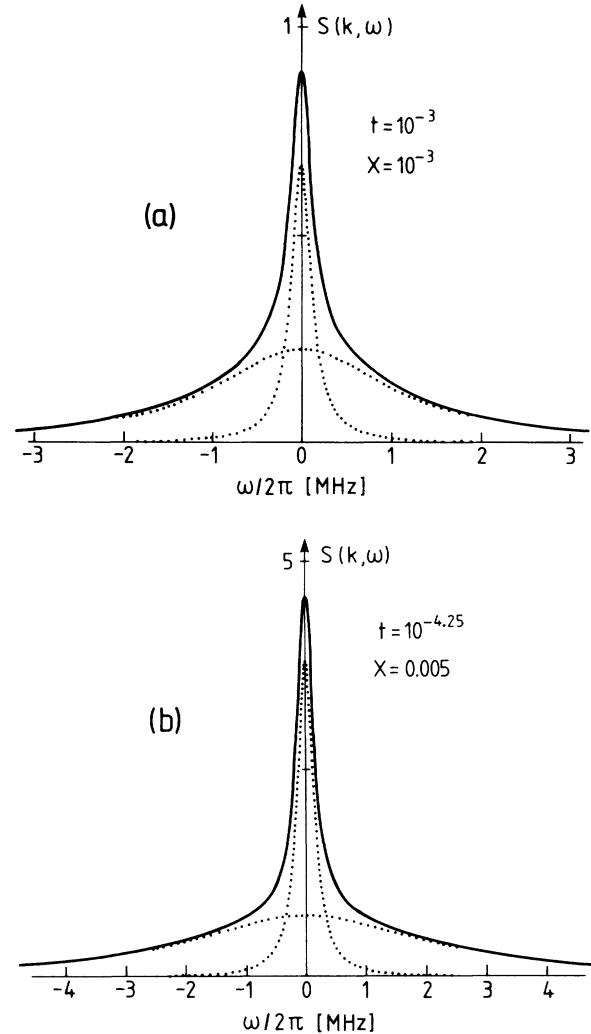

FIG. 13. Theoretical prediction for the shape of the dynamic structure factor, Eq. (8.24) (solid curves). The dotted curves represent the Lorentzian contributions $\sim A_0$ and $\sim A_2$ of the two normal modes, with $A_0/A_2 = 0.35$. The frequency scales are given for the example of $k = 1.8 \times 10^5$ cm^{-1} (Ref. 40). In part (a), $t = 10^{-3}$ and $X = 10^{-3}$; in part (b) $t = 10^{-4.25}$ and $X = 0.005$. [Note that the latter case lies in the hydrodynamic region only for $k < 10^5$ cm^{-1}.] The vertical scales of parts (a) and (b) have the same units.

The latter quantities reach their asymptotic values with the fast transient exponent $\epsilon/2$, in agreement with Siggia and Nelson[43] and with Onuki [J. Low Temp. Phys. (in press)], provided that $X \gtrsim 0.1$. We note that Onuki's theory is restricted to the asymptotic region and therefore does not describe the l dependence of $w_3(l)$. In particular we have found by means of our nonasymptotic theory that Onuki's asymptotic result, Eq. (6.12), should not be observable in the range of the recent experiment by Gestrich, Dingus, and Meyer mentioned above. We

thank H. Meyer and A. Onuki for useful correspondence.

APPENDIX: STATIC QUANTITIES

In this appendix we present the necessary information on the static quantities employed in the comparison with experiments. Following the convention of the experimental literature[24-26] we shall use, instead of c and Δ, the molar quantities X and ϕ. The molar concentration is given by

$$X = \frac{N_3}{N_3 + N_4} = \frac{n_3}{n_3 + n_4} , \quad (A1)$$

where n_i denotes the number of moles of ^{3}He or ^{4}He atoms. In terms of X, Eq. (2.19) becomes

$$g_2 = \frac{k_B T}{\hbar} \frac{m_3 m_4 X}{[m_3 X + m_4 (1-X)]^2} \frac{V_{mol}}{N_A} , \quad (A2)$$

where $V_{mol} = V/(n_3 + n_4)$, with V being the total volume of the mixture and $N_A = 6.02 \times 10^{23}$ mole^{-1} is Avogadro's constant.

The chemical potential conjugate to X is defined as $\phi = (\partial g / \partial X)_{P,T}$, with $g = G/(n_3 + n_4) = g(T,P,X)$ being the Gibbs free energy per mole of solution. This implies

$$\phi = \mu_3 - \mu_4 = N_A (\tilde{\mu}_3 - \tilde{\mu}_4) , \quad (A3)$$

where $\tilde{\mu}_i$ and μ_i denote the chemical potentials per particle (see the definition in Sec. II) and per mole, respectively, with

$$\mu_3 = (\partial G / \partial n_3)_{P,T,n_4} = N_A \tilde{\mu}_3$$

and similarly $\mu_4 = N_A \tilde{\mu}_4$. Our ϕ is identical with ϕ used in Refs. 24 and 75 and with Δ used in Refs. 20–22 and 41. Furthermore, our $\Delta, \tilde{\mu}_i$, and μ_i are identical with $\phi^K, m_i \mu_i^K$, and μ_i, respectively, of Refs. 24 and 75. [Note that Eq. (3.8) of Ref. 75 has been corrected by Eqs. (2.1.75) and (2.1.76) of Ref. 24, but μ_i^K is not correctly defined in Eq. (2.6) of Ref. 75 or in Eqs. (2.2.35) and (2.2.36) of Ref. 24.] With the use of the relation between $(\partial \phi / \partial X)_{P,T}$ and $(\partial \Delta / \partial c)_{P,T}$ given by Eq. (2.2.40) of Ref. 24 one can express X_c, Eq. (2.5), in terms of X and ϕ as
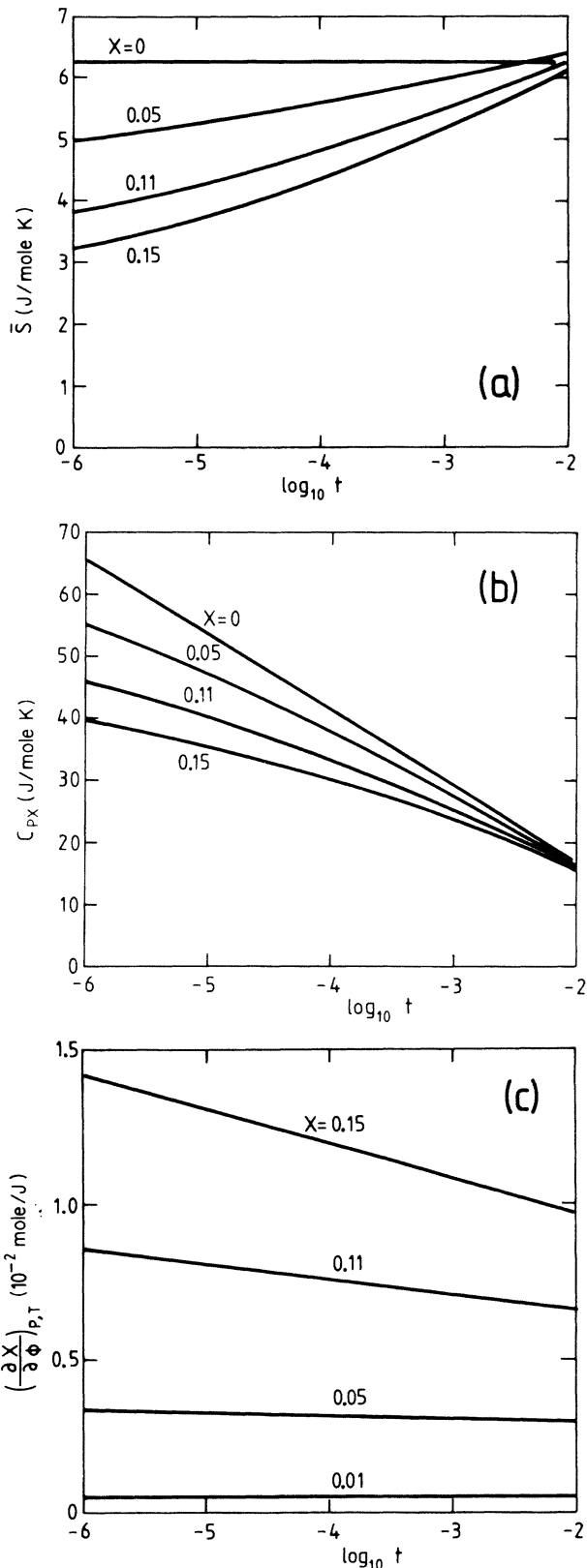

FIG. 14. Static quantities, Eqs. (A5) and (A6), and $(\partial X / \partial \phi)_{P,T}$ taken from experiments (for references see text). See also Fig. 1 of Ryschkewitsch and Meyer [J. Low Temp. Phys. 35, 103 (1979)].

TABLE I. Experimental values for static quantities at $t = 10^{-1.5}$. For $X = 0.05$ they are used in Eqs. (7.30)—(7.33) for calculating from Eqs. (7.24)—(7.28) the parameters given in Eqs. (7.34)—(7.38). For $X = 0.11$ and 0.15 they are used in Eqs. (7.30)—(7.33), with the parameters of Eqs. (7.34)—(7.38) kept fixed, to extrapolate the dynamic parameters w_{i0} and f_{i0} from $X = 0.05$ to $X = 0.11$ and 0.15. The extrapolated values are given in lines 7 and 8 of Table II.

X	g_1 (10^{11} sec^{-1})	g_2 (10^{-13} cm^{3}sec^{-1})	χ_q (10^{22} cm^{-3})	χ_c (10^{-24} cm^3)
0.053	2.19	5.18	2.72	1.41
0.11	2.12	10.8	2.79	3.19
0.154	2.06	15.1	2.80	4.58

$$\chi_c = \frac{k_B T V_{\text{mol}} m_3^2 m_4^2}{[m_3 X + m_4(1-X)]^4} \left[\frac{\partial X}{\partial \phi}\right]_{P,T} . \quad (A4)$$

We shall use the entropy per mole of solution $S = -(\partial g/\partial T)_{P,X}$ and the specific heat per mole $C_{P,X} = T(\partial S/\partial T)_{P,X}$ at constant P and X. These quantities satisfy the relations

$$\bar{S} \equiv S - X \left[\frac{\partial S}{\partial X}\right]_{P,T} = N_A m_4 \left[\sigma - c \left[\frac{\partial \sigma}{\partial c}\right]_{P,T}\right]$$

$$(A5)$$

and

$$C_{P,X} = V_{\text{mol}} \rho C_{P,c} . \quad (A6)$$

Thus we obtain from Eqs. (2.18) and (2.8)

$$g_1 = \frac{T}{\hbar N_A} \left[S - X \left[\frac{\partial S}{\partial X}\right]_{P,T}\right] \quad (A7)$$

and

$$\chi_q = \frac{C_{P,X}}{k_B V_{\text{mol}}} . \quad (A8)$$

In our paper we use experimental values for g_1, g_2, χ_q, and χ_c, which are primarily based on the experiments by Gasparini and Moldover[101] and on the analysis of Ahlers.[24,75] In the range $0.05 \leq X \leq 0.15$ we have determined these quantities in the following way. In Eqs. (A2), (A4), (A7), and (A8) we set $T = T_\lambda$, $S = S_\lambda$, and $V_{\text{mol}} = V_\lambda$ with T_λ, S_λ, and V_λ taken from Table II and Eq. (3.21) of Ahlers.[75] Furthermore, we determine the temperature dependence of $(\partial S/\partial X)_{P,T}$ and of $C_{P,X}$ from Eq. (3.19) and Table II of Ref. 75 and from Eqs. (3.11)—(3.15) and Table I of Ref. 75, respectively. The derivative $(\partial X/\partial \phi)_{P,T}$ can be expressed in terms of other thermodynamic quantities, according to Eq. (3.18) of Ahlers,[75] which are given in Table II of Ref. 75, except for $C_{P\phi}$ which we have taken from Eq. (1) and Table I of Gasparini and Gaeta.[102] For convenience we have plotted the resulting temperature dependence of $S_\lambda - X(\partial S/\partial X)_{P,T}$, of $(\partial X/\partial \phi)_{P,T}$, and of $C_{P,X}$ in Fig. 14. The corresponding curves for B^{expt} are shown in Fig. 3. We note that the parameters at $X = 0.011$ given in Table I of Gasparini and Moldover[101] can be employed for interpolations in the range $0.01 \lesssim X \lesssim 0.05$.

TABLE II. Initial conditions for the effective parameters $w_i(l)$ and $f_i(l)$ at $l = l_0$ corresponding to $t = t_0 = 10^{-1.5}$ at various ^{3}He concentrations X. The values for $B = g_1^2 \chi_c / g_2^2 \chi_q$ are experimental values at $t = 10^{-1.5}$. For $X = 0.053$, we have adjusted f_1, f_2, w_1, and w_3 in fitting the data of Fig. 2. For all other values of $X > 0$, w_i and f_i have been calculated according to the extrapolation procedure described in Sec. VII E. In all cases, B is an l-independent constant according to the invariance property of Eq. (5.3). The cases $X = 0$ refer to model-E fits to the thermal-conductivity data of cell D and cell A (bottom line), respectively. The numbers in the last column indicate the figures where the initial conditions have been used.

X	l_0	f_1	f_2	w_1	w_2	w_3	B	Figs.
10^{-6}	9.70×10^{-2}	0.298	6×10^{-5}	0.764	7.31	-2×10^{-4}	5×10^5	7,8,10,11
0.001	9.68×10^{-2}	0.298	5.8×10^{-3}	0.764	7.31	-6.8×10^{-3}	491	8,9,11,13
0.005	9.59×10^{-2}	0.298	0.029	0.764	7.31	-0.015	98	7—9,11,12
0.01	9.48×10^{-2}	0.298	0.058	0.764	7.31	-0.022	49	4,7—9,11
0.053	8.84×10^{-2}	0.298	0.308	0.764	7.31	-0.050	9.26	1,2,4,7—10
0.053	8.84×10^{-2}	0.137	0.281	1.24	7.63	-0.019	3.0	
0.11	8.2×10^{-2}	0.281	0.592	0.784	7.31	-0.065	4.4	4,5
0.154	7.73×10^{-2}	0.266	0.810	0.787	7.31	-0.072	3.05	6
0	9.70×10^{-2}	0.253		0.572				
0	9.70×10^{-2}	0.186		0.759				7

Since no experimental data for the quantities[24,75] $(\partial\phi/\partial T)_\lambda$ and $(\partial S/\partial T)_\lambda$ are available in the dilute regime $X < 0.01$ we have to resort to a reasonable extrapolation for $X \to 0$. Within the theory for dilute ideal solutions one has $(\partial\phi/\partial T)_\lambda \sim X^{-1}$ and $(\partial S/\partial T)_\lambda \sim \ln X$ as $X \to 0$ [see Eqs. (2.1.86) and (2.1.87) of Ref. 24]. Thus we assume, as an approximate representation for small X,

$$\left| \frac{\partial\phi}{\partial T} \right|_\lambda = aX^{-1} \qquad (A9)$$

and

$$\left| \frac{\partial S}{\partial T} \right|_\lambda = b + R \left| \frac{\partial X}{\partial T} \right|_\lambda \ln X , \qquad (A10)$$

with R being the gas constant and $(\partial X/\partial T)_\lambda = -0.714$ K^{-1} according to the $X = 0$ value given in Table II of Ref. 75. The constants a and b can be determined such that the rhs of Eqs. (A9) and (A10) reproduce the estimated values of $(\partial\phi/\partial T)_\lambda$ and $(\partial S/\partial T)_\lambda$ at $X = 0.05$ given in Table II of Ahlers.[75] This yields $a = -13.75$ J mole K^{-1} and $b = 0.783$ J mole^{-1}K^{-2}. For $C_{P,X}$ we have used Eqs. (3.11)–(3.15) of Ref. 75 also in the dilute regime $X < 0.01$. For all other thermodynamic quantities that remain finite in the $X \to 0$ limit we have taken their $X = 0$ (^{4}He) values. This defines our extrapolation procedure for the static quantities in producing the curves for $X < 0.05$ in Figs. 4 and 7–14.

For our nonlinear renormalization-group analysis we need background values at some t_0 far from $T_\lambda[X]$. We have chosen

$$t_0 = \frac{T_0 - T_\lambda[X]}{T_\lambda[X]} = 10^{-1.5} , \qquad (A11)$$

although the noncritical background region may be even farther from T_λ. The limited accuracy of the present model, however, does not allow for a fully quantitative treatment of the range $t \gtrsim 10^{-1.5}$. Experimental values for the static quantities at t_0 for $X \gtrsim 0.05$ are collected in Table I. Using these values and the constants given in Eqs. (7.34)–(7.38) we can calculate from Eqs. (7.30)–(7.33) the initial conditions $w_i(l_0)$ and $f_i(l_0)$ at l_0 corresponding to $t_0 = 10^{-1.5}$ without adjustable parameters. The resulting initial conditions are presented in Table II. The following comments should be made. (i) For $X \leq 0.05$, $f_1(l_0)$ and $w_1(l_0)$ are independent of X because we have approximated the static values g_1^2 and $\mathcal{X}_q$ in Eqs. (7.30) and (7.31) by their $X = 0.05$ values. For $X > 0.05$ we have used the values of Table I. (ii) $w_2(l_0)$ is independent of X in our procedure because we keep K_0 and $\lambda_0/\mathcal{X}_c$ fixed at the values given in
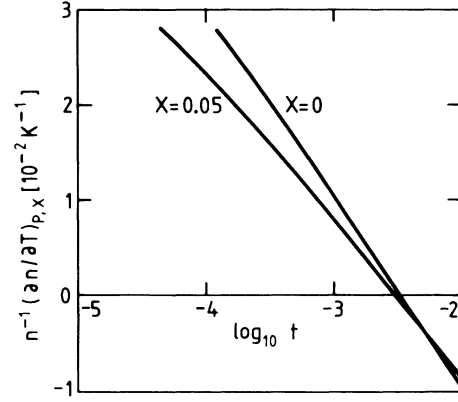

FIG. 15. Thermal expansion coefficient, Eq. (A14), taken from experiments (for references see text).

Eqs. (7.35) and (7.36). (iii) The X dependence of $w_3(l_0)$ and $f_2(l_0)$ results from the X dependence of the coefficients $\mathcal{X}_c^{1/2}/X(1-X)$ and $\mathcal{X}_c/g_2^2$ in Eqs. (7.32) and (7.33).

Now we turn to the relation between the flow parameter l and the relative temperature t, Eq. (7.22), used in the figures. As is well known,[85] the distance t from T_λ for a path at constant c or X is different from the distance $t_\Delta = t_\phi$ at constant Δ or ϕ. The relation between t_ϕ and t is given (for $T < T_\lambda$) in Eqs. (8.2)–(8.4) of Ref. 75. According to Eq. (7.15) we have $l = (t_\phi)^\nu$ with[103] $\nu = 0.675$. Expressing t_ϕ in terms of t and using the relation $(\partial\phi/\partial T)_{P,X} = -(\partial S/\partial X)_{P,T}$, as well as Eq. (3.19) of Ref. 75, we finally obtain

$$l = \left\{ t + \left| \frac{\partial T}{\partial\phi} \right|_{\lambda,P} \left| \frac{\partial T}{\partial X} \right|_{\lambda,P} \right.$$
$$\left. \times \left[t \left| \frac{\partial S}{\partial T} \right|_{\lambda,P} - \frac{1}{T_\lambda} \int_0^t C_{P,X} dt \right] \right\}^\nu , \qquad (A12)$$

where the derivatives are taken along the λ line at constant P. Experimental values for the λ-line parameters and for $C_{P,X}$ are given in Tables II and I of Ref. 75. At given t the rhs of Eq. (A12) is still X dependent. This is the reason for the slight X dependence of l_0 in Table II. For $X = 0.05$, the corresponding values for l and t are given in the lower and upper scale of Figs. 1(a)–1(e). See also Fig. 16 of Ref. 102.

In order to determine the static coefficients a_{qq}, a_{qc}, and a_{cc} entering the dynamic structure factor, Eq. (8.3), we need in addition experimental values for $(\partial n/\partial c)_{P,T}$ and $(\partial n/\partial T)_{P,c}$. For

$$\left| \frac{\partial n}{\partial c} \right|_{P,T} = \left| \frac{\partial n}{\partial X} \right|_{P,T} \frac{[m_3 X + m_4(1-X)]^2}{m_3 m_4} \qquad (A13)$$

we have taken the λ-line values given in Sec. 5.3 of Ref. 40. For $(\partial n/\partial T)_{P,c} = (\partial n/\partial T)_{P,X}$ we use the relation for the thermal expansion coefficient

$$-\frac{1}{n}\left[\frac{\partial n}{\partial T}\right]_{P,X} = \left[V_\lambda T_\lambda \left[\frac{\partial P}{\partial T}\right]_{\lambda,X}\right]^{-1} C_{P,X}$$

$$-\frac{1}{V_\lambda}\left[\frac{\partial S}{\partial P}\right]_{\lambda X} \qquad (A14)$$

[see Eq. (3.22) of Ref. 75]. Here the derivatives are taken along the λ line in the P-T plane at constant X. For $V_\lambda T_\lambda (\partial P/\partial T)_{\lambda,X}$ and $(\partial S/\partial P)_{\lambda,X}$ we have used interpolations between the values given in Table IV of Kakizaki and Satoh[104] and in Table II of Buchal and Pobell,[7] respectively. The resulting temperature dependence is shown in Fig. 15. The vanishing of $(\partial n/\partial T)_{P,X}$ near $t = 10^{-2.5}$ corresponds to the minimum of the molar volume shown in Fig. 4 of Ref. 104.

---

*Present address: Physikdepartment, Technische Universität München, D-8046 Garching, Germany.

†Permanent address.

[1]T. P. Ptukha, Zh. Eksp. Teor. Fiz. <u>40</u>, 1583 (1961) [Sov. Phys.—JETP <u>13</u>, 1112 (1961)].

[2]G. Ahlers, Phys. Rev. Lett. <u>24</u>, 1333 (1970).

[3]R. H. Webeler and D. C. Hammer, Phys. Lett. <u>33A</u>, 213 (1970); Phys. Rev. A <u>5</u>, 1820 (1972).

[4]C. M. Drabkin, V. A. Noskin, V. A. Trunov, A. F. Shchebetov, and A. Z. Yagud, Zh. Tekh. Fiz. <u>42</u>, 180 (1972) [Sov. Phys.—Tech. Phys. <u>17</u>, 142 (1972)]; C. M. Drabkin, V. A. Noskin, and A. Z. Yagud, Zh. Eksp. Teor. Fiz. Pis'ma Red. <u>15</u>, 504 (1972) [JETP Lett. <u>15</u>, 357 (1972)]; G. M. Drabkin, V. A. Noskin, E. C. Tarovik, and A. Z. Yagud, Phys. Lett. <u>43A</u>, 83 (1973).

[5]G. Ahlers and F. Pobell, Phys. Rev. Lett. <u>32</u>, 144 (1974).

[6]P. Leiderer, D. R. Nelson, D. R. Watts, and W. W. Webb, Phys. Rev. Lett. <u>34</u>, 1080 (1975); P. Leiderer, in *Quantum Fluids and Solids*, edited by S. B. Trickley, E. D. Adams, and J. W. Dufty (Plenum, New York, 1977).

[7]C. Buchall and F. Pobell, Phys. Rev. B <u>14</u>, 1103 (1976); C. Buchall, F. Pobell, and W. C. Thomlinson, Phys. Lett. <u>51A</u>, 19 (1975).

[8]W. C. Thomlinson, G. G. Ihas, and F. Pobell, Phys. Rev. B <u>11</u>, 4292 (1975).

[9]P. Lucas, D. A. Penman, and A. Tyler, Phys. Lett. <u>53A</u>, 453 (1975); <u>54A</u>, 387 (1975); <u>55A</u>, 289 (1975).

[10]P. Lucas and A. Tyler, J. Low Temp. Phys. <u>27</u>, 281 (1977).

[11]D. B. Roe, G. Ruppeiner, and H. Meyer, J. Low Temp. Phys. <u>27</u>, 747 (1977).

[12]D. B. Roe and H. Meyer, J. Low Temp. Phys. <u>28</u>, 349 (1977).

[13]M. Tanaka, A. Ikushima, and K. Kawasaki, Phys. Lett. <u>61A</u>, 119 (1977).

[14]M. Tanaka and A. Ikushima, Phys. Lett. <u>64A</u>, 402 (1978); J. Low Temp. Phys. <u>35</u>, 9 (1979).

[15]D. B. Roe, H. Meyer, and A. Ikushima, J. Low Temp. Phys. <u>32</u>, 67 (1978).

[16]L. S. Dikina, C. Y. Kotenev, and E. Y. Rudavskii, Fiz. Nizk. Temp. <u>5</u>, 5 (1979) [Sov. J. Low Temp. Phys. <u>5</u>, 1 (1979)].

[17]B. Lambert, R. Perzynski, and D. Salin, J. Phys. Lett.

<u>40</u>, 477 (1979).

[18]G. Ruppeiner and H. Meyer, Phys. Lett. <u>70A</u>, 433 (1979).

[19]T. Kobayashi and Y. Narahara, J. Low Temp. Phys. <u>38</u>, 641 (1980).

[20]G. Ruppeiner, M. Ryschkewitsch, and H. Meyer, J. Low Temp. Phys. <u>41</u>, 179 (1980).

[21]R. P. Behringer and H. Meyer, J. Low Temp. Phys. <u>46</u>, 407 (1982).

[22]R. P. Behringer and H. Meyer, J. Low Temp. Phys. <u>46</u>, 435 (1982).

[23]D. Gestrich and H. Meyer, Bull. Am. Phys. Soc. <u>27</u>, 516 (1982); H. Meyer (private communication); D. Gestrich, R. Walsworth, and H. Meyer (unpublished).

[24]G. Ahlers, in *The Physics of Liquid and Solid Helium, Part I*, edited by K. H. Bennemann and J. B. Ketterson (Wiley, New York, 1976), p. 85.

[25]H. Meyer, G. Ruppeiner, and M. Ryschkewitsch, in *Proceedings of the International Conference on Dynamic Critical Phenomena*, edited by C. P Enz (Springer, New York, 1979).

[26]A. Ikushima, Jpn. J. Appl. Phys. <u>19</u>, 2315 (1980).

[27]See, e.g., L. P. Kadanoff, in *Proceedings of the International School of Physics "Enrico Fermi"*, Course LI, edited by M. S. Green (Academic, New York, 1973); R. B. Griffiths, Phys. Rev. Lett. <u>24</u>, 1479 (1970).

[28]I. M. Khalatnikov, *An Introduction to the Theory of Superfluidity* (Benjamin, New York, 1965).

[29]K. Kawasaki and J. D. Gunton, Phys. Rev. Lett. <u>29</u>, 1661 (1972).

[30]R. A. Ferrell, N. Menyhárd, H. Schmidt, F. Schwabl, and P. Szépfalusy, Phys. Rev. Lett. <u>18</u>, 891 (1967); Ann. Phys. (NY) <u>47</u>, 565 (1968).

[31]J. Kerrisk and W. E. Keller, Bull. Am. Phys. Soc. <u>12</u>, 550 (1967); Phys. Rev. <u>177</u>, 341 (1969).

[32]M. Archibald, J. M. Mochel, and L. Weaver, Phys. Rev. Lett. <u>21</u>, 1156 (1968).

[33]G. Ahlers, Phys. Rev. Lett. <u>21</u>, 1159 (1968).

[34]G. Ahlers, in *Proceedings of the Twelfth International Conference on Low Temperature Physics*, edited by E. Kanda (Keigaku, Tokyo, 1971), p. 21.

[35]G. Ahlers, in *Quantum Liquids*, edited by J. Ruvalds and T. Regge (North Holland, Amsterdam, 1978), p. 1.

36P. Leiderer and W. Bosch, Phys. Rev. Lett. 45, 727 (1980).

37A. Griffin, Can. J. Phys. 47, 429 (1969).

38W. F. Vinen, in *Physics of Quantum Liquids*, edited by R. Kubo and F. Takano (Syokabo, Tokyo, 1971), p. 1.

39M. K. Grover and J. Swift, J. Low Temp. Phys. 11, 751 (1973).

40D. A. Rockwell, R. F. Benjamin, and T. J. Greytak, J. Low Temp. Phys. 18, 389 (1975).

41M. Papoular, J. Low Temp. Phys. 24, 105 (1976).

42M. J. Stephen, in Ref. 24, p. 307.

43E. D. Siggia and D. R. Nelson, Phys. Rev. B 15, 1427 (1977).

44E. D. Siggia, Phys. Rev. B 15, 2830 (1977).

45L. Peliti, in Ref. 25, p. 189.

46P. C. Hohenberg and B. I. Halperin, Rev. Mod. Phys. 49, 435 (1977).

47C. De Dominicis and L. Peliti, Phys. Rev. B 18, 353 (1978).

48V. Dohm and H. K. Janssen, Phys. Rev. Lett. 39, 946 (1977); V. Dohm, Kernforschungsanlage Jülich Report No. JÜL-1578 (unpublished).

49V. Dohm, Z. Phys. B 31, 327 (1978); 33, 79 (1979).

50R. A. Ferrell and J. K. Bhattacharjee, Phys. Rev. Lett. 42, 1638 (1979); 44, 403 (1980); and in Ref. 25, p. 152.

51V. Dohm and R. Folk, in *Festkörperprobleme (Advances in Solid State Physics)*, edited by P. Grosse (Vieweg, Braunschweig, 1982), Vol. XXII, p. 1.

52V. Dohm and R. Folk, Phys. Rev. Lett. 46, 349 (1981).

53V. Dohm and R. Folk, Z. Phys. B 40, 79 (1980).

54V. Dohm and R. Folk, Z. Phys. B 41, 251 (1981).

55G. Ahlers, P. C. Hohenberg, and A. Kornblit, Phys. Rev. B 25, 3136 (1982); P. C. Hohenberg, Physica (Utrecht) 109-110B, 1436 (1982).

56V. Dohm and R. Folk, Z. Phys. B 45, 129 (1981); Physica 109-110B, 1549 (1982).

57E. Brézin, J. C. Le Guillou, and J. Zinn-Justin, in *Phase Transitions and Critical Phenomena*, edited by C. Domb and M. S. Green (Academic, New York, 1976), Vol. VI; see also E. Brézin, in *Phase Transitions, Cargese 1980*, edited by M. Lévy, J. C. Le Guillou, and J. Zinn-Justin (Plenum, New York, 1982), p. 331; also E. Brézin, in *Order and Fluctuations in Equilibrium and Nonequilibrium*, edited by G. Nicolis, G. Dewel, and J. W. Turner (Wiley, New York, 1981), p. 1.

58D. J. Amit, *Field Theory, The Renormalization Group and Critical Phenomena* (McGraw-Hill, New York, 1978).

59(a) R. Bausch, H. K. Janssen, and H. Wagner, Z. Phys. B 24, 113 (1976); (b) H. K. Janssen, in Ref. 25, p. 25.

60B. I. Halperin, P. C. Hohenberg, and E. D. Siggia, Phys. Rev. B 13, 1299 (1976); 21, 2044(E) (1981).

61H. Meyer (private communication).

62The corresponding data from Duke University will be shown in Fig. 8 of Sec. VII.

63V. Dohm (unpublished).

64L. D. Landau and I. M. Lifshitz, *Statistical Physics* (Addison-Wesley, Reading, Mass., 1969), Chap. XII.

65L. D. Landau and I. M. Lifshitz, *Fluid Mechanics* (Pergamon, London, 1959), Chap. VI.

66J. Swift, Phys. Rev. 173, 259 (1968).

67E. D. Siggia, B. I. Halperin, and P. C. Hohenberg, Phys. Rev. B 13, 2110 (1976).

68H. K. Janssen, Z. Phys. B 23, 377 (1976).

69C. de Dominicis, J. Phys. (Paris), Colloq. 37, C1-247 (1976).

70P. C. Martin, E. D. Siggia, and H. A. Rose, Phys. Rev. A 8, 423 (1973).

71V. Dohm and R. Folk, Z. Phys. B 35, 277 (1979).

72G. 't Hooft and M. Veltman, Nucl. Phys. B 44, 189 (1972).

73I. D. Lawrie, J. Phys. A 9, 961 (1976).

74D. R. Nelson, Phys. Rev. B 14, 1123 (1976).

75G. Ahlers, Phys. Rev. A 10, 1670 (1974).

76This result was obtained independently also by L. Peliti (unpublished).

77This parameter appears also in the work of P. C. Hohenberg and D. R. Nelson, Phys. Rev. B 20, 2665 (1979) [see Eq. (3.33)].

78B. I. Halperin and P. C. Hohenberg, Phys. Rev. 177, 952 (1969).

79V. Dohm and R. A. Ferrell, Phys. Lett. 67A, 387 (1978).

80J. K. Bhattacharjee, V. Dohm, and H. K. Janssen (unpublished).

81P. C. Hohenberg, B. I. Halperin, and D. R. Nelson, Phys. Rev. B 22, 2373 (1980).

82D. R. Nelson and D. S. Fisher, Phys. Rev. B 16, 4945 (1977).

83On the basis of dynamic scaling theory it has been predicted (Refs. 78,5, and 24) that D above T_λ can be expressed in terms of the second-sound velocity c_2 below T_λ as $D = A_D c_2 \xi_\Delta$ with a temperature-independent amplitude A_D. This agrees with our result in the asymptotic limit $T \to T_\lambda$ provided that $w^* > 0$. Furthermore, from Eq. (2.37), from the relation between Ψ_0 and ρ_s according to Eq. (2.17), and from $\rho_s = m_4^2 k_B T \hbar^{-2} \xi_T^{-1}$ [Eq. (4.4) of Ref. 60] we obtain the explicit expression for the amplitude A_D as $A_D = R^*_{He}(\xi_T/\xi_\Delta)^{1/2}(1+B)^{-1}$, with ξ_T being the transverse correlation length below T_λ. We see that for $w^* \sim O(0.1)$ and $B \sim O(1)$, A_D is of order unity, thus confirming previous assumptions (Refs. 5 and 24). For very small c or c very close to $c_{tricrit}$, however, $A_D \ll 1$ since $B \gg 1$ in these cases. Similar comments apply to $D_s = A_s c_2 \xi_\Delta$ and $A_s = A_D B$.

84P. C. Hohenberg, A. Aharony, B. I. Halperin, and E. D. Siggia, Phys. Rev. B 13, 2986 (1976).

85M. E. Fisher, Phys. Rev. 176, 257 (1968); B. J. Lipa and M. J. Buckingham, Phys. Lett. 26A, 643 (1968); Y. Imry, O. Entin-Wohlman, and D. J. Bergman, J. Phys. C 6, 2846 (1973).

86More precisely, we have minimized the sum of squares of the relative deviations $(R_\alpha^{expt} - R_\alpha)/R_\alpha$.

87We have also tried to study the effect of the temperature dependence of $B^{expt}(t)$ in the following phenomeno-

logical way. We have dropped the flow equation for $w_2(l)$ and instead have determined $w_2(l)$ from the relation $w_2(l) = B^{\text{expt}}(t) w_1(l) f_2(l)/f_1(l)$, now with the temperature-dependent quantity $B^{\text{expt}}(t)$. Using this $w_2(l)$ in the flow equations for $w_1(l)$, $w_3(l)$, $f_1(l)$, and $f_2(l)$, and carrying out a least-squares fit yields the initial conditions $w_1(l_0) = 1.51$, $w_3(l_0) = 0.001$, $f_1(l_0) = 0.108$, and $f_2(l_0) = 0.203$, which implies $w_2(l_0) = 26.3$. The fit quality, however, is not improved by this procedure. We feel that, although part of the model-F-type effects are taken into account by this procedure, this is not a controlled way to improve the present model. From the analysis of ^{4}He, we know (Ref. 56) that only a consistent loop-wise calculation (Ref. 63) can avoid the shortcomings of phenomenological "improvements" (Ref. 55).

[88]J. O. Hirschfelder, C. F. Curtis, and R. B. Bird, *Molecular Theory of Gases and Liquids* (Wiley, New York, 1954); R. Paul, A. J. Howard, and W. W. Watson, J. Chem. Phys. **43**, 1622 (1965).

[89]W. L. Taylor, in *Proceedings of the Thirteenth International Conference on Low-Temperature Physics*, edited by K. D. Timmerhaus, W. J. O'Sullivan, and E. F. Hammel (Plenum, New York, 1974), Vol. I, p. 631.

[90]G. Careri, J. Reuss, F. Scaramussi, and J. O. Thomson, in *Proceedings of the Fifth International Conference on Low-Temperature Physics*, edited by J. R. Dillinger (University of Wisconsin Press, Madison, 1958), p. 155.

[91]F. Careri, J. Reuss, and J. M. Beenakker, Nuovo Cimento **13**, 148 (1959).

[92]J. J. M. Beenakker, K. W. Taconis, E. A. Lynton, Z. Dokoupil, and G. Van Soest, Physica (Utrecht) **18**, 433 (1952).

[93]The interpretation of the parameters in Eqs.

(7.34)—(7.38) as background quantities is, of course, inaccurate since the background region is farther from T_λ than $t_0 = 10^{-1.5}$. Nevertheless, we note that there is rough agreement, at least in order of magnitude, with the background values measured in Refs. 4, 21, 31, and 89—92.

[94]G. Ahlers and R. P. Behringer, as quoted in Ref. 55 [Phys. Rev. B **25**, 3136 (1982)].

[95]The corresponding formula suggested by Ahlers and Pobell (Ref. 5) differs by a factor π^{-2}.

[96]G. Ahlers, Phys. Rev. Lett. **43**, 1417 (1979).

[97]M. J. Crooks and B. J. Robinson, Physica (Utrecht) **107B**, 339 (1981) and unpublished.

[98]See, e.g., Eq. (4.5.24) of Ref. 42, and Fig. 7 of Ref. 54.

[99]We note that further measurements of k_T at $X = 0.15$ have been performed by Lucas and Tyler [Ref. 10 and P. Lucas (private communication)]. Unfortunately, there seem to be difficulties in obtaining reliable absolute values for k_T; the published values (Ref. 10) differ from those of Ref. 23 by about 30%; therefore, a comparison with our theory does not seem possible at present.

[100]P. C. Hohenberg and S. Sarkar, Phys. Rev. B **24**, 3800 (1981).

[101]F. M. Gasparini and M. R. Moldover, Phys. Rev. B **12**, 93 (1975).

[102]F. M. Gasparini and A. A. Gaeta, Phys. Rev. B **17**, 1466 (1978).

[103]See Eq. (2.5) and footnote 41 of Ref. 55 [Phys. Rev. B **25**, 3136 (1982)].

[104]A. Kakizaki and T. Satoh, J. Low Temp. Phys. **24**, 67 (1976).

[105]R. A. Ferrell and J. K. Bhattacharjee, Phys. Rev. B **20**, 3690 (1979).